HANDBOOK

AND

PROCEEDINGS

OF THE

TENNESSEE JUNIOR

ACADEMY OF SCIENCE

2014

Sponsored by the
Tennessee Academy of Science

Edited by Jack Rhoton, Director
Tennessee Junior Academy of Science
P.O. Box 70301
East Tennessee State University
Johnson City, TN 37614
RhotonJ@etsu.edu

TENNESSEE JUNIOR ACADEMY

OF SCIENCE

ANNUAL MEETING

Belmont University

Nashville, Tennessee

Friday, April 25, 2014

Sponsored by the

TENNESSEE ACADEMYOF SCIENCE

TABLE OF CONTENTS

TENNESSEE ACADEMY OF SCIENCE OFFICERS: 2014

Dr. Kim Cleary Sadler ……..…..…….. … President
Middle Tennessee State University, Murfreesboro

Dr. Gilbert Pitts…...…….…… ...President-Elect
Austin Peay State University

Mandy Carter-Lowe ..…….....Immediate Past President
Columbia State Community College, Columbia

Teresa Fulcher…….…….…… …….Secretary
Pellissippi State Technical Community College, Knoxville

C. Steven Murphree…….…….…….…….Treasurer
Belmont University, Nashville

Dr. Rachel Rigsby……..……Managing Editor
Tennessee Academy of Science Journal, *Belmont University, Nashville*

.

Abigail M. Goosie……..……Assistant Editor
Tennessee Academy of Science Journal, *Walter's State Community College*

TENNESSEE JUNIOR ACADEMY OF SCIENCE

Sponsored by the

TENNESSEE ACADEMY OF SCIENCE

Jack Rhoton…..……..…..Director, Tennessee Junior Academy of Science
East Tennessee State University, Johnson City

READING COMMITTEE 2013-2014

Jack Rhoton..…….…….East Tennessee State University

Chih-Che Tai…..……..……..East Tennessee State University

Timothy McDowell..…..…….East Tennessee State University

Gary Henson..…..……...East Tennessee State University

JUDGES

Joel Harp..…..……Vanderbilt University

E. Lewis Myles...……..…….Tennessee State University

Preston J. MacDougall..…..……...Middle Tennessee State University

LOCAL ARRANGEMENTS

C. Steven Murphree..…...…….Belmont University

INSTRUCTIONS FOR PARTICIPATION IN THE
TENNESSEE JUNIOR ACADEMY OF SCIENCE

Purpose. The Tennessee Junior Academy of Science (TJAS) is designed to further the cause of science education in Tennessee high schools by providing an annual program of scientific atmosphere and stimulation for capable students. It is comparable to scientific meetings of adult scientists. The Junior Academy supplements other efforts in the encouragement of able students of science by providing one venue of stimulation and expression

Rewards and Prizes. The student's primary rewards are the honor of being selected to appear on the program, experience in presenting his/her paper, opportunity to discuss this work with other students of similar interests, membership in the Tennessee Junior Academy of Science, and publication of his/her paper in the *Handbook and Proceedings of the Tennessee Junior Academy of Science.* However, the top two student writers will receive $500 each from the Tennessee Academy of Science, and other top writers will receive $200 for each paper published in the *Handbook.* In addition, the TAS will award $500 to each of the top two writers to participate in the Annual Meeting of the American Junior Academy of Science (AJAS). The AJAS meeting is held in a different city each year. All students who present papers to the TJAS are encouraged to enter their papers in other competitive programs, such as the Westinghouse Science Talent Search and the International Science and Engineering Fair. Students are also encouraged to solicit scholarships from individuals, companies, or institutions.

Preparation of the Report. The report should be an accurate presentation of a science or mathematics project completed by the student. It should be comprehensive, yet avoid excessive verbosity. Maximum length should be 1500 words. The report and the project it describes must be original with the student, not just a review of another article. It should be obvious that the experimentation and/or observations have been scientifically made. The paper should reflect credit on the writer and the school represented.

Visual aids such as slides, mock-ups, and charts may be used in presentation of the report. **PLEASE NOTE THE FOLLOWING: ILLUSTRATIONS WITHIN THE REPORT MUST BE RESTRICTED TO TABLES AND/OR SIMPLE LINE DRAWINGS. These must be done in BLACK ON 8 ½ X 11 WHITE PAPER. COLORED FIGURES CANNOT BE PRINTED IN THE HANDBOOK. Total width of the illustration itself cannot be more than 7". Illustrations submitted with the paper MUST be originals, NOT COPIES, and MUST be BLACK AND WHITE.**

The report must be **DOUBLE-SPACED** on 8 ½" by 11" paper. Give careful attention to spelling and grammar. **IT IS VERY IMPORTANT that YOU prepare a COVER SHEET** for the report, giving **ALL** the required information as specified, INCLUDING YOUR HOME TELEPHONE NUMBER **AND E-MAIL ADDRESS.** IF YOUR PAPER SHOULD BE SELECTED FOR PUBLICATION, IT MAY BE NECESSARY FOR OUR EDITORS TO CONTACT YOU. FAILURE TO PROVIDE CONTACT INFORMATION COULD PREVENT YOUR PAPER FROM BEING PUBLISHED. The cover sheet included with this material may be duplicated as needed. Prepare an abstract to accompany your paper (not more than 100

words). **NO PAPER WILL BE CONSIDERED UNLESS IT IS ACCOMPANIED BY AN ABSTRACT.**

Scientific or Technical Report Writing. A very important phase of the research of a scientist is the effective reporting of the research project attempted and completed. The technical report is different from other kinds of informative writing in that it has a single, predetermined purpose: to investigate an assigned subject for particular reasons. Technical reporting is done in the passive voice. Use of personal pronouns should be avoided except in rare instances. The telling portion of the research job is often underrated. Thus, communication is a very necessary part of research work. Any breakdown in communication means that the report has failed. The following functional analysis of the parts of the report is suggested to aid in organizing and presenting the results of scientific and experimental efforts.

I. Introduction
   A. Purpose of the investigation (why the work was done)
   B. How the problem expands/clarifies knowledge in the general field
   C. Review of related literature

II. Experimental procedure (how the work was done)
   A. Brief discussion of experimental apparatus involved
   B. Description of the procedure used in making the pertinent observations and obtaining data

III. Data (what the results were)
   A. Presentation of specific numerical data in tabulated or graphic form
   B. Observations made and recorded
   C. Any and all pertinent observations made that bear on the answer to the problem being investigated

IV. Conclusions (final contributions to knowledge)
   A. General contributions the investigations have made to the answer to the problem
   B. Further investigation suggested or indicated by the work

V. References –should be the **WORKS CITED ONLY** (the literature sources that are ACTUALLY **CITED** in the paper)
   A. Items arranged alphabetically by author's surname
      1. Author (surname, with initials only)
      2. Date, in parentheses
      3. Title, capitalize first work only
      4. Source: (periodical) (NO ABBREIVATIONS)
         (book) city, state of publication, publisher.

Each item in the Works Cited **MUST ALSO BE CITED WITHIN THE TEXT** of the student paper, using the parenthetical format of the APA Style Manual. Plagiarism is a serious offense, and is **not** limited to direct quotations. Any word, thought, statement, or instruction written by

another author and used in the student paper must be appropriately cited in the student paper presented to the Junior Academy.

Submission of the Report. Each report must bear an OFFICIAL COVER SHEET, which may be obtained in advance from Junior Academy link on Tennessee Academy of Science web page.

Director of the Tennessee Junior Academy of Science
Dr. Jack Rhoton
East Tennessee State University
Box 70301
Johnson City, TN 37614
E-mail: Rhotonj@etsu.edu

The ORIGINAL COPY of the report should arrive on or before **March 1, 2015**. The parts of each report should be stapled or clipped, not bound. Heavy covers increase the cost of postage. The student should keep a copy of the report; the original cannot be returned. (We **MUST** have the **ORIGINAL** of all papers –and illustrations- for publication.)

Selection of the Report. Each report submitted must be endorsed by a local science or mathematics teacher. The teacher should approve the report as the first member of a selection committee. IT SHOULD BE APPROVED ONLY IF IT IS OF HIGH QUALITY AND REPRESENTS THE STUDENT'S OWN WORK IN RESEARCH AND PREPARATION. The science or math faculty submitting two or more papers in a given category will be asked to serve as judges for those papers and rate them in the order of 1, 2, 3, 4, etc., according to merit before submission to the Tennessee Junior Academy of Science for final judging. The report will then be read by a committee of two or more additional scientists in the field appropriate to the report. Reports will be selected on the basis of research design (30 points), creative ability (20 points), analysis of results (20 points), grammar and spelling (20 points), and general interest (10 points).

TENNESSEE JUNIOR ACADEMY OF SCIENCE CALENDAR FOR 2015

March 1	Final Date for Receiving Reports
March 20	Completion of Report Evaluation
March 30	Mailing of Invitations
April 17	Annual Meeting – Nashville

RESEARCH GRANTS FOR SCIENCE PROJECTS BY HIGH SCHOOL STUDENTS

The Tennessee Academy of Science has available a limited number of small research grants ($100-$300 per student) to assist high school students involved in developing scientific projects for the TJAS program. These grants are intended to be need-based. That is, we want to support good proposals from motivated students of adequate ability, where lack of some outside financial support might result in a poor project or possibly no project at all. These grants should not be regarded as competitive merit awards for outstanding proposals or outstanding students, and should not be given to students whose families, or whose project mentors, can readily provide

the resources needed. For instance, a project being conducted under the mentorship of a university professor would not, in general, be a good choice for a TAS grant, no matter how able the student and how good the proposed project. It is intended that the TAS research grants program create opportunities for adequately motivated students with access to limited resources to conduct significant, competitive projects. The Tennessee Academy of Science will depend on the sponsoring science or math teachers to provide input into the decision-making process as it concerns the need of applying students and worthiness of their proposed projects.

The application form for the TAS research grant included in these materials may be duplicated as needed. Please note the deadline for receiving grant applications is ***NOVEMBER 15, 2014***. However, the earlier grant applications are received, the sooner grant application funds can be distributed. If you desire further information concerning the TAS research grants program, please write to Dr. Jack Rhoton, Division of Science Education, Box 70684, East Tennessee State University, Johnson City, TN 37614 or E-mail: Rhotonj@ETSU.edu.

TENNESEE JUNIOR ACADEMY OF SCIENCE
SPRING MEETING – 2014

The 71th Annual Meeting of the Tennessee
Junior Academy of Science was held in
Nashville (Belmont University) on Friday, April 25, 2014

All Tennessee high schools are invited to participate in the TJAS program leading up to the spring meeting. The program provides state-wide and national recognition for high school students' investigative or research-type science projects

TENNESSEE JUNIOR ACADEMY OF SCIENCE REGULATIONS

The following regulations have been developed to govern the Tennessee Junior Academy meeting by the Standing Committee on Junior Academies of the Academy Conference. Papers must be of a research problem type, with evidence of creative thought. Papers presented should be suitable for publication (typewritten, double-spaced, one side of paper only, name and address on each sheet) and between 1000 and 1500 words in length. Oral presentation will be limited to 10 minutes. Projectors and other audiovisual equipment will be available. Questions on paper presentation will be limited to 3 minutes. All papers should be postmarked **NO LATER THAN MARCH 1, 2015**, and sent to Dr. Preston MacDougall, Hon 229, Department of Chemistry, Middle Tennessee State University, Murfreesboro, TN 37132 or e-mail Preston Macdougall [Preston.Macdougall@mtsu.edu]. Certificates will be presented to all participants. Sponsoring schools or clubs should have insurance coverage to protect school participants. The Tennessee Junior Academy of Science can assume no responsibility in this matter.

WHAT YOU CAN DO NOW

If there is no science club at your high school, why not start one? A science club will provide many opportunities to work on problems that will be fun and relaxing. The ready, mutual exchange of ideas can provide a challenging experience in proposing, designing, and completing research into the unknown. Begin now to work on a scientific project to present at the next annual meeting of your local, state, and national Junior Science Clubs. For further information on the Junior Academy program, contact:

Tennessee Junior Academy of Science
Dr. Jack Rhoton, Director
PO Box 70301
East Tennessee State University
Johnson City, TN 37614
Phone: 423-439-7589
E-mail: Rhotonj@etsu.edu
Fax: 423-439-7530

PURPOSE OF THE ACADEMIES OF SCIENCE

The purpose of the various state and municipal Junior Academies is to promote science as a career at the secondary school level. The basic working unit is the science club or area in each school where the extracurricular science projects and activities are supervised by science teachers/sponsors. The American Junior Academy serves a state or city organization much the same as do the professional societies, and it functions in a similar manner; e.g., holding annual meetings for presenting research papers. The parent sponsor of a Junior Academy of Science is the State Academy of Science. The primary activity of the American Junior Academy of Science is the Annual Meeting held with the Annual Meeting of the American Association for the Advancement of Science and the Association of Academies of Science. Top young scientists in each state or city academy are encouraged to present papers and exchange research ideas at the national level. Tours and social hours are also arranged.

DIRECTORS OF THE TENNESSEE JUNIOR ACADEMY OF SCIENCE

1942-2014

The Tennessee Academy of Science has been the sponsor of the Tennessee Junior Academy of Science since its initial organizational meeting on the Vanderbilt University campus in 1942.

The Directors of the Junior Academy of Science since 1942 are as follows:

Dr. Frances Bottom – 1942-1955…….**.....** George Peabody College
Nashville

Dr. Woodrow Wyatt – 1955-1958……...The University of Tennessee
Knoxville

Dr. Myron S. McCay – 1958-1963……..The University of Tennessee
Knoxville

Dr. Robert Wilson – 1963-1965……..The University of Tennessee
Chattanooga

Dr. John H. Bailey – 1965-1976…….East Tennessee State University
Johnson City

Dr. William N. Pafford – 1976-1992……..East Tennessee State University
Johnson City

Dr. Jack Rhoton – 1992-2014…….East Tennessee State University
Johnson City

TENNESSEE JUNIOR ACADEMY OF SCIENCE
Sponsored by the
TENNESSEE ACADEMY OF SCIENCE
Annual Meeting

Belmont University
Nashville, Tennessee
Friday, April 25, 2014

PROGRAM

9:00 –9:30 a.m.	Registration
9:30 – 9:40 a.m.	Welcome
9:40 –11:30 a.m.	Paper Presentations
11:35 a.m.	Special Presentations
12:00 –1:00 p.m.	Lunch
1:30 –4:00 p.m.	Paper Presentations
4:00 p.m.	Adjournment

TENNESSEE JUNIOR ACADEMY OF SCIENCE

Papers to be Presented at Annual Meeting
Title of Paper, Student's Name, School, City

EFFICACY OF SIMULATED MARTIAN AND LUNAR REGOLITH AS SHEILD — **Physics**

Lillith Bulawa, Grace Gass
Greeneville High School, Greeneville

LOW LEVELS OF CAFFEINE PROTECT THE BRAIN FOLLOWING STROKE — **Zoology**

Faris Wasim
Montgomery Bell Academy, Nashville

CHARACTERIZING UNKNOWN MICROBIAL SPECIES AND ANALYZING MICROBIAL STABILITY IN CAVE WATER ENVIRONMENTS — **Microbiology**

Alex Jolly, Catherine English, Jacob Hill, Yae Eun Yang
School for Science and Math at Vanderbilt, Nashville

THE AGE AND DISTANCE OF THE OPEN CLUSTER NGC 2126 — **Astronomy**

Kayla Jenkins
Sullivan South High School, Kingsport

TESTING THE BAYESIAN MODEL OF HYPOTHESIS EVALUATION — **Behavioral Psychology**

Vijaya Dasari
White Station High School, Memphis

THE INFLUENCE OF HUE, LIGHTNESS, AND SATURATION ON ANT's FORAGING BEHAVIOR — **Zoology**

Susanna Edwards
Pope John Paul II High School, Hendersonville

REDOX REACTIONS OF IRON IN THE BODY — **Chemistry**

Chardia Csizmadia and Abigail Schilling
Northwest High School, Clarksville

TESTING THE ENZYMATIC CAPACITY OF ß-glucosidase — **Biochemistry**

Samuel Rafter and Camron Shirkhodaie
School for Science and Math at Vanderbilt, Nashville

DETERMINATION OF PROTEIN MOLECULAR WEIGHT — **Biochemistry**

Aubrey Baxter and Carleigh Wilson
Northwest High School, Clarksville

A COMPARISON OF WATER PARAMETERS, VEGETATION, AND MACRO-INVERTEBRATES OF A STREAM BEFORE, AFTER, AND AS PASSES THROUGH WATERVILLE GOLF COURSE — **Environmental**

Heidi Barringer
Cleveland High School, Cleveland

MACROINVERTEBRATES AS INDICATORS OF ANTHROPOGENIC EFFECTS ON WATER QUALITY — **Environmental Science**

Caroline Dodd, Julia Sculley and Christina Webb
Siegel High School, Murfreesboro

MICROORGANISM PRESENCE IN THE DECOMPOSITION OF FLESH — **Zoology**

Emily McRen
Pope John Paul II High School, Hendersonville

VOLTAGE MEASURED RELATIVE TO ANGLE OF SOLAR PANEL — **Physics**

Sam Smith, Kyra Wilson and Christian Taylor
St. Andrew's-Sewanee School, Sewanee

THE DEVELOPMENT OF A FROG-LOGGING ANDROID APPLICATION — **Technology**

Valeria Garcia, Nhung Hoang and Susannah E. Price
School for Science and Math at Vanderbilt, Nashville

BIIOMASS TO BIOFUELS: AN ECONOMICAL STUDY — **Chemistry**

Rachel Baker
Camden Central High School, Camden

THE EFFECT OF RIVER PROXIMITY ON THE MICROBIAL PHYLLOSPHERE OF THE SYCAMORE TREE, *Platanus occidentalis* — **Microbiology**

Cooper Thome
Central Magnet High School, Murfreesboro

THE PROCESS OF EUTROPHICATION AND THE EFFECTS OF NUISANCE ALGAE GROWTH AND NUTRIENT ENRICHMENT — **Environmental**

Anna Ferenchuk
Cleveland High School, Cleveland

GARLIC DERIVATIVES AS A NOVEL THERAPY FOR PANCREATIC CANCER — **Medicine and Health**

Anjali Chandra
Girl's Preparatory School, Chattanooga

EVALUATION OF PRIMERS FOR MICROBIAL SOURCE TRACKING OF DEER AND BOVINE IN MIDDLE TENNESSEE — **Biology**

Forrest Richardson
Hillsboro High School, Nashville

DETERMINING SOIL ELECTRICAL CONDUCTIVITY USING ELECTROMAGNETIC INDUCTION ON AN AUTONOMOUS ROBOT — **Physics**

Efrain Salazar and Able Shi
School for Science and Math at Vanderbilt, Nashville

ANTHROPOGENIC EFFECTS ON THE WATER QUALITY OF THE WATER QUALITY OF THE STONES RIVER IN MURFREESBORO, TN — **Environmental Science**

Morgan Bowling and Rachel Nichols
Siegel High School, Murfreesboro

SEQUENCING OF sIL-6Rά TO IDENTIFY A POTENTIAL CLEAVAGE SITE FOR sIL-6Rά TRANS-SIGNALING IN GLAUCOMA — **Biology**

Emma Kingsbury
Hillsboro High School, Nashville

MEASURING WETLAND HEALTH WITH GEOCHEMICAL DATA LOGGERS — **Environmental Engineering**

Dheeraj Namburu, Arturas Malinauskas, Gray Tettleton and Daniel Mehus
School for Science and Math at Vanderbilt, Nashville

Students Who Submitted Papers to the Tennessee Junior Academy of Science

Ahmed, Zheer; Martin Luther King Academic School, Nashville
Anderson, Kortni; Northwest High School, Clarksville
Ayers, John; Hillsboro High School, Nashville
Baker, Rachel; Camden Central High School, Camden
Barbour, Craig; Northwest High School, Clarksville
Barker, Hannah; Northwest High School, Clarksville
Barringer, Heidi; Cleveland High School, Cleveland
Baxter, Aubrey; Northwest High School, Clarksville
Bergman, Melissa; Northwest High School, Clarksville
Bompers, Aliayah; Northwest High School, Clarksville
Bowen, Jordan; Siegel High School, Murfreesboro
Bowling, Morgan; Siegel High School, Murfreesboro
Brown, Akiya; Northwest High School, Clarksville
Bulawa, Lillith; Greeneville High School, Greeneville
Campos, Elena; Northwest High School, Clarksville
Carter, Alex C.; Hillsboro High School, Nashville
Cerda, Alaina; Northwest High School, Clarksville
Chandra, Anjali; Girls Preparatory School, Chattanooga
Claiborne, Jewel; Northwest High School, Clarksville
Cruz, Virginia; School for Science and Math at Vanderbilt, Nashville
Csizmadia, Chardia; Northwest High School, Clarksville
Dail, DeShaun; Northwest High School, Clarksville
Dasari, Vijaya; White Station High School, Memphis
Debesai, Fenan; School for Science and Math at Vanderbilt, Nashville
Denmark, Devonta; Northwest High School, Clarksville
Dodd, Caroline; Siegel High School, Murfreesboro
Drake, Evelyn, G.; Central Magnet High School, Murfreesboro
Driscoll, Kelsey; School for Science and Math at Vanderbilt, Nashville
Edwards, Susanna; Pope John Paul II High School, Hendersonville
Emory, Crawford; St. Andrew's Sewanee School, Sewanee
English, Catherine; School for Science and Math at Vanderbilt, Nashville
Fairfield, Diona; Northwest High School, Clarksville
Faulk, Helen; Northwest High School, Clarksville
Ferenchuk, Anna; Cleveland High School, Cleveland
Fischer, Jacob; Northwest High School, Clarksville
Fonger, Haley; Northwest High School, Clarksville
Freeman, Mason; Hillsboro High School, Nashville
Garcia, Valeria; School for Science and Math at Vanderbilt, Nashville
Gass, Grace; Greeneville High School, Greeneville
Gilstrap, Teresa; Pope John Paul II High School, Hendersonville
Gordon, Evan; School for Science and Math at Vanderbilt, Nashville
Groves, Kacey; Northwest High School, Clarksville
Harris, Varik; School for Science and Math at Vanderbilt, Nashville

Harrison, Ashley, Northwest High School, Clarksville
Hernandez, Mayra; School for Science and Math at Vanderbilt, Nashville
Hill, Jacob; School for Science and Math at Vanderbilt, Nashville
Hoang, Nhung; School for Science and Math at Vanderbilt, Nashville
Hobbs, Annie; Cleveland High School, Clarksville
Hughes, Hallie; Cleveland High School, Clarksville
Hurt, Haley; Northwest High School, Clarksville
Ige, Isaac; School for Science and Math at Vanderbilt, Nashville
Irion, Courtlyn; Northwest High School, Clarksville
Jenkins, Kayla; Sullivan High School, Kingsport
Johnson, Andriana; School for Science and Math at Vanderbilt, Nashville
Johnson, Kelsey; Northwest High School, Clarksville
Johnson, Owen; Clarksville Academy, Clarksville
Johnson, Sydney; Northwest High School, Clarksville
Jolly, Alex; School for Science and Math at Vanderbilt, Nashville
Kassenbaum, Ellie E.; Siegel High School, Murfreesboro
Katsiaficas, Nathan; Hillsboro High School, Nashville
Keck, Amanda; Northwest High School, Clarksville
Kingsbury, Emma; Hillsboro High School, Nashville
Lasley, Camille; Hillsboro High School, Nashville
Lawson, Mikayla; Northwest High School, Clarksville
Logan, Michael; Cleveland High School, Clarksville
Long, Kennedy; Northwest High School, Clarksville
McDonald, Xena; School for Science and Math at Vanderbilt, Nashville
MacPherson, Elizabeth; School for Science and Math at Vanderbilt, Nashville
Malinauskas, Arturas; School for Science and Math at Vanderbilt, Nashville
McLaughlin, Kaitlin; Northwest High School, Clarksville
McRen, Emily; Pope John Paul II High School, Hendersonville
Mehus, Maylan Daniel; School for Science and Math at Vanderbilt, Nashville
Milford, Ashton; St. Andrew's Sewanee School, Sewanee
Namburu, Dheeraj; School for Science and Math at Vanderbilt, Nashville
Needham, Amy E.; Hillsboro High School, Nashville
Nichols, Rachel; Siegel High School, Murfreesboro
Nickels, Cooper; St. Andrew's Sewanee School, Sewanee
Ogburn, Keyia; Northwest High School, Clarksville
Park, Jun; Northwest High School, Clarksville
Phillips, Shanee; Northwest High School, Clarksville
Price, Susannah E.; School for Science and Math at Vanderbilt, Nashville
Rafter, Samuel; School for Science and Math at Vanderbilt, Nashville
Ramos, Chris; Northwest High School, Clarksville
Reynolds, Emma M.; Hillsboro High School, Nashville
Richardson, Forrest; Hillsboro High School, Nashville
Salazar, Efrain; School for Science and Math at Vanderbilt, Nashville
Schilling, Abigail; Northwest High School, Clarksville
Scott, Kamica; Kenwood High School, Clarksville
Sculley, Julia; Siegel High School, Murfreesboro

Seiber, Gracie; Northwest High School, Clarksville
Sharpe, Tyson Scott; Hillsboro High School, Nashville
Shi, Zaixing "Able"; School for Science and Math at Vanderbilt, Nashville
Shirkhodaie, Camron; School for Science and Math at Vanderbilt, Nashville
Simann, Nabil; Hillsboro High School, Nashville
Sipes, Tyler; Northwest High School, Clarksville
Smith, Sam; St. Andrew's Sewanee School, Sewanee
Taylor, Christian; St. Andrew's Sewanee School, Sewanee
Tettleton, Gray; School for Science and Math at Vanderbilt, Nashville
Thomas, Sam; St. Andrew's Sewanee School, Sewanee
Thome, Cooper; Central Magnet High School, Murfreesboro
Toler, Jill; Northwest High School, Clarksville
Ward, Charlotte; Cleveland High School, Clarksville
Wasim, Faris; Montgomery Bell Academy, Nashville
Way, Antwaun; Northwest High School, Clarksville
Webb, Christina; Siegel High School, Murfreesboro
Wiesen, Sarah. E; Hillsboro High School, Nashville
Wilson, Carleigh; Northwest High School, Clarksville
Wilson, Kyra; St. Andrew's Sewanee School, Sewanee
Yang, Yae Eun; School for Science and Math at Vanderbilt, Nashville
Yu, Haoran; Hillsboro High School, Nashville
Zapata, Shayna; Northwest High School, Clarksville

Papers of Excellence

Testing the Enzymatic Capacity of β-glucosidase

Samuel Rafter and Camron Shirkhodaie
School for Science and Math at Vanderbilt, Nashville

Abstract

The purpose of this experiment was to measure the enzymatic activity of β-glucosidase, an enzyme that breaks down disaccharides, in various mushroom species. This specific process is of interest because it is both the cost and time limiting step in the breakdown of cellulose and, by extension, the production of ethanol biofuel. Various mushrooms in Nashville, Tennessee were collected to extract the β-glucosidase. After these mushrooms were identified using field identification guides, they were processed in order to produce an aqueous extract containing the β-glucosidase enzyme for testing. The enzymatic activity over time was measured colorimetrically using an artificial substrate, and the concentration of product was determined from absorbance readings using a standard curve. Additional tests were run with an initial glucose concentration to see if glucose, which is the typical product of the reaction, would inhibit the reaction and to what degree at varying concentrations. It was discovered that the β-glucosidase of different mushroom species responded differently to glucose inhibition, indicating competitive inhibition. The β-glucosidases also had significant differences in their normal enzyme reaction. This means that the type of β-glucosidase used in the production of ethanol could have an impact on the efficiency of the process.

Introduction

The objective of this research project was to measure the enzymatic activity of β-glucosidase, an enzyme found in fungal species that hydrolyses disaccharides (Figure 1) (Pei, Pang, Zhao, Fan & Shi, 2012). β-glucosidase enzymes are of considerable interest to the scientific and biofuel manufacturing communities because they catalyze the time and cost-limiting step in the breakdown of cellulose from which biofuels are produced (Pei et al., 2012). Tests were run to measure the reaction progress over time and to see if an initial glucose concentration would inhibit the reaction and to what degree at varying concentrations. It was discovered that different species of mushrooms responded differently to this and had large differences in the base reaction rates of their β-glucosidase enzymes.

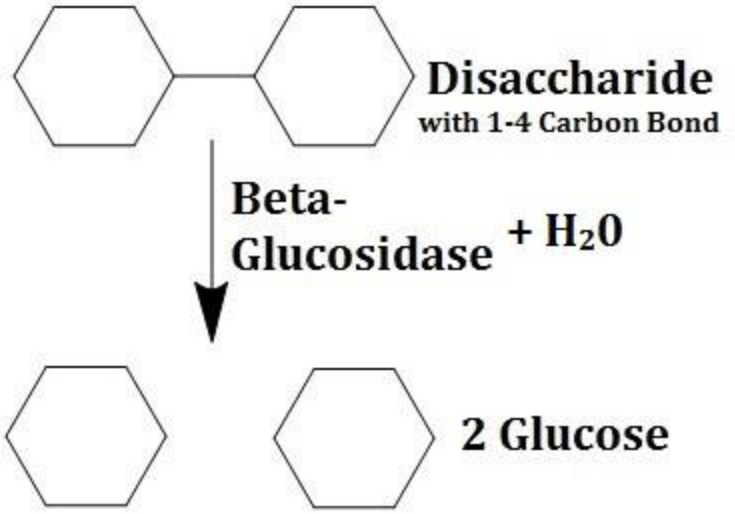

Figure 1: The reaction catalyzed by β-glucosidase enzymes in nature.

Methods

Collection and Identification

Fungi used in the experiment were collected at Vanderbilt University and Shelby Bottoms Park in Nashville, Tennessee, and identified using morphology characteristics and a field guide (McKnight & McKnight, 1987).

Enzyme Extraction

A sample of each collected mushroom was cut and measured for use in each experiment. First, 2g of the mushroom were used for the time progression tests and 5 g of the mushroom were used for the glucose inhibition tests. To the weighed sample of the mushroom, a number of milliliters equal to double the number of grams of sample was added (1g needs 2mL) of extraction buffer (solution of Tris, MgCl2, Triton X-100, pH 7.2, from Bio-Rad). Next, this solution was ground thoroughly until the mushroom sample was completely dispersed throughout. The solution was then centrifuged for two minutes at 11,000 rpm. Afterwards, the supernatant was taken out and collected. In order to produce the solution to be used for the experiments, 500μL of resuspension buffer (sodium acetate, pH 5.0) and 1mL of 1.5mM p-nitrophenol-glucosidase, an artificial substrate, was added to the solution with the supernatant. This substrate acts exactly like disaccharide in a natural environment. However, the differing

product, p-nitrophenol, creates a yellowish tint which is able to be quantified using a spectrophotometer set at 410nm wavelength.

Time Progression Tests

The production rate of the enzyme reactions could be measured by measuring the intensity of the yellow color. Time progression tests began when the substrate was added to the solution. At specified time intervals, the solution was taken and put into a cuvette containing stop solution (carbonate buffer, pH 9.5). The solution was then tested and measured for its product concentration based on the absorbance of the product.

Glucose Inhibition Tests

Glucose inhibition tests were done by adding starting concentrations of 0mM, 5mM, or 10mM glucose to the enzymatic reactions. These tests were carried out like the time tests to the extent that there were prepared stop solution cuvettes ready and samples were taken from the reaction and stopped at certain time intervals. The same controls were used. Controls for both experiments were used that contained resuspension buffer, p-nitrophenol, and stop solution. A correction value for the natural color of the enzyme was found by finding the absorbance value of the control. This value was subtracted from the absorbance at other time intervals. The amount of p-nitrophenol was quantified by using standards with a known concentration of the substrate. These standards were done at 0, 12.5, 25, 50, and 100 nM concentrations.

Results

Two of the mushrooms collected were identified to be *Trametes versicolor* and *Ganoderma lucidum*. Another one was unable to have its species identified; however, the genus of the mushroom was found to be *Bjerkandera*.

The results show significant variation ($p>.05$) in the capacity of the enzyme as it varies among mushrooms. *Trametes versicolor* had the highest activity and least glucose inhibition. The glucose-inhibition tests also showed that glucose inhibited the enzymatic reaction, supporting previous studies that had been done with other species of fungi (Chauve, Mathis, Huc, Casanave, Monot & Ferreira, 2010).

The left column of Fig 2 shows the time progress of each reaction, which was often

consistent and linear or logistic. In the *G. lucidum* test shown here, the concentration of product fluctuated erratically, which may have been due to error, but this is unlikely due to the constancy with which this happened during *G. lucidum* tests. The right column shows the comparison of simultaneous tests of reactions with various starting concentrations of glucose. The tests showed some inhibition, but the degree varied greatly between mushrooms.

Figure 2: *These graphs shows the concentration of p-nitrophenol (y-axis) over time (x-axis) for reactions involving each of the three species tested.*

Species	Time Progressions Tests (20 min)	Glucose Inhibition Tests (10 min)
G. lucidum	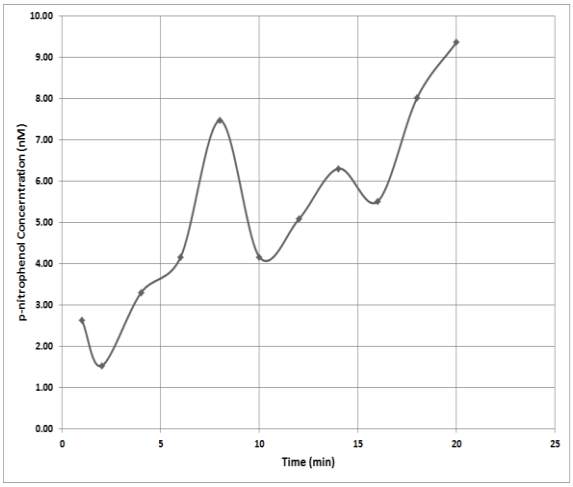	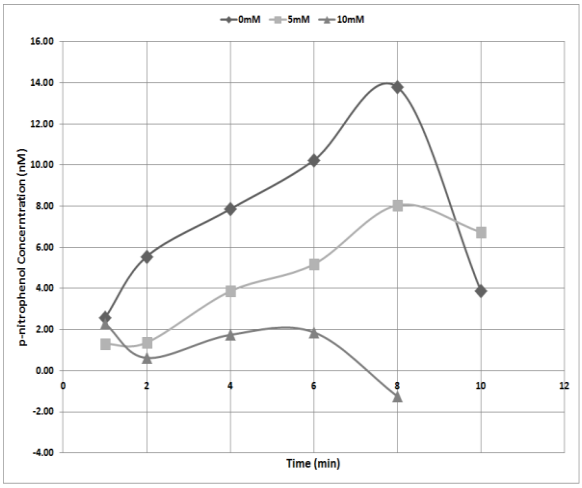
T. versicolor	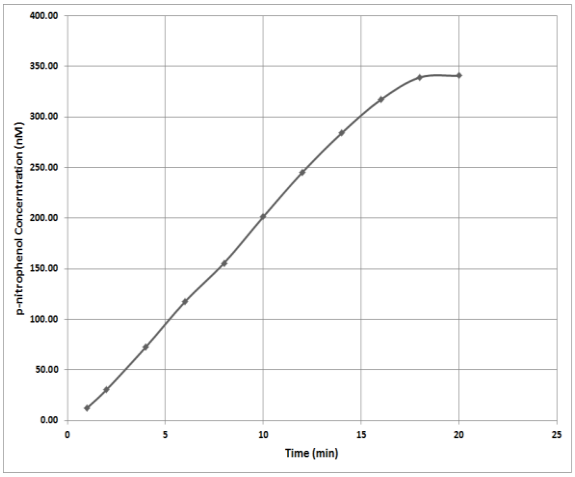	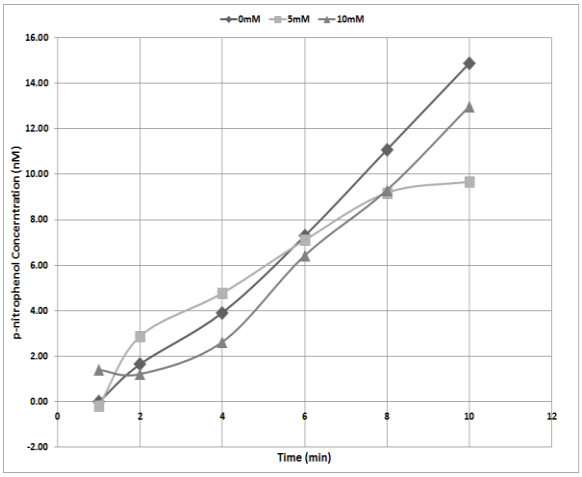

Bjerkandera	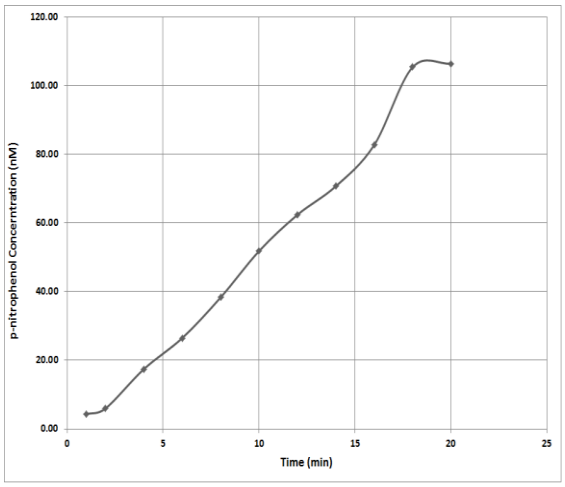	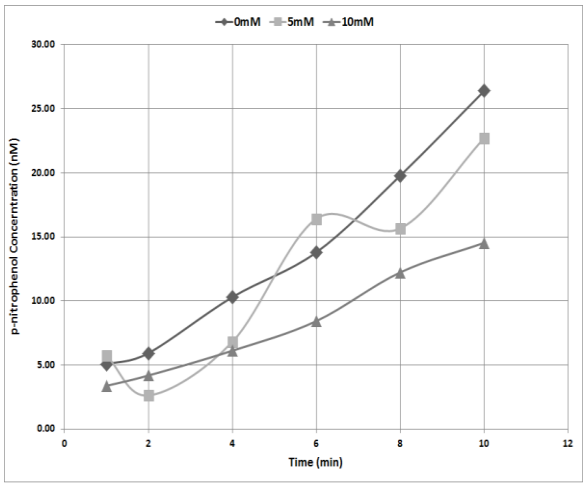

Conclusions

The data is valuable because it has shown the possibility of measuring the reaction progress and shown that glucose, a product found in abundance in the industrial process, does inhibit the desired reaction. It will also be necessary to produce an enzyme reaction model with an exact inhibition constant, which should also vary among mushrooms. This information will help those in industry which versions of the enzyme are better not only at catalyzing the reaction, but also which are better in higher concentrations of glucose, which could lead to the use of multiple versions of the enzyme for the optimal process. Testing β-glucosidase at various conditions with different temperature and pH level would help to find the optimal condition of the most active enzymes. Such a mixture of enzymes should also be tested to see if the enzymatic reaction is able to produce more of the product if it relies on multiple types of enzymes, which have the potential to do better at different stages of the reaction. Furthermore, sequencing the DNA of the β-glucosidase gene in species found to have useful enzymes will make producing the enzyme easier and allow a better understanding of how the enzyme works.

Acknowledgments

We would like to thank all of the instructors and students at the School for Science and Math at Vanderbilt for helping us during our project. In particular, we would like to thank Dr.

Angela Eeds, whose guidance during our project was crucial to our success. Finally, we would like to thank Dr. Jason Slot for helping us in identifying our collected mushrooms.

Literature Cited

Chauve, M., Mathis, H., Huc, D., Casanave, D., Monot, F., & Ferreira, N. L. (2010). Comparative kinetic analysis of two fungal β-glucosidases. *Biotechnology for Biofuels*, *3*(3), 3-10. doi: 10.1186/1754-6834-3-3

McKnight, K., & McKnight, V. (1987). *A Field Guide to Mushrooms*. New York: Houghton Mifflin Company.

Pei, J., Pang, Q., Zhao, L., Fan, S., & Shi, H. (2012). *Thermoanaerobacterium thermosaccharolyticum* β-glucosidase: a glucose-tolerant enzyme with high specific activity for cellobiose. *Biotechnology for Biofuels*, 5(31), 31-40. doi: 10.1186/1754-6834-5-31

Wang, B., & Xia, L. (2011). High efficient expression of cellobiase gene from *Aspergillus niger* in the cells of *Trichoderma reesei*. *Bioresource Technology*,*102*(6), 4568-4572. doi: 10.1016/j.biortech.2010.12.099

The Development of a Frog-logging Android Application

Valeria Garcia, Nhung Hoang, and Susannah E. Price
School for Science and Math at Vanderbilt, Nashville

Abstract

Frogs play a major role in the ecosystem as an environmental indicator, due to their semi-permeable skin, and as a predator of mosquitoes, the carriers of malaria. Although it is known that the populations of frog species are in overall decline, there is little data available to support the implementation of conservation acts for this endangered species. Currently, some parks and nature centers are using a method called frog-logging in an attempt to maintain a record of the frog population. However, this is a complex process that requires extensive training and experience. RibbID is an Android application created to increase the amount and reliability of frog-logging data by allowing people with little experience to identify frog calls through visual analysis instead of auditory analysis. The application was developed through the Eclipse IDE program, using JAVA and XML coding languages. It contains a database of waveform images depicting the calls of nine frog species found in Middle Tennessee, and provides a recording function that successfully translates audio tracks into visible waveforms, which the user visually compares to the database for identification. Overall, RibbID connects modern technology to the environmental crisis, in an attempt to subside its effects.

Introduction

Frogs play a major role in the ecosystem as an environmental indicator, due to their semi-permeable skin, and as a predator of mosquitoes, the carriers of malaria (Butler). Unfortunately, modern environmental changes, such as habitat destruction, have caused the worldwide frog population to decline at an alarming rate of 3.7% each year since 2002, endangering the delicate balance of the ecosystems in which they live (Butler). In order to prevent further population decline, it is necessary for conservation and protection acts to be established as soon as possible for the frogs, especially the species nearest to extinction. A significantly large amount of reliable population data must be collected in order to create and implement such acts, causing many methods of collecting frog population data to being developed within the recent years. Frog-logging is currently the most common process to be used in areas such as parks and nature centers. It occurs during the frogs' mating season, when the males croak constantly for attention from the females, and involves a herpetologist or naturalist with an expert level of training observing and keeping a written record of each detected frog species during the time period. He or she must be able to identify the frogs based on the unique frequencies of each call, as heard by

ear (Behler, Behler, Peeling & Peeling, 2008). Although frog-logging seems easy to implement, the data collection tends to be unreliable, as it depends heavily on the assumption that the frog-loggers were able to correctly identify all frog calls despite potential hearing subjectivity and background noise. Studies involving such date typically don't factor in the possible human errors. It is also difficult for large amounts of data to be collected since each frog-logging session must be conducted by a limited number of experienced professionals, reducing the possibility for volunteers to collect reliable data. This restricts the use of the rising number of citizen scientists and nature observers, two groups that would have a noticeable impact if they had a chance to work together as a team. This project consisted of developing an Android application, RibbID, as a more efficient and organized method of frog-logging. RibbID relies on visual comparisons of similar waveforms instead of audio identification and analysis, which broadens the range of people that can use it. The goal of RibbID is to serve as a user-friendly application that aids the frog-logging process, reduce the amount of training and experience required to collect population data, and increase the reliability of the data collected so that larger amounts of dependable data can be collected and analyzed. The collection of more reliable data will increase the likelihood of active conservation acts for frog species worldwide, thus calming an upset environmental balance.

Methods

Code Development

A simple user-interface plan was designed at the start of the project as the basis for development and regularly altered as the application criteria changed over time. The development of RibbID was conducted on the Eclipse IDE program. Android Developer was used as a guide for basic code writing in XML and Java, for the user-interface and implemented functions, respectively. Once a simple layout of RibbID was developed, open sources were accessed for adaption of code for complex functions. Each adapted code proceeded to go through a trial and error cycle, where it would be incorporated into RibbID to fit a specific function need, run through an emulator or Android device for testing, and then edited after an analysis of the errors noted by the Eclipse IDE program. Each set of code was repeatedly edited and tested until the function ran successfully. Open source codes were in the languages of Java and SQLite.

Audacity

It was not viable to collect frog calls from nature centers or parks, because the application was not ready for field tests, thus calls from the nine frogs were collected from online sources with minimal to no background noise ("Frog Sounds" & "Sing to Me"). Once the calls were collected, they were analyzed using Audacity, in order to determine the viability of a visual comparison conducted by the user. The calls were then recorded with RibbID to determine if the distinctive characteristics of the waveforms produced by the app correlated with those produced by Audacity.

Results

It was discovered through Audacity that the frog calls of the nine Middle Tennessee frog species, eight native and one non-native, were different enough that they could be identified visually as individuals. This resulted in RibbID becoming a manual visual analysis application, with the layout shown in Figure 1. RibbID is able to successfully record, playback, and store frog calls in an automatically created file folder within the phone. The application converts sound files, recorded in wav format and accessible from a directory list, into plotted waveforms. RibbID presents the generated waveform on an analysis screen that displays a database of the nine frog calls in waveform, which allows the user to perform a visual comparison. The analysis screen also provides a location textbox, the time and date of which the call was recorded, and a save button that stores all the information as a file. The waveform database generated by RibbID's audio recorder was compared to the frog calls recorded on Audacity to determine the application's ability to correctly record sound. RibbID's waveforms resembled Audacity's sufficiently to prove that the audio recorder function is viable, as shown in Figure 2.

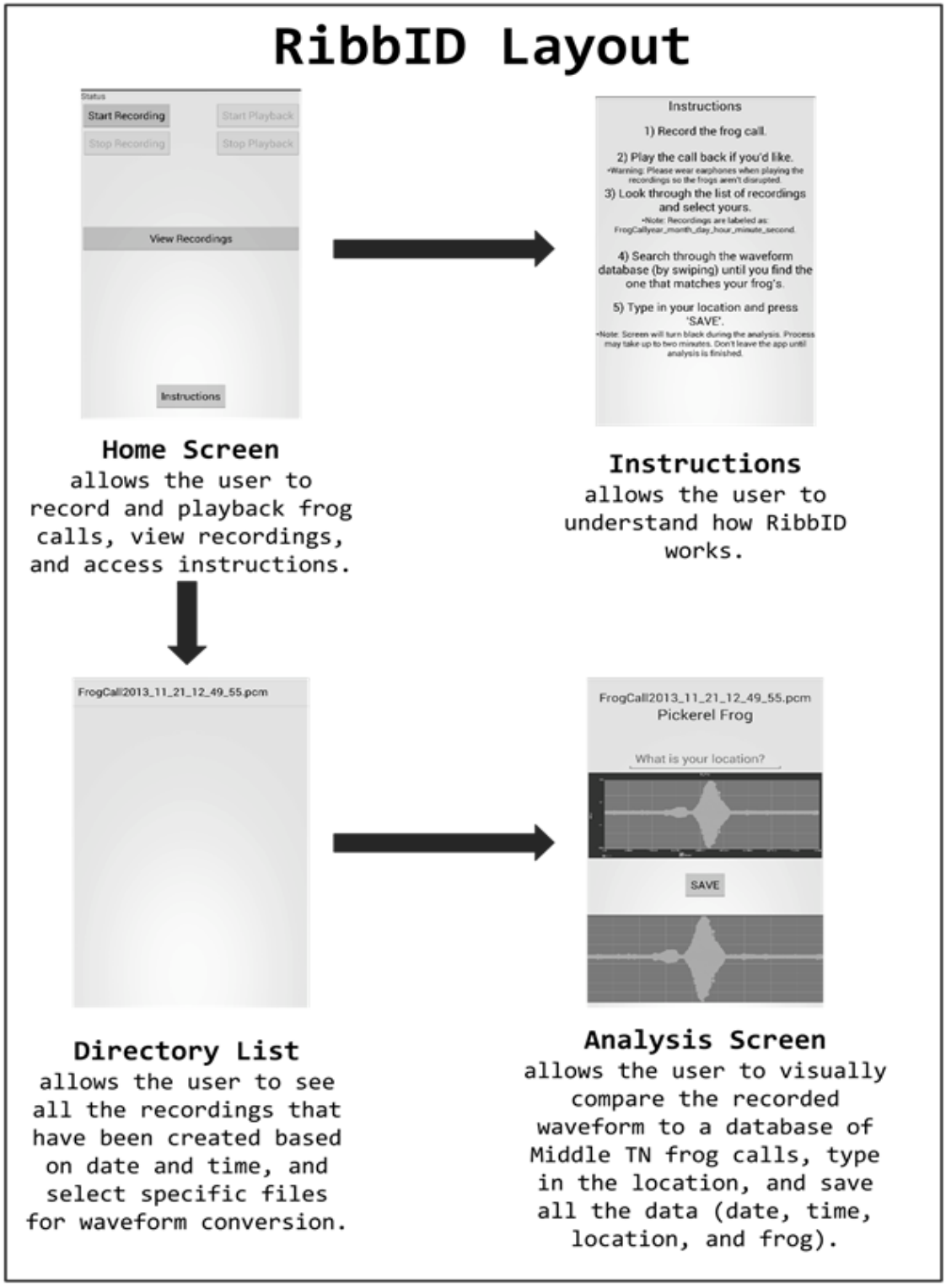

Figure 1 displays the interface layout of RibbID. The application is able to record and playback sound, as well as convert the recording into a visual waveform. The save function allows the recording and its information (time, date, location, and frog species) to be kept in one file.

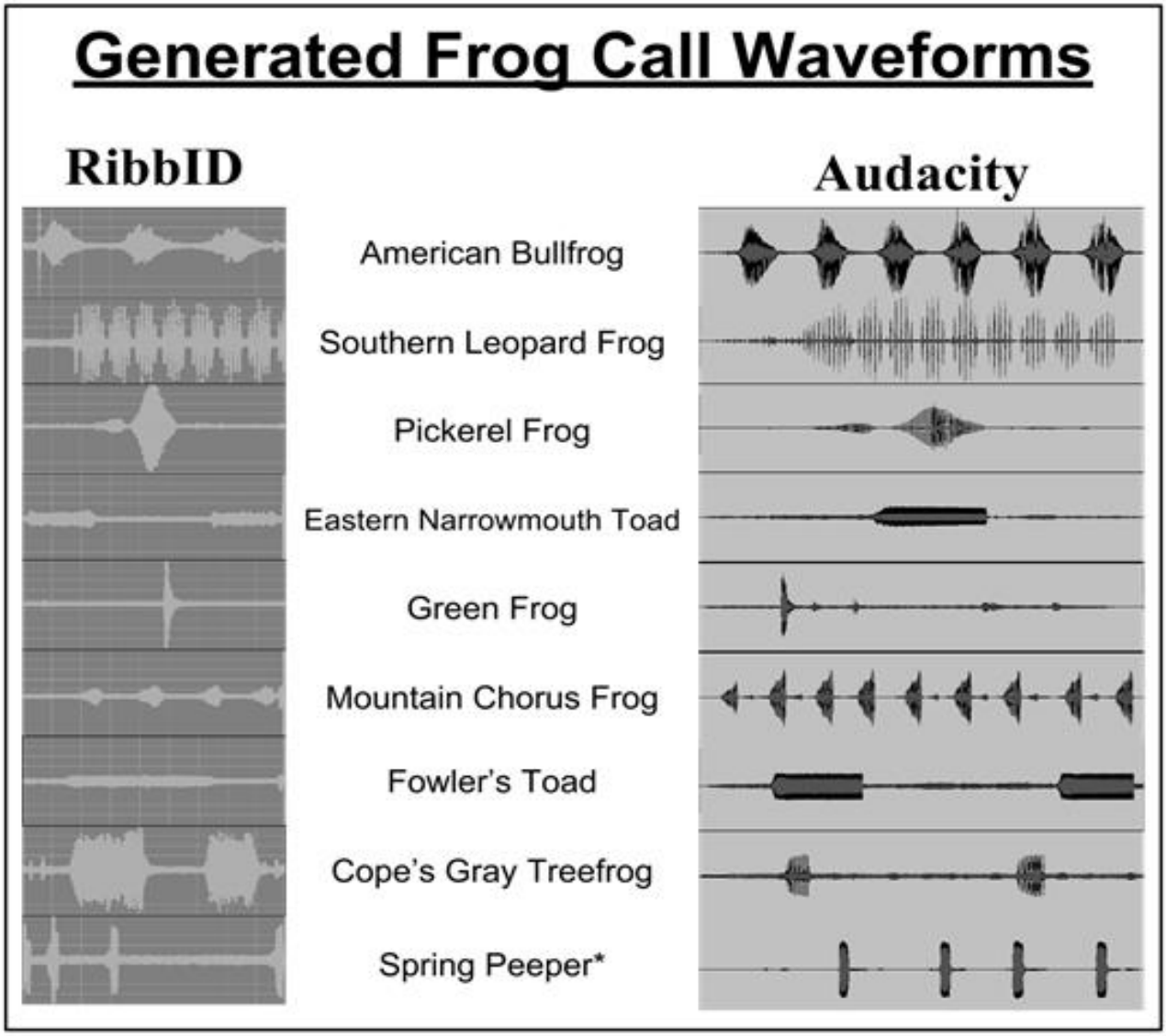

Figure 2 shows RibbID's ability to correctly record sound through a comparison with Audacity. Although not as detailed as Audacity's, the waveforms generated on RibbID are visually different enough from one another that they are feasible on the application.
*All of the frog species presented are native to Tennessee except for the Spring Peeper, which is native to North Carolina, but has been spotted in Middle Tennessee parks.

Conclusions

Currently RibbID relies on a visual analysis conducted by the user, which should be more reliable for inexperienced researchers than the current methods of frog-logging, but is still subjective. Future directions for RibbID involve incorporating automatic image analysis into the app so that it produces the most likely match for an audio file along with a confidence interval

for that match. The app will also require a method of analysis for overlapping frog calls, as the current version does not identify multiple calls within a recording. Following this refinement, field-testing must be done to evaluate the effectiveness of the app. We could expand the app to include frogs outside of Tennessee, in fact RibbID is now able to produce a waveform for the Spring Peeper wich is not native to Middle Tennessee. This demonstrates RibbID's ability for expansion by extending thewaveform database. Other limitations that should be addressed include distortion of the waveform because of background noise and the amount of memory taken up by the recordings. The background noise could possibly be addressed by recording baseline noise at the location to be subtracted from the calls. The memory issue has created an issue with phones that don't have a lot of available memory, because very few recordings can be taken. This could be addressed by editing the code so that RibbID converts the uncompressed Wav file into a compressed file after analysis.

A related study focused on techniques such as acoustic signaling, Hidden Markov models, and Fast Fourier Transform to filter recordings taken during the nights and identify the species and frequency of various cricket chirps and frog calls (Brandes, Naskrecki, & Figueroa, 2006). Although this study used high-powered computer software and microphones, the methods can be a reference point for writing analyses techniques into RibbID's code. Other applications have been created that analyze sound recordings, such as Shazam and iBird Pro ("Shazam," 2012& "ibird pro," 2013). Shazam identifies songs and provides information about them, based on the audio signatures found in recordings. iBird Pro has an audio identification component for bird calls to aid birders. Components of these apps can be used to determine the best way to incorporate analysis into the app itself.

RibbID currently records and saves audio files, which are then converted into waveforms. These waveforms can be compared visually to an internal database of frog calls heard in Middle Tennessee, to determine if the recorded audio is that of a call distinctive to one of Middle Tennessee's frog species, and if so the species can be identified. The app is unable to replace a trained frog-logger in its current form, but it can aid the analysis and identification of the calls and allow for confirmation of the species after the frog-logging session using the recordings. RibbID demonstrates the possibility of implementing technology such as android applications to aid frog-logging or similar studies, and provides a base for future frog-logging apps as well. The

usage of such technology can increase the reliability and frequency of recorded population data to improve the prospects for conservation of endangered frog species.

Acknowledgements

This project would not have been possible without the guidance and support of many people. First and foremost, we would like to thank Dr. Creamer for providing us with guidance and support throughout the project and Mr. Sterling, whose instruction involving code and app development was crucial to the creation of RibbID. We would also like to thank Dr. Loveless for her advice and assistance with the code and the background knowledge needed to develop the app. We would like to show our appreciation to Kim Bailey of Warner Parks in Nashville, Tennessee for teaching us about frog-logging and providing information that was essential to the project. Finally, we would like to express our gratitude to the School for Science and Math at Vanderbilt for providing us with the facilities and means necessary to develop RibbID.

Literature Cited

Brandes, T., Naskrecki, P., & Figueroa, H. (2006, November). Using image processing to detect and classify narrow-band cricket and frog calls.. Retrieved from http://www.ncbi.nlm.nih.gov/pubmed/17139751

Behler, J., Behler, D., Peeling, C., & Peeling, C. (2008).Frogs: A chorus of colors. (p. 135). New York City: Sterling Publishing Company Inc. Retrieved from http://books.google.com/books?id=QUf4_BxTUT4C&pg=PA135&lpg=PA135&dq=frog-logging description&source=bl&ots=GXTAevdQIL&sig=NIfIj40Xi7BZhldA7MskYs2ikb8&hl=en&sa=X&ei=CJygUvewOIrIkAec6YDwDA&ved=0CG4Q6AEwBw

Butler, R. (2007, April 16). Bad news for frogs; amphibian decline worse than feared global warming, not disease, may be the culprit this time. Retrieved from http://news.mongobay.com/2007/0416-frogs.html

Frog sounds. (n.d.). Retrieved from http://www.junglewalk.com/sound/frog-sounds-P4.htm

Sing to me baby! .ribbit!. (n.d.). Retrieved from http://www.junglewalk.com/popup.asp?type=a&AnimalAudioID=13915

Adams, M. (2013). Trends in amphibian occupancy in the United States. *PLoS One*, *8*(5), e64347. doi: 10.1371/journal.pone.0064347

The Age and Distance of the Open Cluster NGC 2126

Kayla Jenkins
Sullivan South High School, Kingsport

ABSTRACT

The open star cluster NGC 2126 was examined in order to determine its age and distance from the earth. The cluster was imaged with "B" and "V" photometric filters using the 0.9-meter SARA telescope at Kitt Peak, Arizona. NGC 2126 was found to lie at a distance of 2800 parsecs (9100 light years) from the earth and to have an age of about 21 million years, based on a Main-Sequence-Turn-Off point of stellar type B5. Few red stars were evident in the cluster.

INTRODUCTION

An open cluster is a group of stars-- all of the same age, all the same distance from the Earth, and all of similar chemical composition-- which are held together by gravity. Stars in a cluster have different masses, which makes them age at different rates (Dutton, 2014). It is thought that our solar system was once part of a large open cluster which dispersed over time (MacRobert, 2007). Determining the ages and distances of open clusters is important in understanding our own solar system, and others that may have formed under similar conditions.

Although it had been covered by previous studies, NGC 2126 was chosen because it had not been examined in this particular way before. It also was favorably located in the sky during the period that access to the telescope was available. Images of the cluster were acquired on the night of January 18, 2014, using a 1024 x 1024 pixel CCD camera attached to the 0.9-meter SARA telescope. SARA is the Southeastern Association for Research in Astronomy, which is a consortium of several southern US colleges and universities. SARA operates two telescopes: the 0.9-m SARA-North at Kitt Peak, Arizona, and the 0.6-m SARA-South at Cerro Tololo, Chile.

When the V filter magnitudes are subtracted from the B filter magnitudes, the stars' color-index can be determined. Light from objects in space travels through interstellar dust, making the stars appear both redder and dimmer than they actually are. Reddening for the cluster was 0.2, but the error was +/- 0.15 – which is very large given the size of the

measurement. Given the uncertainty in the actual reddening values, they were ignored in this study.

OBSERVATION AND DATA REDUCTION

The images of the cluster were taken through two photometric filters, B (blue) and V (green). The true colors of the stars, known as the color index, were determined using the equation,

B-V = color index of the star eq. 1

The data were reduced to account for hot pixels, cold pixels, and other instrumental issues that could influence the results. Hot pixels are pixels with excessive charge compared to the surrounding pixels, while cold pixels are less sensitive than the surrounding pixels or have no sensitivity at all (STSCI, 2013).

Ten images in the B filter, each 20 seconds long, were taken. These images were "stacked" in order to produce a single exposure equivalent to 200 seconds. Ten images in the V filter (10 seconds each) were taken as well. These images were also stacked, producing the equivalent of a single 100 second exposure. The computer program, *MaxImDL*, was then used to examine the stacked images. Using the photometry tool feature of the program, each labeled star (see Image 1) was examined. The numbering system of Cuffey (1942) was used.

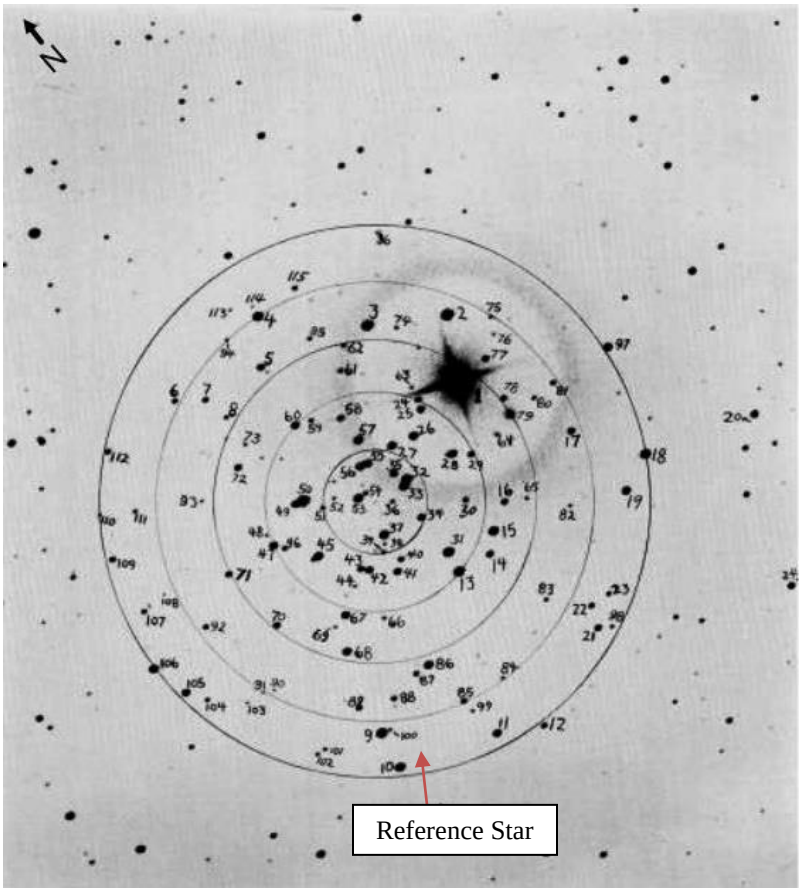

Image 1. *This image shows the cluster NGC 2126, the reference star pointed to by a small arrow in the lower left-hand corner. The brightest star in the image, star NGC 2126-1, was so bright that it saturated the CCD detector and its magnitude could not be measured. The magnitude values for this star were those published by the AAVSO.*

The brightness of each star was compared to that of a reference star. A reference star is a star whose brightness is known and to which the brightness of the target stars could be compared. Above is an image of the cluster in the V filter. The colors in image 1 were reversed so the stars were easier to examine.

Image 2. *NGC 2126 as seen in the night sky. Image by Peter Wienerroither.*

The reference star's brightness in the V filter was recorded as 15.320. Its brightness in the B filter was recorded as 12.025 (Simbad, 2014). The reference star is a known variable star, but its variation is small enough (about 0.08 mag.) that it would not impact the results. When each star was selected in the photometry tool, the computer compared it to the reference star's brightness. This data was then saved to a Microsoft Excel document, where it was examined.

After the data were analyzed, it was imported into the program *LoggerPro*. The graph produced by LoggerPro was then placed on top of a graph of the ZAMS (zero-age-main-sequence) line. A ZAMS line is a graph of a group of stars of all spectral types which have just entered the main sequence. A main sequence star is one that is fusing hydrogen into helium in its core.

Once a star's hydrogen has been used up, the star begins fusing heavier elements into still heavier ones. The star leaves the ZAMS line at this point and begins moving toward the upper

right-hand corner of the graph as it changes into a red giant (McGoodwin, 2012). By looking at the shared curve between the cluster data and the ZAMS line, the stellar age of the stars' which have left the main sequence becomes evident. Data points which move in that direction on the graph represent stars that are becoming red-giants who are burning themselves out with helium gases once all their hydrogen gasses are depleted. The curve will indicate at what age the stars use up their hydrogen, and this determines the age of the cluster as a whole.

Table 1

Sp. Type	O5	B0	A0	F0	G0	K0	M0
Mass (solar)	40	15	3.5	1.7	1.1	0.8	0.5
B – V	**-1.2**	**-0.3**	**0.0**	**0.3**	**0.6**	**0.8**	**1.4**
MS Lifetime	1.0×10^6	1.1×10^7	4.4×10^8	3.0×10^9	8.0×10^9	1.7×10^{10}	5.6×10^{10}

Table 1. *The relation between spectral type, the mass, B-V values, and a star's lifespan is shown here.*

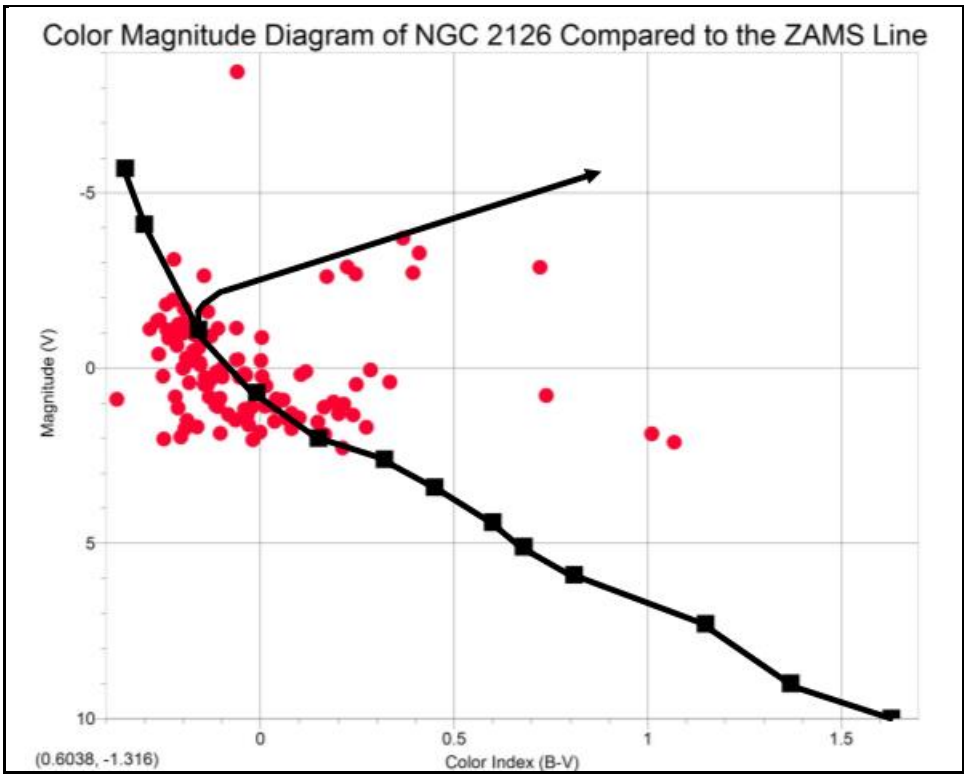

Image 3. *When a ZAMS line is overlaid upon a color-magnitude (H-R) diagram of the open cluster and the (B-V) axes aligned, the point where stars begin turning off of the main sequence can be established. This allows the age of the cluster to be estimated.*

ANALYSIS AND RESULTS

When searching for the reddening values of the cluster, the WEBDA listed the reddening value as 0.20. When applied to the data collected, the stars in the cluster registered far above the O-spectral type (they came out too blue). In cross-referencing the WEBDA information with a paper by Gaspar, et al. (2003), the reddening value was found to have large error bars, almost the size of the measurement itself (0.2 +/- 0.15). In light of this large uncertainty in the values, reddening was not applied to the stars in the cluster—further determination of the reddening values is needed and represents an area for further study.

Spectral types of stars are sorted into 7 categories from hot to cool (O, B, A, F, G, K, and M). One particular star in the image was very prominent. The star labeled as number 1 in Cuffey's numbering system was significantly brighter than any of the other stars in NGC 2126. Its brightness was such that MaximDL was unable to measure it (it had saturated the detector), B

and V values for it were obtained through the AAVSO (American Association of Variable Star Observers). Although first thought to just be a bright star, comparison to the rest of the cluster indicates that star 1 is not in the cluster at all, but rather is a foreground star. The B-V values were determined for all data collected, and the results showed that NGC 2126 is composed of many brighter B stars and also several A stars. Its O-type stars had already left the main sequence. Since most of the stars measured were type B, they are very hot and very young. B stars are blue-white stars at a temperature of anywhere between 10,000 and 30,000 kelvin (K). No cooler, fainter, redder stars were detected, in agreement with Cuffey (1943).

B-type stars are young, hot, and bright stars. However, the range of ages for B-type stars can be anywhere from 10,000,000 (B0) to 100,000,000 (B9) years old. NGC 2126 was determined to be approximately 21,000,000 years old. This marks it as a young cluster.

The distance to a star may be determined by comparing its true brightness (absolute magnitude) to its apparent brightness (apparent magnitude) according to the following equation:

$$d = 10^{(m - M + 5)) / 5} \qquad \text{eq.2}$$

Where, d=distance in parsecs, m= the star's apparent magnitude and M=the star's absolute magnitude

Using star NGC-2126-9 as the star closest to the ZAMS line turn-off produces a distance to the cluster of 2800 parsecs or about or about 9100 light years. This value is larger than that mentioned by Cuffey (1943) or Gaspar (2003).

DISCUSSION

By determining the age of NGC 2126, the relative ages of star clusters like it can also be estimated. NGC 2126 was determined to be approximately 21,000,000 years old. Absolute magnitude is the magnitude the star would have if it were placed at a distance of 10 parsecs from the Earth. Apparent magnitude of a star tells how bright that star appears at its great distance from Earth (Las Cumbres Observatory Global Telescope Network, 2012). The published values

of an analog to a star in the cluster were used. The star examined was a type B5, and by researching stars that are also in class B5, the absolute and apparent magnitudes of other stars in the same category should be the same. By applying equation 2, the cluster comes out to be 2800 parsecs from the Earth. This makes it 9100 light years away. The turn off in the ZAMS line (shown previously) indicates the cluster's young age and relative brightness.

SUMMARY

To conclude, this study determined the age of NGC 2126; which was around 21,000,000 years. The distance of NGC 2126 from the Earth was also determined to be 2800 parsecs 9100 light years). NGC 2126 is a young cluster composed mainly of B and A type stars. This was indicated by the turn off in the ZAMS line on the HR Diagram. It is a very bright and very blue cluster. In addition to the cluster's age and distance, additional aspects of NGC 2126 were discovered; including uncertainty in the reddening and dimming values. Star 1 was too bright to measure, stars 24 and 63 were too close to the bleed-through of star 1, star 79 was a "ghost" and not real (Cuffey, 1943).

ACKNOWLEDGEMENTS

I would like to thank Mr. Tom Rutherford for his aid and direction in this project, along with his patience and perseverance. Also, thanks to Dr. Gary Henson, East Tennessee State University, and SARA for providing the images of the cluster. Special thanks to Julie Vaughn, Secretarial Text Message Translator, and a big thank you to my friends and family for putting up with my rambling about star clusters every night for the past three months. Astronomy is a new adventure in my life that I will carry on into college and adulthood, and this project has only given me more inspiration to make that dream happen.

Literature Cited

Cuffey, James. (December 28, 1942). "The Galactic Clusters NGC 2126 and NGC 2194." Astrophysical Journal,: (93-97). NASA Astrophysics Data System.

Gaspar, A. (2003). "The First CCD Photometric Study of the Open Cluster NGC 2126." Astronomy & Astrophysics, 410, 879-885 (2003).

Palmer, Christopher. (2014). Measuring the Age of an Open Cluster. Penn State Department of Astronomy and Astrophysics. Retrieved February 2, 2014 from https://www.e-education.psu.edu/astro801/content/l7_p6.html.

JEB. (May 13, 2013). Stellar Ages from Middle Age to Death. The University of Oregon. Retrieved February 12, 2014 from http://pages.uoregon.edu/jimbrau/astr122/Notes/Chapter20.html.

MacRobert, Alan. "The Lives of Open Star Clusters." Sky and Telescope 113.3 (2007): 75.

Armstrong, J. D. "Absolute Magnitude." Los Cumbres Global Telescope Network. (2012). Retrieved February 17, 2014 from https://lcogt.net/spacebook/what- absolute-magnitude.

COSMOS - The SAO Encyclopedia of Astronomy › Z. (2014).Zero Age Main Sequence. Zero Main Age Sequence (ZAMS). February 23, 2014 from https://astronomy.swin.edu.au/cosmos/Z/Zero+Age+Main+Sequence

Space Telescope Science Institute/ NASA/ AURA (2014). "Hubble Space TelescopeHot and Cold Pixels." Retrieved January 30, 2014 from http://www.stsci.edu/hst/nicmos/performance/anomalies/hotcoldpix.html

WEBDA. Institute for Astronomy of the University of Vienna. "NGC 2126." Retrieved 04 September 2013 from http://www.univie.ac.at/webda/cgi-bin/ocl_page.cgi?dirname=ngc2126.

Nave, Carl R., (2014). HyperPhysics. Georgia State University. Stellar Spectral Types. Retrieved February 15, 2014 from http://hyperphysics.phy-astr.gsu.edu/hbase/starlog/staspe.html.

Larson, Ana. (2013). Astronomy 101A University of Washington. "Determining the Age of Star Clusters Using Color Magnitude Diagrams." http://www.astro.washington.edu/users/anamunn/Astro101/CoursePackPDFS/cp06b_ages_clusters_cmd.pdf

Southeastern Association for Research in Astronomy. (2014) SARA. Retrieved January 18, 2014 from http://saraobservatory.org/.

McGoodwin, Michael. (June 29, 2012). University of Washington. Stars, Galaxies,, and Beyond (page 45). Retrieved February 28, 2014 from http://www.mcgoodwin.net/pages/astrophysics_2012.pdf

American Association of Variable Star Observers. (2014) VSP. Chart 13243BFD. Retrieved January 27, 2014 from http://www.aavso.org/vsp/chart/compstar/.

Appendix 1: Data Table

Star ID	B	V	B-V
NGC-1	5.990	6.050	-0.060
NGC-2	11.165	10.797	0.368
NGC-3	11.626	11.216	0.410
NGC-4	12.067	11.821	0.246
NGC-5	13.756	13.915	-0.159
NGC-6	14.845	14.982	-0.137
NGC-7	14.707	14.835	-0.128
NGC-8	15.215	14.968	0.247
NGC-9	11.723	11.869	-0.146
NGC-10	12.179	11.785	0.394
NGC-11	13.382	13.552	-0.170
NGC-12	14.668	14.706	-0.038
NGC-13	11.843	11.619	0.224
NGC-14	14.196	14.353	-0.157
NGC-15	12.867	13.128	-0.261
NGC-16	15.238	14.904	0.334
NGC-17	14.305	14.506	-0.201
NGC-18	12.330	12.556	-0.226
NGC-19	13.360	13.595	-0.235
NGC-20	13.839	14.102	-0.263
NGC-21	14.206	14.268	-0.062
NGC-22	14.742	14.926	-0.184
NGC-23	15.447	15.563	-0.116
NGC-24	*	*	*
NGC-25	14.054	14.235	-0.181
NGC-26	13.042	13.216	-0.174
NGC-27	13.396	13.612	-0.216

NGC-28	13.300	13.362	-0.062
NGC-29	14.707	14.761	-0.054
NGC-30	15.293	15.406	-0.113
NGC-31	12.065	11.894	0.171
NGC-32	12.448	12.692	-0.244
NGC-33	12.892	13.159	-0.267
NGC-34	14.034	14.226	-0.192
NGC-35	14.413	14.512	-0.099
NGC-36	15.528	15.487	0.041
NGC-37	12.612	12.809	-0.197
NGC-38	16.082	15.843	0.239
NGC-39	15.602	15.591	0.011
NGC-40	14.719	14.602	0.117
NGC-41	13.844	14.018	-0.174
NGC-42	13.631	13.628	0.003
NGC-43	14.258	14.414	-0.156
NGC-44	15.719	15.757	-0.038
NGC-45	12.757	12.893	-0.136
NGC-46	14.843	14.559	0.284
NGC-47	13.307	13.506	-0.199
NGC-48	16.021	15.921	0.100
NGC-49	13.287	13.496	-0.209
NGC-50	11.177	11.401	-0.224
NGC-51	17.394	16.383	1.011
NGC-52	16.260	16.364	-0.104
NGC-53	13.006	13.206	-0.200
NGC-54	15.640	15.681	-0.041
NGC-55	13.462	13.590	-0.128
NGC-56	13.176	13.418	-0.242
NGC-57	13.413	13.650	-0.237

NGC-58	14.499	14.613	-0.114
NGC-59	15.662	15.474	0.188
NGC-60	13.644	13.860	-0.216
NGC-61	15.426	15.385	0.041
NGC-62	15.748	15.533	0.215
NGC-63	*	*	*
NGC-64	15.821	15.864	-0.043
NGC-65	17.69	16.621	1.069
NGC-66	15.748	15.831	-0.083
NGC-67	13.317	13.546	-0.229
NGC-68	13.129	13.347	-0.218
NGC-69	16.189	16.041	0.148
NGC-70	14.116	14.297	-0.181
NGC-71	14.199	14.257	-0.058
NGC-72	13.85	14.018	-0.168
NGC-73	16.019	16.183	-0.164
NGC-74	16.037	16.232	-0.195
NGC-75	16.092	16.123	-0.031
NGC-76	16.565	16.399	0.166
NGC-77	14.479	14.731	-0.252
NGC-78	15.026	15.012	0.014
NGC-79	ghost	ghost	ghost
NGC-80	15.816	15.850	-0.034
NGC-81	15.259	15.364	-0.105
NGC-82	16.311	16.231	0.080
NGC-83	15.598	15.621	-0.023
NGC-84	15.919	15.984	-0.065
NGC-85	14.623	14.664	-0.041
NGC-86	13.049	13.261	-0.212
NGC-87	14.795	14.691	0.104

NGC-88	14.652	14.751	-0.099
NGC-89	14.296	14.295	0.001
NGC-90	16.279	16.529	-0.250
NGC-91	16.468	16.195	0.273
NGC-92	14.627	14.770	-0.143
NGC-93	16.012	15.944	0.068
NGC-94	16.007	15.805	0.202
NGC-95	15.807	15.997	-0.190
NGC-96	15.424	15.637	-0.213
NGC-97	13.104	13.390	-0.286
NGC-98	15.880	15.800	0.080
NGC-99	15.785	15.621	0.164
NGC-100	16.026	15.288	0.738
NGC-101	15.489	15.599	-0.110
NGC-102	15.626	15.590	0.036
NGC-103	16.062	16.026	0.036
NGC-104	15.193	15.326	-0.133
NGC-105	13.268	13.378	-0.110
NGC-106	12.351	11.629	0.722
NGC-107	14.749	14.745	0.004
NGC-108	16.531	16.551	-0.020
NGC-109	14.304	14.503	-0.199
NGC-110	16.262	16.468	-0.206
NGC-111	15.475	15.416	0.059
NGC-112	14.826	14.971	-0.145
NGC-113	16.330	16.331	-0.001
NGC-114	16.994	16.782	0.212
NGC-115	15.027	15.398	-0.371
NGC-116	15.100	15.320	-0.220

Sequencing of IL-6Ra to Identify a Potential Cleavage Site for sIL-6Rα Trans-Signaling in Glaucoma

Emma Kingsbury
Hillsboro High School, Nashville

Abstract

The two major risk factors associated with glaucoma are age and elevated intraocular pressure (IOP), which is the only modifiable risk factor. Interleukin-6 (IL-6) is a cytokine that is produced in response to elevated IOP and can be either neuroprotective or neurodestructive for RGCs. Classical and trans-signaling could result in different effects of the IL-6Rα signaling on RGCs. Different forms of IL-6Rα, products of cleavage, have been show to exist in the human retina, but they have yet to be identified in mouse retina. A protein isolation technique was developed to isolate the IL-6Rα in mice retina so a potential cleavage site could be identified.

Introduction

Glaucoma, the second leading cause of blindness worldwide, is characterized by the progressive degeneration of retinal ganglion cells (RGCs) and their axons, which form the optic nerve. Interleukin-6 (IL-6) is a cytokine that is produced in response to elevated IOP and can be both neuroprotective and neurodestructive for RGCs in glaucoma. Classical signaling and trans-signaling are two possible circumstances that could result in different IL-6 signaling outcomes within the retina. IL-6Ra is expressed by RGCs and endothelial cells in the vasculature (Sims et al., 2012). As such, RGCs and endothelial cells are likely targets of classical pathway for IL-6 signaling. Classical signaling occurs via interactions between glycoprotein 130 (gp130) and the membrane bound form of IL-6 receptor alpha (IL-6Rα), which can produce both pro- or anti-inflammatory effects. Trans-signaling occurs when a soluble form of the IL-6Rα (sIL-6Rα) binds to IL-6 extracellularly. This IL-6 signaling pathway can both alter the classical signaling pathway and confer IL-6 sensitivity to any cell expressing gp130. Astrocytes and Müller glia express gp130 and as such, are potential targets for IL-6 trans-signaling (Echevarria et al., 2013). RGCs and vasculature could also experience IL-6 trans-signaling in addition to classical signaling. In humans, sIL-6R is formed by both de novo synthesis and cleavage of IL-6Rα, but thus far, only de novo synthesis has been linked to the sIL-6R formation in mice. There is evidence that shows the presence of three forms of IL-6Rα, suggesting that the sIL-6Fα is produced by cleavage in mouse. The Sappingon laboratory's recent work suggests that: 1)

elevated IOP may induce IL-6 trans-signaling and 2) that sIL-6Rα may be formed by proteolytic cleavage of membrane-bound IL-6Rα (Sappington et al 2009). Preliminary work was performed with recombinant IL-6Rα in order to identify the potential cleavage site in mouse, but the recombinant protein was incomplete and lacked the c-terminus. In the human form of IL-6Rα, the cleavage site is present in the c-terminus, and it is suspected that the cleavage site in mouse would be located on a similar site on the receptor. A protein isolation method was developed so that the presence of sIL-6Rα in retina from mice with experimentally-induced glaucoma was confirmed, and possible cleavage sites in IL-6Rα could be identified and sequenced using mass spectrometry.

Materials and Methods

Protein Extraction

To isolate proteins for purification and mass spectrometry analysis, all proteins were first extracted from brain and retina of C57Bl/6 mice. Extraction of both the GFAP and IL-6Rα was performed using brain tissue and retinal tissue from mice. Five mL Radioimmuno precipitation assay (RIPA) buffer and a protease cocktail (12.5mg of sodium (Na) deoxycholate, PMSF dissolved in ethanol (EtOH), protease inhibitor cocktail, and phosphate inhibitor) solution was made. The tissue was acquired and 1.5mL RIPA buffer/protease cocktail solution was added to the tissue, which was homogenized using an ultrasonificator. The tissue was incubated on ice for 30 minutes after which 15µL SDS was added to the solution creating a total volume of 0.1% SDS. The sample was then centrifuged for 15 minutes at 14,000 RPM at 4°C. The supernatant was collected and transferred to centrifuge tubes and stored at 4°C. The pellets were discarded.

BCA Protein Assay

BCA protein assays were utilized to determine the amount of total protein present in samples isolated from brain and retina of C57Bl/6 mice. 16µL of both the RIPA buffer and extracted protein sample were pipetted into a centrifuge tube. 40µL of the RIPA buffer was pipetted in wells S_1 to S_7 of a 96 well plate. 80µL of albumin standard was pipetted into S_1, and then 40µL was pipetted out of S_1 and put in S_2. This continued until 40µL from S_5 was pipetted into S_6. 10µL of the extracted protein sample was pipetted in the first three wells of the row beneath the S_1-S_7 wells.

A working solution was made by combining 200µL of Reagent B with 10mL of Reagent A. 200µL of this working solution was pipetted into each well, and the plate was shaken for 30

seconds. The plate was then incubated at 37°C for 30 minutes. The absorbance at 562 nm was recorded using a UV-Vis spectrometry using SOFTmax PRO software.

Protein Isolation

Four hundred μL of protein sample collected from the tissue was pipetted into a centrifuge tube, to which a 1:10 dilution of the 1° antibody was added (either GFAP or IL-6Rα). This was incubated for 30 minutes at 4°C. 100μL of μMACS streptavidin microbeads was added to the sample, which bind instantly to the primary antibody.

A column was placed in a magnetic holder, and rinsed with 100μL of protein equilibration buffer. The column was then rinsed twice with 100μL of Tris (40mM). The extracted protein sample was run through the column, and the run-through was collected. Subsequent washes with 100 mL of Tris were also collected. The sample was eluted using 150μL of the appropriate elution buffer provided in the μMACS Strepavidin Kit. The eluted protein was stored at -20°C.

Western Blot

Western blotting techniques were used to determine whether or not the isolated protein was the intended protein, GFAP or IL-6Rα. 27.8 μL of the isolated protein sample and the collected washes were pipetted into a centrifuge tube. 9.25μL of 4x Loading Dye was added to each centrifuge tube. The samples were incubated for 10 minutes at 70°C in a dry bath. A Criterion Precast 4-20% Tris-HCl gel's wells were flushed with running buffer (100mL Tris/Glycine/SDS buffer and 900mL ddH_2O) to clear the wells. The gel was placed in a electrophoresis apparatus, and running buffer was poured into the chambers on either side of the gel to the fill line. 15μL of ladder was pipetted into wells 1 and 5. 35μL of the extracted protein sample and each wash was pipetted into the remaining wells.

The gel was run for 10 minutes at 100 volts, and then the voltage was increased to 150 V and the gel ran until the bands could be resolved (approximately 45 minutes).

A PVDF membrane was prepared and washed in methanol for 30 seconds. It was washed in ddH_2O for 2 minutes and 10 minutes in transfer buffer (200mL methanol, 200mL 10x Tris/CAPS buffer, and 1600mL ddH_2O). The sponges and filter paper were soaked in cold transfer buffer. The gel was removed from the apparatus and soaked in cold transfer buffer for 5 minutes.

The gel holder was set up, and the bubbles were removed from the holder, and the gel was placed in the blotting apparatus. An ice pack was placed in the apparatus with transfer buffer to the fill line, and it a voltage of 100 V was applied for 1 hour on a stirring plate. The gel was washed for 5 minutes in ddH_2O and then washed in a total protein stain (Coomassie blue or Ponceau S).

The membrane was washed in washing buffer for 5 minutes (100mL 10x PBS, 500mL Tween 20, 900mL ddH_2O). A milk blocking solution was made: 10g nonfat milk powder, 200mL washing buffer. 80µL of the primary antibody was added to 19.92mL of milk blocking solution. This was added to the membrane and gently stirred on a stir plate overnight at 4°C.

The membrane was washed four times with washing buffer for 15 minutes each time. The secondary antibody was made in a 1:1000 dilution in 15 mL of milk solution, added, and shaken at room temperature for 1 hour. The membrane was washed 4 times for 15 minutes each time in washing buffer after the 2° antibody was removed. The membrane was imaged using the LICOR Odyssey.

Results

Preliminary Mass Spectrometry Digestion Conditions used for Recombinant IL-6Rα Sequencing

Table 1: Shows all of the previously tested mass spectrometry digestion conditions that were utilized to try and sequence the recombinant for of the IL-6Rα. However, the recombinant form of the receptor was incomplete and lacked the c-terminus, where the potential cleavage site was thought to be located, so the percent coverage found is not an accurate representation of the percent sequenced. The final total coverage, was 72%, but had been closer to 95% when taking into account the missing c-terminus. These conditions can be utilized for isolated IL-6Rα in retinal tissue from C57Bl/6 mice. Mass spectrometry involves the digestion of proteins to small peptides that are then identified by mass to charge ratio. The more proteins that are in your sample, the harder it is to align the peptide sequences into the full-length protein sequence of your target protein-- IL-6Ra. This is especially true for low abundant proteins, like IL-6Ra, which could be easily overwhelmed by peptides from more abundant proteins.

Table 1

Digestion Enzyme	**Coverage**
AspN 15%	MLTVGCTLLVALLAAPAVALVLGSCRALEVANGTVTSLPGATVTLICPGKEA AGNVTIHWVYSGSQNREWTTTGNTLVLRDVQLSDTGDYLCSLNDHLVGTV PLLVDVPPEEPKLSCFRKNPLVNAICEWRPSSTPSPTTKAVLFAKKINTTNG KSDFQVPCQYSQQLKSFSCQVEILEGDKVYHIVSLCVANSVGSKSSHNEAFH SLKMVQPDPPANLVVSAIPGRPRWLKVSWQHPETWDPSYYLLQFQLRYRP VWSKEFTVLLLPVAQYQCVIHDALRGVKHVVQVRGKEELDLGQWSEWSPE VTGTPWIAEPRTTPAGILWNPTQVSVEDSANHEDQYESSTEATSVLAPVQE SSSMSLPTFLVAGGSLAFGLLLCVFIILRLKQKWKSEAEKESKTTSPPPPPYS LGPLKPTFLLVPLLTPHSSGSDNTVNHSCLGVRDAQSPYDNSNRDYLFPR
Chymotrypsin 38%	MLTVGCTLLVALLAAPAVALVLGSCRALEVANGTVTSLPGATVTLICPGKEA AGNVTIHWVYSGSQNREWTTTGNTLVLRDVQLSDTGDYLCSLNDHLVGTV PLLVDVPPEEPKLSCFRKNPLVNAICEWRPSSTPSPTTKAVLFAKKINTTNG KSDFQVPCQYSQQLKSFSCQVEILEGDKVYHIVSLCVANSVGSKSSHNEAFH SLKMVQPDPPANLVVSAIPGRPRWLKVSWQHPETWDPSYYLLQFQLRYRP VWSKEFTVLLLPVAQYQCVIHDALRGVKHVVQVRGKEELDLGQWSEWSPE VTGTPWIAEPRTTPAGILWNPTQVSVEDSANHEDQYESSTEATSVLAPVQE SSSMSLPTFLVAGGSLAFGLLLCVFIILRLKQKWKSEAEKESKTTSPPPPPYS LGPLKPTFLLVPLLTPHSSGSDNTVNHSCLGVRDAQSPYDNSNRDYLFPR
Trypsin 47%	MLTVGCTLLVALLAAPAVALVLGSCRALEVANGTVTSLPGATVTLICPGKEA AGNVTIHWVYSGSQNREWTTTGNTLVLRDVQLSDTGDYLCSLNDHLVGTV PLLVDVPPEEPKLSCFRKNPLVNAICEWRPSSTPSPTTKAVLFAKKINTTNG KSDFQVPCQYSQQLKSFSCQVEILEGDKVYHIVSLCVANSVGSKSSHNEAFH SLKMVQPDPPANLVVSAIPGRPRWLKVSWQHPETWDPSYYLLQFQLRYRP VWSKEFTVLLLPVAQYQCVIHDALRGVKHVVQVRGKEELDLGQWSEWSPE VTGTPWIAEPRTTPAGILWNPTQVSVEDSANHEDQYESSTEATSVLAPVQE SSSMSLPTFLVAGGSLAFGLLLCVFIILRLKQKWKSEAEKESKTTSPPPPPYS LGPLKPTFLLVPLLTPHSSGSDNTVNHSCLGVRDAQSPYDNSNRDYLFPR
Asp N 56% Coverage	mltvgctllvallaapavaLVLGSCRALEVAngtvtslpgatvtlicpgkeaagnvtihwvysg SQNREWTTTGNTLVLRdvqlsDTGDYLCSLNDHLVGTVPLLVDVPPEEPKLS CFRKNPLVNAICEWRPSSTPSPTTKavlfakkinttngkSDFQVPCQYSQQLKSF SCQVEILEGDKVYHIVSLCVANSVGSKSSHNEAFHSLKmvqpdPPANLVVSAI PGRPRwlkVSWQHPETWDPSYYLLQFQLRyrpvwskeftvlLLPVAQYQCVIH DALRGVKHVVQVRGKEELDLGQWSEWSPEVTGTPWIAeprTTPAGILWNP TQVSVEdsanheDQYESSTEATSVLAPVQesssmslptflvaggslafglllcvfiilrlkqk wkseaekesktttsppppppyslgplkptfllvplltphssgsdntvnhsclgvrdaqspydnsnrd ylfpr
Chymo 53% Coverage	mltvgctllvallaapavaLVLGSCrALEVANGTVTSLPGATVTLicpgkEAAGNVTI HWvySGSQNREWTTTGNTLVLRDVQLSDTGDYLCSLNDHLVGTVPLLVDV PPEEPKlscfrKNPLVNAICEWRPSSTPSPTTKavlfakkinttngkSDFQVPCQYS QQLKSFSCQVEILEGDKVYHIVSLCVANSVGSKSSHNEAFHSLKMVQPDPPA NLVVSAIPGRPRwlkVSWQHPETWDPSYYllqfqlryrpvwskEFTVLLLPVAQ YQCVIHDALRgvkHVVQVRGKEELDLGQWSEWSPEVTGTPWiaeprttpagil wnptqvsvedsanhedqyessteatsvlapvqesssmslptflvaggslafglllcvfiilrlkqkw kseaekesktttsppppppyslgplkptfllvplltphssgsdntvnhsclgvrdaqspydnsnrdyl fpr
Tp 60% Coverage	mltvgctllvallaapavaLVLGSCrALEVANGTVTSLPGATVTLICPGKEAAGNVT IHWVYSGSQNREWTTTGNTLVLRDVQLSDTGDYLCSLNDHLVGTVPLLVD VPPEEPKlscFRKNPLVNAICEWRPSSTPSPTTKAVLFAkkinttnGKSDFQVP CQYSQQLKSFSCQVEILEGDKVYHIVSLCVANSVGSKSSHNEAFHSLKMVQP DPPANLVVSAIPGRPRwlkVSWQHPETWDPSYYLLQFQLRyrpvwskEFTVL LLPVAQYQCVIHDALRGVKHVVQVRGKEELDLGQWSEWSPEVTGTPWIAE

	PRttpagilwnptqvsvedsanhedqyessteatsvlapvqesssmslptflvaggslafglllcvf iilrlkqkwkseaekeskttsppppyslgplkptfllvplltphssgsdntvnhsclgvrdaqspy dnsnrdylfpr
Tp/AspN 66% Coverage	mltvgctllvallaapavaLVLGSCrALEVANGTVTSLPGATVTLICPGKEAAGNVT IHWVYSGSQNREWTTTGNTLVLRDVQLSDTGDYLCSLNDHLVGTVPLLVD VPPEEPKlscfrKNPLVNAICEWRPSSTPSPTTKavlfakkinttnGKSDFQVPCQ YSQQLKSFSCQVEILEGDKVYHIVSLCVANSVGSKSSHNEAFHSLKmvqpDP PANLVVSAIPGRPRwlKVSWQHPETWDPSYYLLQFQLRYRPVWSKEFTVLL LPVAQYQCVIHDALRGVKHVVQVRgkeelDLGQWSEWSPEVTGTPWIAEPR TTPAGILWNPTQVSVEdsanheDQYESSTEATSVLAPVQesssmslptflvaggsla fglllcvfiilrlkqkwkseaekeskttsppppyslgplkptfllvplltphssgsdntvnhsclgvr daqspydnsnrdylfpr	
Glu C 71% Coverage	mltvgctllvallaapavaLVLGSCRALEVANGTVTSLPGATVTLICPGKEAAGNVT IHWVYSGSQNREWTTTGNTLVLRDVQLSDTGDYLCSLNDHLVGTVPLLVD VPPEEPKLSCFRKNPLVNAICEWRPSSTPSPTTKAVLFAKkinttngkSDFQVP CQYSQQLKSFSCQVEILEGDKVYHIVSLCVANSVGSKSSHNEAFHSLKMVQP DPPANLVVSAIPGRPRWLKVSWQHPETWDPSYYLLQFQLRYRPVWSKEFT VLLLPVAQYQCVIHDALRGVKHVVQVRGKEELDLGQWSEWSPEVTGTPWI AEPRTTPAGILWNPTQVSVEDSANHEDQYEsteATSVLAPVQEsssmslptflv aggslafglllcvfiilrlkqkwkseaekeskttsppppyslgplkptfllvplltphssgsdntvnh sclgvrdaqspydnsnrdylfpr

Total Coverage:

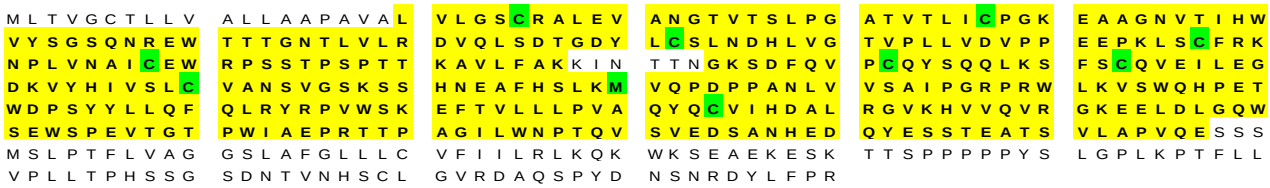

Trial One

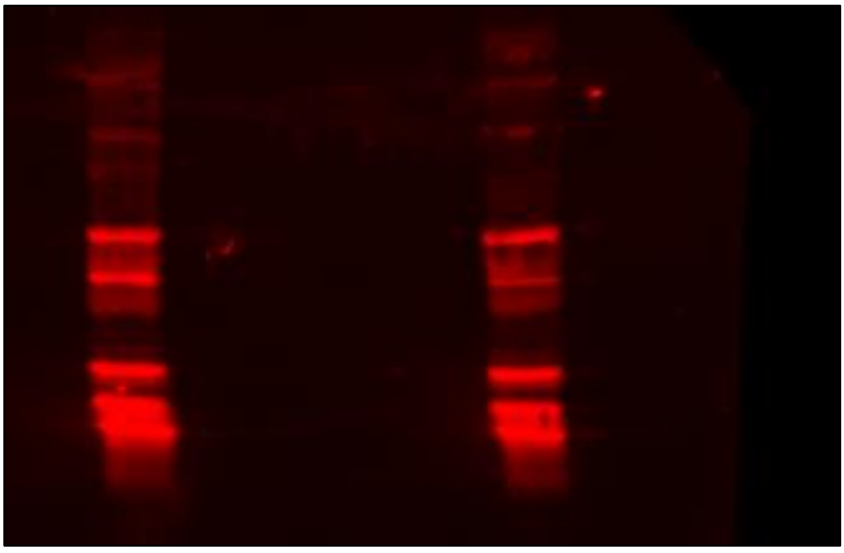

Figure 1: Western Blot Analysis of GFAP from Brain Lysate: Trial one was completed by isolating GFAP from brain lysate. Only the ladders appear in the imaged membrane, with all of the other lanes appearing empty. This shows that no GFAP was detected by the Western Blot.

Trial Two

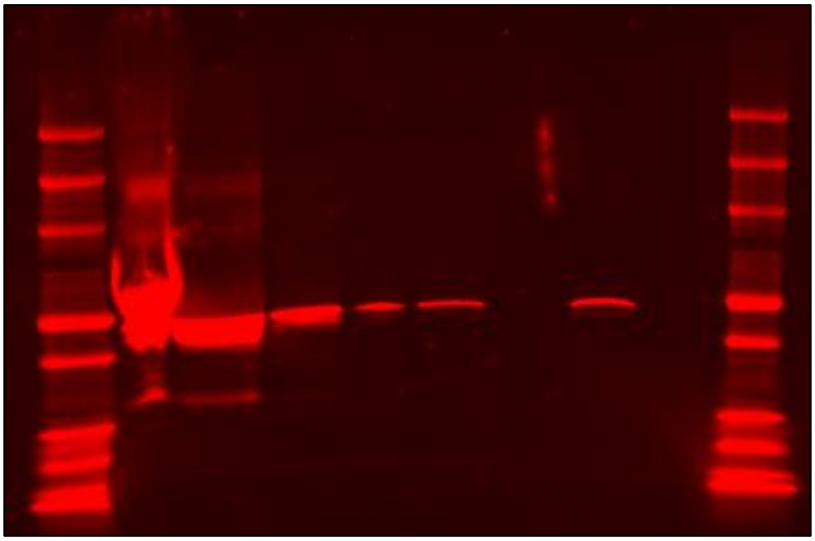

Figure 2: Western Blot of GFAP from Brain Lysate: shows the PVDF membrane with GFAP proteins lighting up. The first lane is the ladder, lanes two through 6 are: initial flow through, wash 1, wash 2, wash 3, and wash 4. Lane 8 contains the isolated GFAP protein eluted in tris. Finally, the last lane is an additional ladder.

Trail 2 Continued

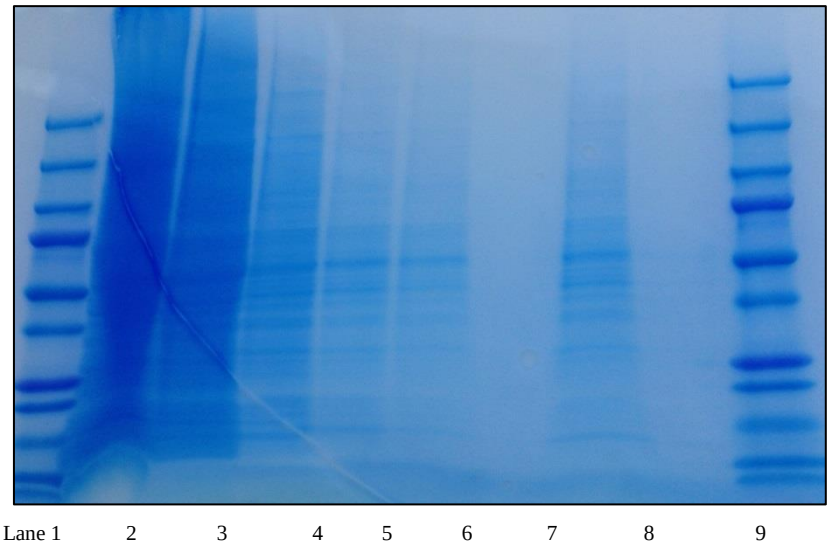

Figure 3: Gel of GFAP from Brain Lysate: shows a gel of brain lysate that ran through a µMACS column. This is the same samples as the membrane in figure 1 shows, but this gel has been stained with Coomassie Blue. The isolated protein was GFAP. All of the washes are shown in lanes 2 through 6.

Trial 3

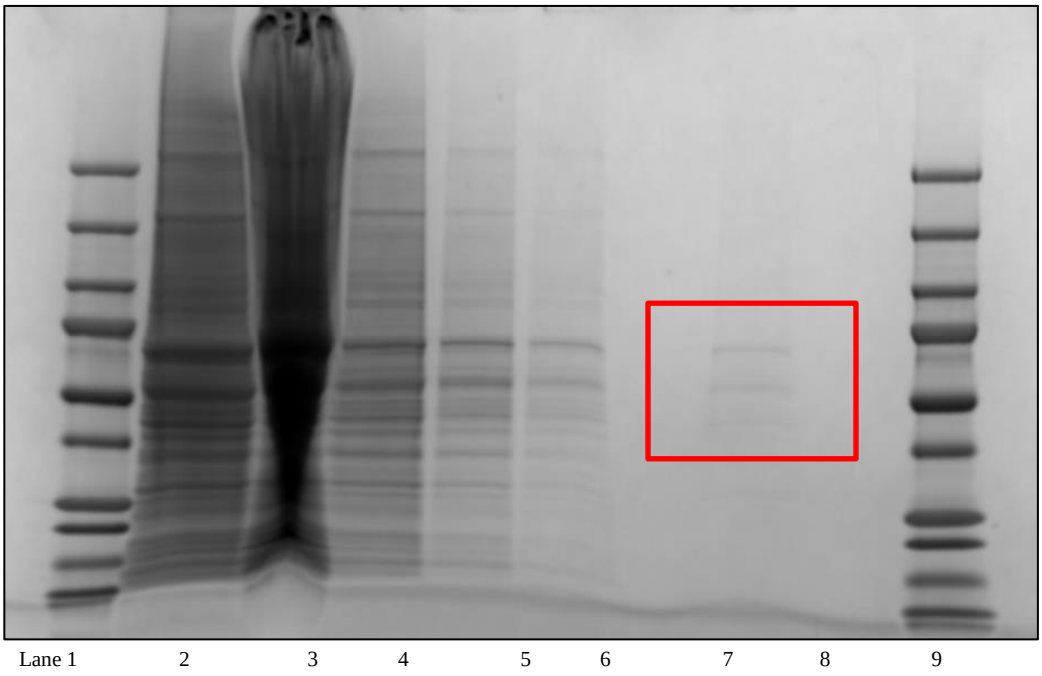

Figure 4: Gel of IL-6Rα from Brain Lysate: is an image of a gel from a brain lysate that ran through a μMACS column. The isolated protein was the IL-6Rα, and each wash from the column is represented on this gel. Lane 1 and the final lane contain the ladder, lane 2 is wash 1, lane 3 is the initial flow through, and washes 2 through 4 are in lanes 4 through 6. This gel was stained with Coomassie Blue. The final eluted protein shows specific bands: one at ~75kDa and another at ~40kDa. The band at ~40kDa is the sIL-6Rα, and the band at ~75kDa is the entire IL-6Rα. However, the final eluted sample is very similar to all of the washes, which could mean that the column is isolating non-specifically bound proteins.

Trial 4

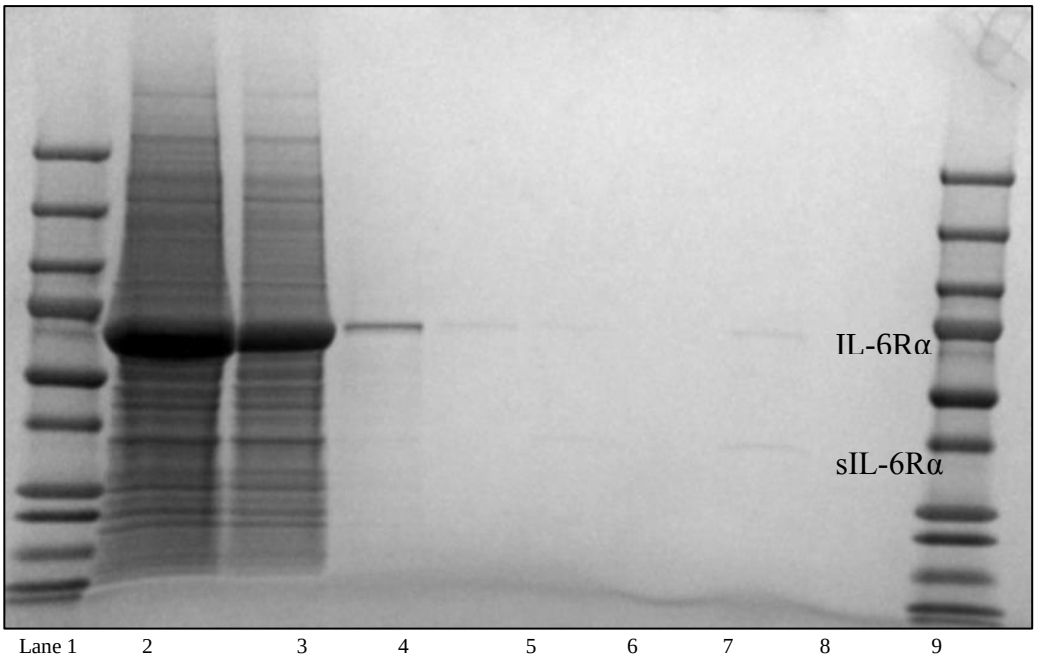

Figure 5: is an image of a gel from a retinal lysate sample. The lysate collected was from a pool of ten retinas. The bands from IL-6Rα show both the membrane bound and soluble form of the receptor. The antibody binding was specific and only the two forms of the IL-6Rα appear in the sample eluted from the column. The gel was stained with Coomassie Blue.

Trial 5

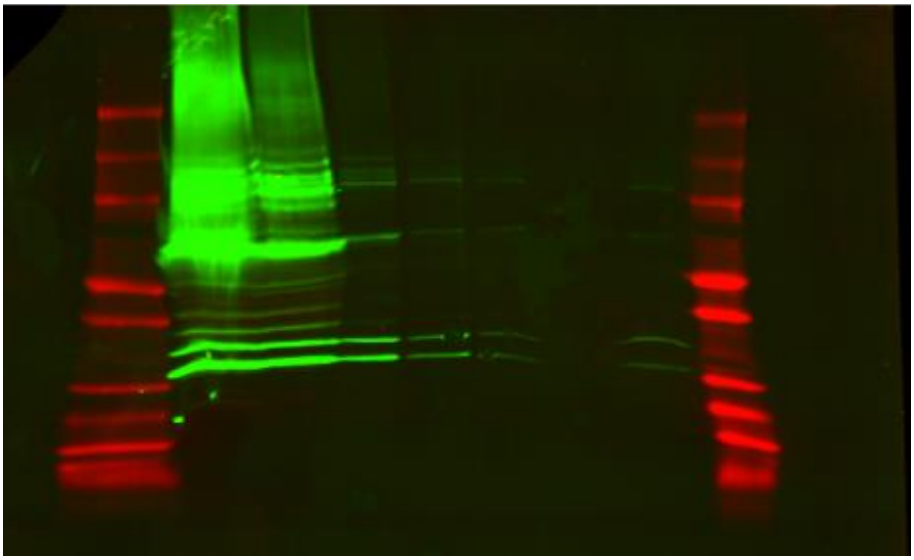

Lane 1 2 3 4 5 6 7 8 9

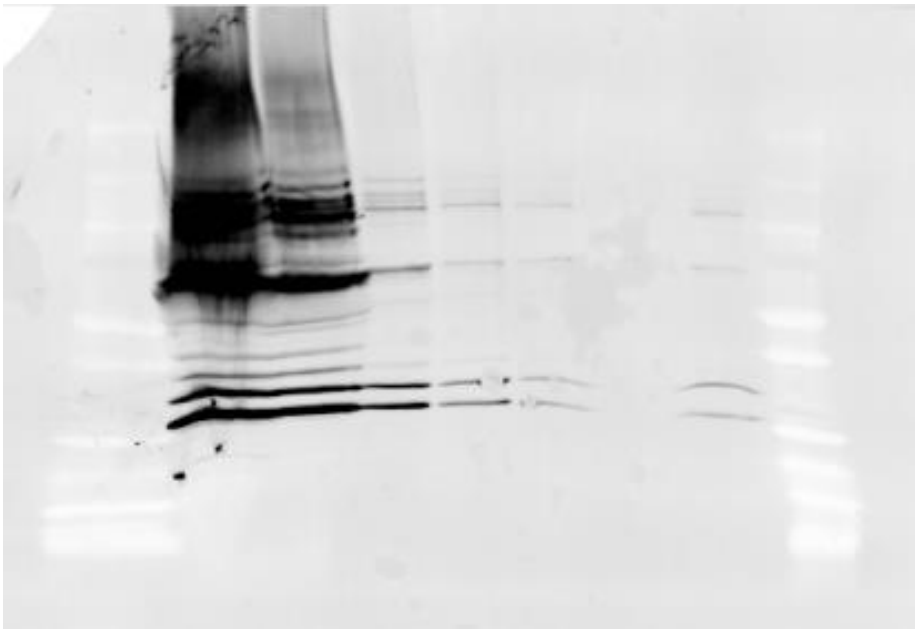

Lane 1 2 3 4 5 6 7 8 9

Figures 6 & 7: are images of a western blot run on isolated IL-6α from a sample of brain lysate isolated from C57Bl/6 mice. This membrane utilized IL-6Ra M-20 antibody from Santa Cruz. The antibody is detecting IL-6Rα at approximately 125, 75, 25, and 20 kilodaltons (kD). This is significant because the whole-length receptor is approximately 80kD, the soluble form is

approximately 50kD, and the potential cleavage product is 37kD. The antibody is picking up another form of the receptor, which could possibly be an additional cleavage product. The antibody incubation times were 24 hours.

Trial 5 Continued

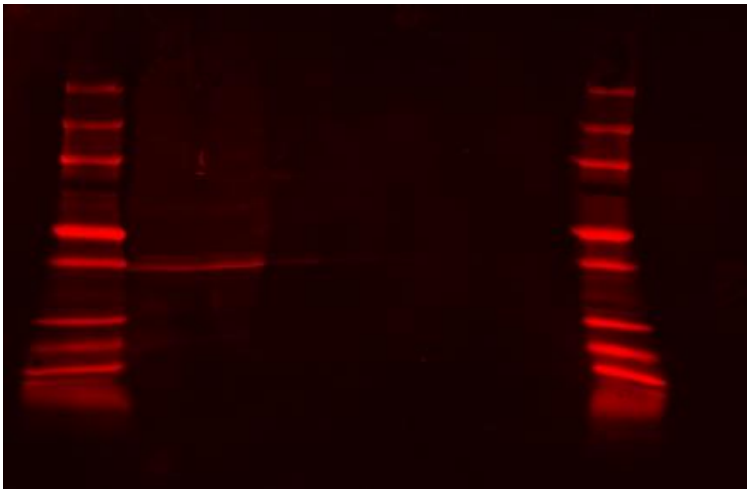

Lane 1 2 3 4 5 6 7 8

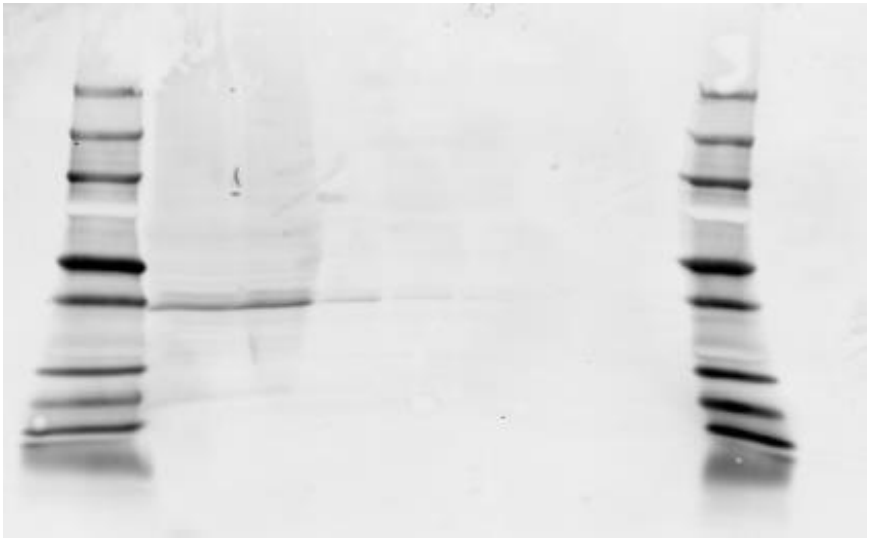

Lane 1 2 3 4 5 6 7 8 9

Figures 8 & 9: represent a western blot run on isolated IL-6Rα. The antibodies were from R&D during this trial instead of Santa Cruz. The antibody utilized was the IL-6Ra CD126. This trial's purpose was to determine the potential difference between the two antibodies and determine which one had the most specific binding. Both parts of trial 5 were being performed in order to ensure that the cell separation column was successfully isolated the intended biotinylated protein. The column technique was being tested for the first time throughout the course of this experiment, and its effectiveness had yet to be determined. A 24 hour incubation time was used for the antibodies.

Trial 6

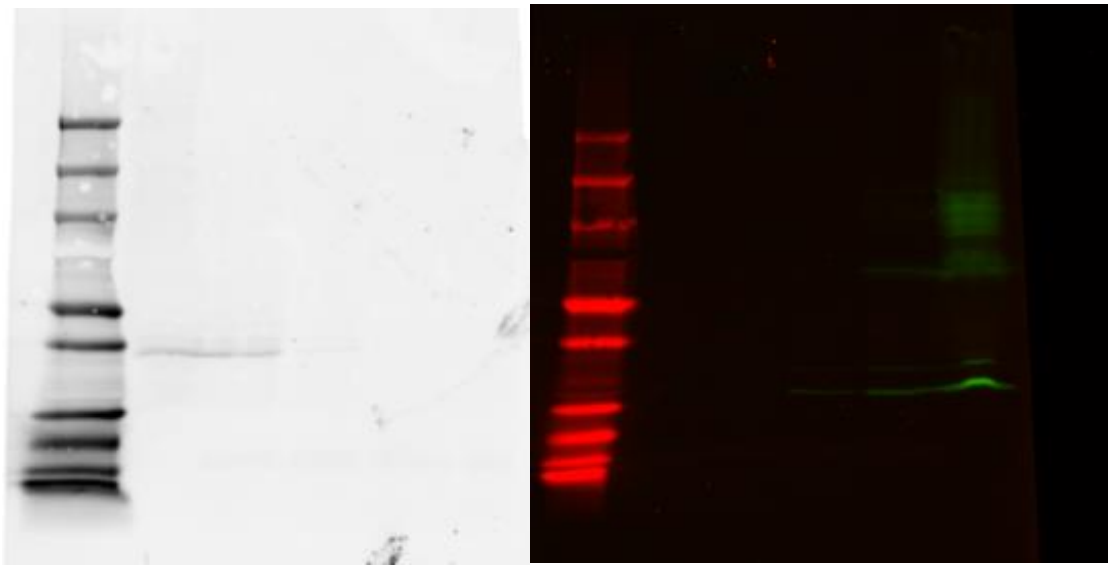

Figures 10 & 11: shows an image of a western blot with CD126 IL-6Rα antibodies. The incubation for these westerns, with proteins isolated from brain lysate, was increased to five hours. The previous incubation times had ranged from 30 minutes to 2 hours. This was the longest incubation time utilized to test the effectiveness of the cell separation column and how successful it was in isolating the IL-6Rα. The IL-6Rα band in figure 10 can only been seen in the initial flow through and wash one. In figure 11, the receptor did not light up, and there was probably an issue with the binding, not the protein isolation method.

Discussion

Trials one through three were completed using brain lysate. This was done because of the prevalence of protein in brain, whereas retinas contain a substantially smaller amount of protein. GFAP was isolated also because of its prevalence in the tissue samples. It provided a good way to test the developing method and to ensure that it was in fact, capable of isolating biotinylated proteins before moving on to experimental tissue. Trial one was not effective, and the antibody incubation times and concentrations were both increased based on the results from trial one. The incubation time was increased from 30 minutes to 2 hours, and the incubation concentration was increased to 1µg (1:10) from its previous concentration: 1:100. After the isolation of GFAP was shown to be possible by trial 2, the experiment could be moved into retinal lysate. The gels were stained with total protein stains (Coomassie Blue or Ponceau S) to see where the column was losing the most protein. Based on the imaged membrane from trial two, the biotinylated proteins were being washed off the column during the 4 washes. There was specific binding of the GFAP protein in washes one through 4. The majority of the biotinylated protein needed to be contained in the column so that it could be eluted so that there was enough protein to cut out from the gel

and sequenced. An adaption to the washes was made, and the 10μL of Np-40 was added to the tris wash for trial 3. Based on the gel from trial 3, which showed very faint IL-6Rα bands on the gel, the Np-40 was taken out of the washes. The Np-40 seemed to make the washes lose even more of the biotinylated protein, which could be a result of non-specific binding. However, based on the size of the final eluted protein samples from trial 3, it was though that the removal of the Np-40 would increase the amount of protein present in the final eluted sample.

Trial four involved a pool of ten retinas to increase the amount of total protein that was being extracted. The amount of IL-6Rα being isolated would be much higher because of the increase of the initial protein. The final eluted protein showed potential, with two very clear bands. However, they are very faint, and washes three, four, and five show similar bands. After seeing this gel, it was proposed to follow the same process, but collect and elute after only one tris wash. This would eliminate the loss of biotinylated protein over the next three washes. It was promising to see two specific IL-6Rα bands, and it was hypothesized that one was the membrane form of the receptor and that the other was the soluble form of the receptor. It is also possible that one is the cleavage product. However, trial four only shows an image of a gel. A western blot had not been performed; therefore the bands cannot be proven to be the IL-6Rα.

Conclusions

The ability to purify IL-6Rα directly from tissue samples will allow us to differentiate between soluble and membrane-bound forms of IL-6Rα and determine whether the soluble form is produced by cleavage in retina from any mouse model of glaucoma. Combined with the optimal digestion paradigm, determined by testing with recombinant IL-6Ra, the endogenous protein in healthy and glaucomatous retina is ready for sequencing. Also, this technique is not limited to the purification of IL-6Rα - it can also be used to target other proteins of interest in the future. This project sought to develop and test the effectiveness of the modified μMACS cell separation column, with the intention of using this new technique to isolate the IL-6Rα.

Literature Cited

Sappington RM, Chan M, Calkins DJ. Interleukin-6 Protects Retinal Ganglion Cells for Pressure-Induced Death. IOVS, July 2006, Vol. 47, No. 7.

Stephanie MS, Holgren L, Cathcart HM, Sapington RM. Spatial Regulation of interleukin-6 signaling in response to neurodegenerative stressors in the retina. Am J Neurodegener Dis 2012;1(2):168-179

Efficacy of Simulated Martian and Lunar Regolith as a Radiation Shield

Lillith Bulawa and Grass Gass
Greeneville High School, Greeneville

Abstract

As space exploration continues beyond low earth orbit (LEO) astronauts will move out of the protection of the earth's magnetosphere and atmosphere and will be exposed to harmful levels of radiation. For any successful future long term space mission the problem of exposure to both Galactic Cosmic Radiation (GCR) and Solar Power Events (SPE) must be addressed. Not only must astronauts be protected during space travel, they also must have the ability to establish outposts that provide radiation protection on future space outposts. The establishment of space outposts using native regolith as a radiation shield is investigated in this experiment. An experimental design was constructed and the halving thickness of packed soil and water was calculated and compared to known values. The design was felt to be valid because the calculated values were consistent with known values. The halving thickness of simulated Martian and Lunar regolith was then calculated. It was determined that Martian and Lunar regolith would be potential sources of radiation shields on future space outposts.

Introduction

The future of space exploration must extend beyond the confines of low earth orbit. As astronauts make this journey they will be removed from the protection of the earth's atmosphere and magnetosphere and exposed to harmful levels of both Galactic Cosmic Radiation and Solar Particle Events. This harmful radiation can damage DNA and lead to increased risks of cancer. Radiation has also been linked to a weakened immune system, cataracts, heart disease, strokes and Alzheimer's disease. (NASA Space Faring) NASA's goal is to keep radiation at levels "As Low as Reasonably Possible" or ALARP. Even on the International Space Station astronauts are all equipped with personal dosimeters and are exposed to between 20 to 40 times more radiation in a 6 month period then a scientist on earth. (NASA Understanding Space) NASA's chief medical officer recently stated that, "Even for the shortest of missions we are perilously close to the radiation career health limits we've established for our astronauts" (Klotz, 2013).

The problem of radiation exposure must be addressed not only during space flight, but also during establishment of future space outposts on planets and asteroids. Transportation of materials to and beyond low earth orbit is enormous. The estimated cost of transporting just one liter of water to the International Space Station is $22,000. (NASA Waste Limitation)

Incorporation of native materials to build space outposts would drastically cut costs and make the possibility of construction of a space outpost more feasible.

As thickness is added to a material its radiation shielding capabilities multiply. The mathematical expression that describes this relationship is I=I exp(- x) represents the linear attenuation coefficient, which characterizes how easily a material can be penetrated by radiation. (Maher, 2008) A large attenuation coefficient means that radiation is quickly attenuated, or weakened, as it passes through the material. A small attenuation coefficient means the material is fairly transparent and there is little change in the intensity of the radiation as it passes through the material. This expression is shown in graph 1 below (Maher, 2008).

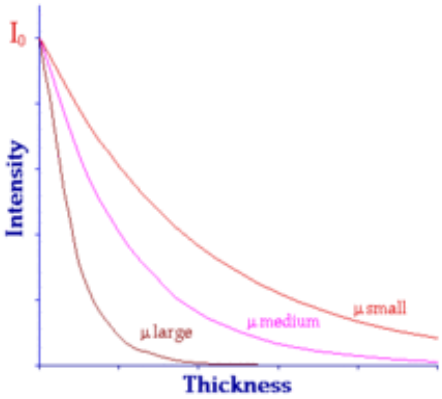

Graph 1

The curve is exponential in nature. All graphs of radiation intensity versus material thickness will have an exponential curve but the rate of decline will vary depending on the materials linear attenuation coefficient. (Maher, 2008)

The efficacy of a material as a radiation shield is more commonly and more easily measured by determining the materials halving thickness. Halving thickness is the amount of material required to effectively block half the radiation it is exposed to. This is illustrated in the graph 2 below (Maher, 2008).

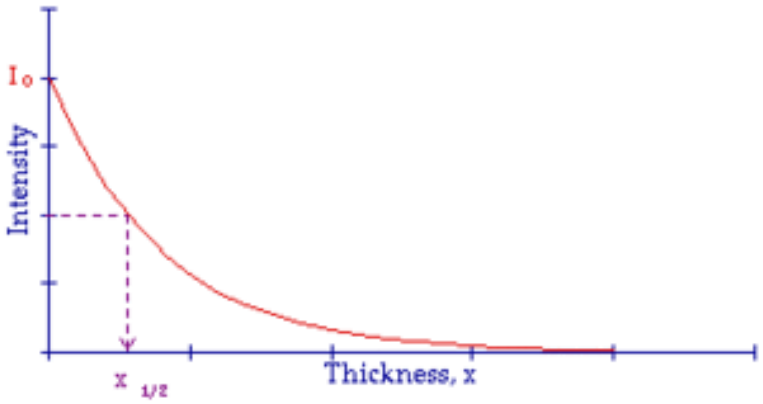

Graph 2

Tables are available of calculated values of halving thickness of common materials (www.nuclead).

Sand bag homes can be constructed quickly and easily and can provide protection from harsh environments and harmful radiation here on earth. (Hunter 2004) There has been much analysis of the composition of both Martian and Lunar regolith and NASA has developed a simulated version of this regolith for use in experiments. (www.orbitec) It is our hope to conduct an experiment to investigate the halving thickness of this simulated regolith to determine if future space outposts can be constructed in the sand bag design that will offer radiation protection and allow for cost effective construction of outposts during future long term space missions.

Materials and Methods

Materials – gamma radiation source, ring stand and clamps, Vernier radiation probe and Labquest data collector, clear plastic fluorescent light bulb cover, simulated Martian and Lunar regolith, packed soil, water, Saran Wrap, a rubber band and a ruler.

Methods – An apparatus was constructed consisting of a Vernier radiation probe attached to a ring stand and suspended over an enclosed source of gamma radiation. Gamma radiation was used as it was felt to most closely simulate harmful radiation that astronauts would face. A clear plastic fluorescent bulb casing was cut and a piece of Saran Wrap was secured on the base with a rubber band. The casing was secured to the ring stand over the gamma radiation source. Radiation readings were then taken each hour for six hours. Next two cm of material were added to the tube and readings were again taken each hour for six hours. The average value was calculated for each thickness and then graphed. The graph was analyzed and the thickness was determined that blocked half the radiation was determined.

Initially readings were taken of materials who had known halving thickness values. The halving thickness of water and packed soil was determined and compared to the known values to ensure that our experimental design was accurate.

Data Analysis –

The purpose of this experiment was to determine the halving thickness of simulated Martian and Lunar regolith. Initially the halving thickness of water and packed soil was determined to ensure the experimental design was valid. Table 1 shows the readings that were

obtained when water and packed soil were increased by two cm over the gamma radiation source. Readings were taken at one hour intervals for six hours.

The average radiation readings were plotted against the thickness of the material and this is shown in the graph below. Graphs 3 and 4 show the classical exponential nature in the decline of intensity of radiation versus thickness of material. The halving thickness was then determined from the graph.

Water	Trial 1	Trial 2	Trial 3	Trial 4	Trial 5	Trial 6	Ave
0 cm	4469	4423	4526	4463	4390	4441	4452
2 cm	3835	3887	3978	3962	3873	3997	3922
4 cm	3498	3626	3703	3604	3609	3546	3598
6 cm	3388	3219	3356	3231	3339	3287	3303
8 cm	3141	2889	3012	3013	3043	3038	3023
10 cm	2841	2793	2825	2815	2859	2885	2836
12 cm	2653	2722	2673	2721	2692	2644	2684
14 cm	2546	2525	2536	2511	2539	2493	2525
16 cm	2390	2427	2396	2387	2399	2389	2398
18 cm	2269	2280	2274	2284	2199	2320	2271
20 cm	2179	2203	2162	2184	2165	2187	2180

Table 1: Radiation Count Over One Hour - Water and Packed Soil

Mars	Trial 1	Trial 2	Trail 3	Trial 4	Trial 5	Trial 6	Ave
0 cm	4918	5224	5265	5078	5092	5160	5123
2 cm	4055	4157	4132	4041	4087	4111	4097
4 cm	3497	3790	3732	3391	3693	3623	3686
6 cm	3199	3436	3423	2989	3420	3287	3359
8 cm	3059	3038	3119	3732	3063	3102	3069
10 cm	2845	2709	2830	2930	2806	2765	2814
12 cm	2626	2600	2516	2552	2539	2687	2587
14 cm	2384	2398	2546	2413	2499	2573	2468

Lunar	Trial 1	Trial 2	Trial 3	Trial 4	Trial 5	Trial 6	Ave
0 cm	7560	7401	7640	7589	7374	7410	7496
2 cm	5486	5448	5444	5544	5588	5462	5495
4 cm	4471	4501	4602	4494	4520	4388	4496
6 cm	4106	4000	4149	4037	4079	4086	4076
8 cm	3451	3356	3482	3356	3359	3453	3409
10 cm	2797	2765	2796	2868	2765	2774	2794
12 cm	2385	2340	2438	2364	2404	2423	2392
14 cm	2007	2120	2026	2067	1995	2013	2038

Table 2: Radiation Count Over One Hour - Martian and Lunar Regolith

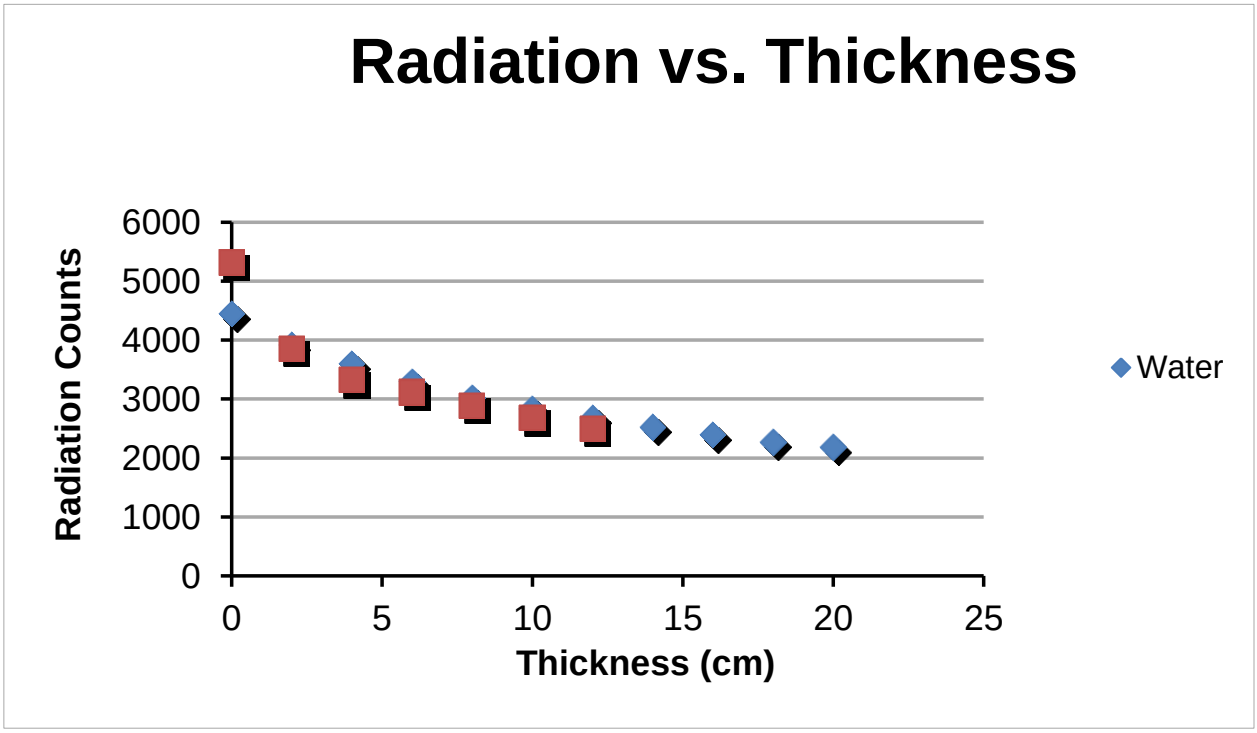

Graph 3

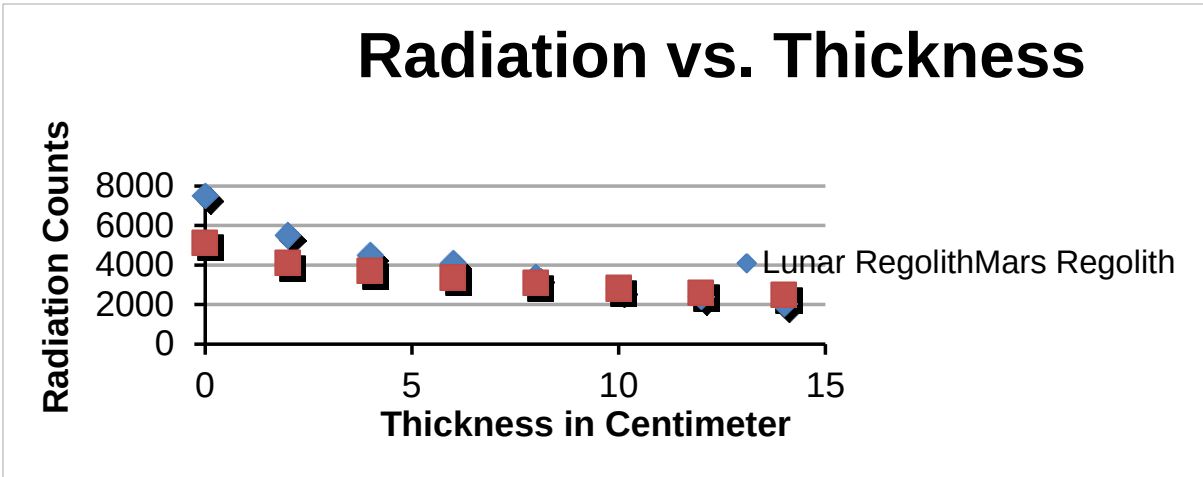

Graph 4

The halving thickness of water was calculated to be 18 cm and that of packed soil was calculated as 9 cm. This was compared to the established values. The values correlated indicating our experimental design was valid. (www.nuclead)

Next we obtained readings of gamma radiation at one hour intervals while the thickness of Martian and Lunar regolith was increased by two cm. Again readings were taken at one hour

intervals for six hours. This is seen in table 2. The average value was then graphed and the halving thickness was calculated. The graph is seen below and again shows exponential decline.

The calculated halving thickness we determined for simulated Martian regolith was 11 cm and for simulated Lunar regolith was 7 cm.

Conclusion

To determine the halving thickness of simulated Martian and Lunar regolith an experiment was designed to analyze radiation protection while the thickness of these materials was varied. The experimental set up was first tested on materials with known halving values to ensure it was accurate. The calculated halving thickness for the simulated regolith was calculated and approximated that of packed soil.

Sand bag homes have been used for many years to construct stable, quick, and inexpensive homes in times of crisis and in areas with few other natural resources. The possibility of constructing regolith structures on future space outposts is particularly advantageous as the need for transport of costly construction materials is greatly reduced.

The experiment demonstrates that both Martian and Lunar simulated regolith can be used as effective radiation shields. Space outposts can be constructed using the sand bag technique and native regolith. This will allow for simple cost effective structures to be established that provide radiation protection. Future studies should be done to analyze the efficacy of using sand bag construction techniques in conditions of diminished gravity with simulated regolith materials. If this technique can be developed it may aid in the development of viable long term space missions and space outposts that allow for radiation protection.

Literature Cited

NASA Space Faring – The Radiation Challenge. Module 2: Radiation Damage in Living Organisms. Pg2-4 EP-2008-08-116-MSFC

NASA Facts – Understanding Space Radiation Oct.2002 FS 2002-10-080JSC

Klotz, Irene "Trip to Mars Would Likely Exceed Radiation Limits for Astronauts" Reuters, Cape Canaveral Florida May 30, 2013

Hunter, Kaki "Earth Bag Building the Tools, Tricks, and Techniques", New Society Publishing June 2004 ISBN-10 086571507

NASA Waste Limitation Management and Recycling Educators Guide Pg 17 EG-2009- 10-107-KSC

Maher, Kiernan “Basic Physics of Nuclear Medicine” Platypus Global Media Copywrite 2004

Determining Soil Electrical Conductivity Using Electromagnetic Induction on an Autonomous Robot

Efrain Salazar and Able Shi
School for Math and Science at Vanderbilt, Nashville

Abstract

Monitoring soil conductivity is crucial in precision agriculture as it shows levels of soil moisture, pH, and depth. However, this process is extremely tedious and labor intensive. Therefore, the use of autonomous vehicles for measuring soil properties such as conductivity presents a viable, efficient, and cost effective solution to precision agriculture. The focus of this project was to design and construct an autonomous robot to detect soil electrical conductivity throughout an agricultural field. The robot would be able to collect data which can be used to compose a map displaying the varying degrees of electrical conductivity throughout an agricultural object, indicating areas of higher soil ion content and allowing for more effective soil management and crop yield. An RC vehicle was modified into an autonomous vehicle relying on the input data collected from mounted obstacle-avoidance distance sensors which observed the robot's environment and used accordingly by the Arduino microcontroller to program the vehicle's navigation. An electromagnetic induction sensor was constructed comprising of two copper solenoids: one a transmitter and the other a receiver fitted to a circuit consisting of a power inverter system, which supplied alternating current to the transmitting inductor. The receiver coil circuit would output a signal, varying with the conductivity of the medium, which can be calculated for EC using the analog input of the Arduino. The EMI sensor was thoroughly tested to determine its functionality and was attached onto the autonomous vehicle with a specific distance between coils calculated given the frequency of the circuit and the geometry of the coils.

Introduction

Precision agriculture with the use of autonomous robots can increase crop production per designated agricultural area. This is due to the site-specific crop management (SSM) implemented with precision agriculture, which allows farmers to address specific issues pertaining to that specific area. With this technology, farmers can better cultivate crops in a definitive area of a field and hopefully generate more produce, thus, increasing overall food production per area and addressing the growing problem of malnourished populations.

Hoping to improve precision agriculture, the primary aim of the project was to develop one of these autonomous robots by modifying a RC vehicle with an Arduino micro-controller, an electromagnetic induction (EMI) meter, and distances sensors in order to provide a cheap, efficient method to precision agriculture. A common problem regarding precision agriculture is its expensive cost for implementation. By modifying an inexpensive RC vehicle, the project hopes to reduce the cost for autonomous robots and instruments required for precision agriculture. Likewise, the materials used were rather modest in price and easily replaced for

repairs or upgrades. One of these instruments was the EMI sensor which would allow the robot to measure soil electrical conductivity using electromagnetic induction without penetrating the soil. This would allow for quick, cost-effective, efficient data-collection without the need for human assistance. Furthermore, the distance sensors will aid the robot's navigational abilities by detecting potential obstacles and impediments in the robots path. All data collected by both the EMI sensor and distances sensors were processed in the Arduino micro-controller. Furthermore, the Arduino was programmed to input a change in direction according to readings made by the distances sensors in order to navigate the robot. Similarly, Arduino also analyzes data collected by the EMI sensor and mediates the intervals at which data is collected. All data is saved to a SD card in order to be further analyzed on a computer. A farmer or scientists may use this map in order to determine specific areas that need particular attention in the form of fertilizers or other agricultural techniques.

In previous research pertaining to precision agriculture, it is revealed that this technique is in fact, rather effective especially in crop yield. In one particular paper, written by Pentjuss, et al., the scientists researched the effectiveness of autonomous robots on a farm. The paper explained robots could accurately measure different qualities of the farmland without the need of human assistance. Furthermore, in order to develop the EMI sensor, equations used to optimize the sensor were taken from a research paper written by Arne Breen. The number of coils (N), the area cm^2 enclosed by the coil (q), and effective coil permeability (ucoil), which was set at 100, were used to calculate inductance (L) with the following equation:

$$L = \frac{4\pi N^2 q \mu_{coil}}{l} \cdot 10^{-9} \text{ hy}$$

These equations reflected Gauss' law and Faraday's law and were rearranged in order to fit the project's criteria.

Therefore, in order to determine the coil design geometry, the equation:

V=L*(di/dt)

was optimized.

With these equations, a schematic was generated for the both the EMI sensor and distance sensors to the Arduino along with resistors and capacitors. All in all, with the research and equations from previous studies, a EMI sensor was built from scratch and integrated into the robot.

Methods

3.1 Autonomous Interfacing:

The designated remote control vehicle was temporarily disassembled and its principal internal component, the RX2 chip, was manually interfaced with an Arduino microcontroller to allow for direct control of the basic functions of the vehicle via a specified output of a signal from the Arduino. Using a diagram of the electrical circuit of the receiver and transmitter components in the RC vehicle (provided by the manufacturing company), wires were soldered to

the respective receiver pins on the RX2 chip, enabling a direct electrical connection to the motor control circuit, and were extended and inserted into their designated digital output ports on the Arduino. Through the Arduino's digital output function, a high signal consisting of 5V DC was transmitted to the designated receiver pin, imitating a similar signal that would have been received from the transmission from the remote, and thus activating a specific function

3.2 Autonomous Code Development:

Once direct communication was established between the Arduino microcontroller and the formerly remote-controlled vehicle, three ultrasonic distance sensors were mounted onto the vehicle and integrated in the Arduino control system. The analog input data, provided by the USD sensors, indicated to the microcontroller the absolute distance between the sensors and any solid object directly in front of the sensor, allowing for a method of environmental perception and qualification. Utilizing basic coding methods and setting up specific distance parameters, logical conditions were implemented in the program modeled after simulated conditions that robot would most likely encounter in the field, creating a repeatable system of behaviors for the robot to abide by that would allow basic maneuverability and obstacle avoidance.

3.3 Electromagnetic Sensor Design:

The method of using electromagnetic induction to determine soil conductivity non-invasively, is based on a basic sensor design which detects the measurement of the change in mutual impedance between a pair of coils, separated at a fixed distance, on or above the soil's surface. This requires the use of alternating current to flow through two solenoids in order produce a constant primary electromagnetic field and detect the resulting field induced in medium, thereby indicating the conductivity of the soil. In order to produce these effects, the electrophysical characteristics of the sensor and circuit were calculated based on the solenoid geometry. The self inductance of the transmitter coil was given by

$$\mathrm{L} = \frac{4\pi \mathrm{N}^2 q \mu_{\mathrm{coil}}}{l} \cdot 10^{-9}\ \mathrm{hy}$$

where N is the number of turns around the core, q is the area in cm² enclosed by the coil and l is the length of the rod in cm. The fixed distance between the coils was calculated based on the practicality of the length of the sensor in relation to the size of the autonomous robot and the frequency of the circuit was obtained according to the relationship between both properties in an electromagnetic device in which the primary field produced will be known and remain constant; this would allow for the direct quantification of impedance of the soil calculated from the detected secondary field subtracted from the known primary. The frequency of the transmitter was produced by integrating a 555 timer, which would oscillate the input signal at any specification given the correct circuit set-up, and the capacitance value for the receiver circuit was calculated based on the formula below in order to match and calibrate the initial impedance of the signal produced by both circuits.

3.4 EMI Circuit Design

The circuit design was customized to the specifications of the electromagnetic sensors. The final circuit was comprised of two sub circuits: receiver circuit and transmitter circuit. The transmitter circuit incorporated a basic 555 timer in order to produce a consistent oscillation of the input signal from the 9V batteries at a calculated frequency. The oscillation was also used as a crude DC-to-AC power inverter, thereby supplying an alternating current to the sensor to induce a magnetic field in the coil. A high-power operational amplifier was included in the transmitter circuit to amplify the output signal from the 555 timer and increase signal strength for the power-demanding transmitter coil induction. The receiver circuit consisted of two high-capacitance capacitors connected in series to allow for matched circuit frequency at which the signal of the transmitter coil is operating and received by the transmitter circuit. The output signal from the receiver circuit is designed to be connected to an arduino analogue port for signal analysis and subsequently, electric conductivity of the medium.

3.5 Testing of EMI Sensor

After the circuit was finalized and the prototype was completed, a series of tests involving an oscilloscope was performed. The EMI design was tested using an oscilloscope which was connected to the input and output of each of the coil circuits that calculated the actual inductance of the coils. The range of the electromagnetic field was also quantified through timed measurements of voltage and displayed in Figure 1 and Figure 2.

Results

The GPS was programmed to display coordinates, but only in open areas. In the laboratory, the GPS could not show any coordinates, but once outside, it had no problem presenting coordinates. Similarly, once the RC car was modified with distance sensors and made autonomous as the result of coding in the Arduino, the robot demonstrated autonomous navigation by avoiding obstacles in its path. Once the distance sensors on the robot detect an obstruction, the robot would stop, back up and adjust its orientation so that it can avoid the impediment. As for the EMI sensor, after both the receiver coil and transmitter coil had been constructed, complete with their many capacitors and resistors as shown in the schematic in Figure 1, and it was successfully tested using an oscilloscope (Fig. 5a-b). In other words, the EMI sensor did produce electromagnetic induction and had a range of approximately 20 cm between the two coils (Fig. 2) with the most favorable distance at 5.4 cm (Fig. 3) given a relatively small and reproducible amount of voltage. However, in order to outfit the EMI sensor completely onto the autonomous car, a portable AC voltage supply was needed to be fitted on the car. Unfortunately, the 9V battery is a rather weak source for electricity for the high-power EMI sensor as shown in Figure 4.

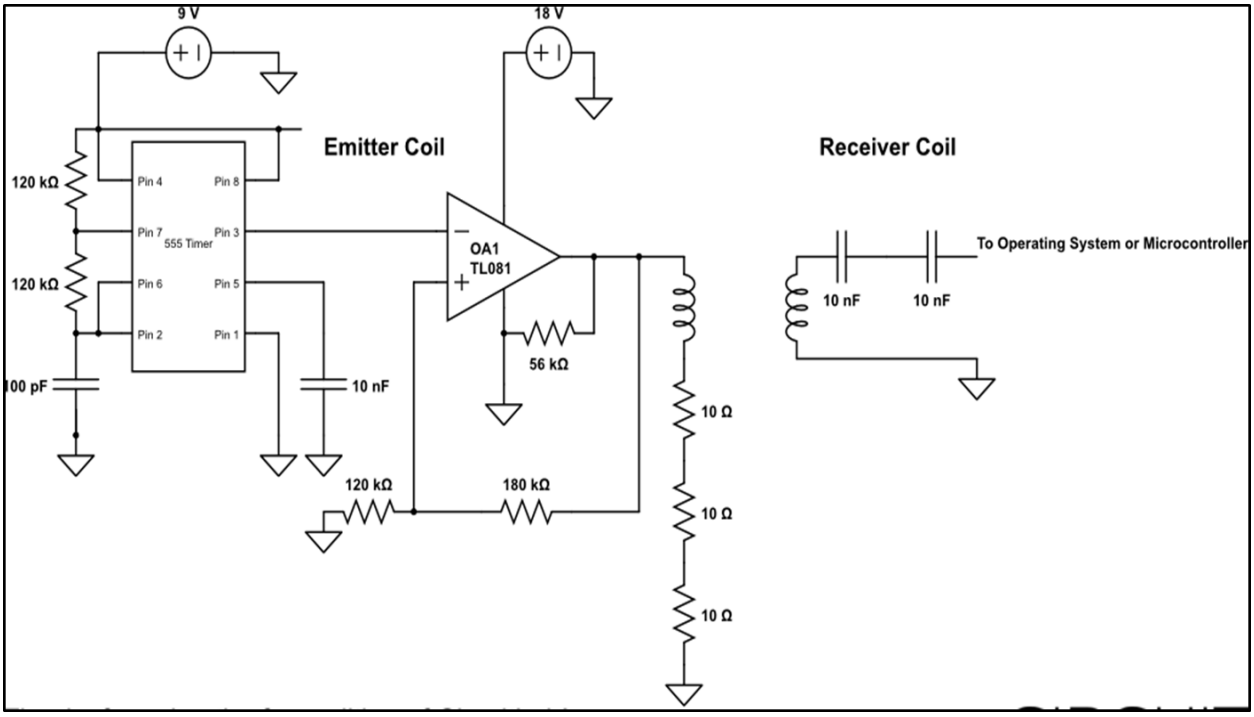

Figure 1: The figure above displays the complete circuit schematic of both coils (emitter and receiver) the EMI sensor.

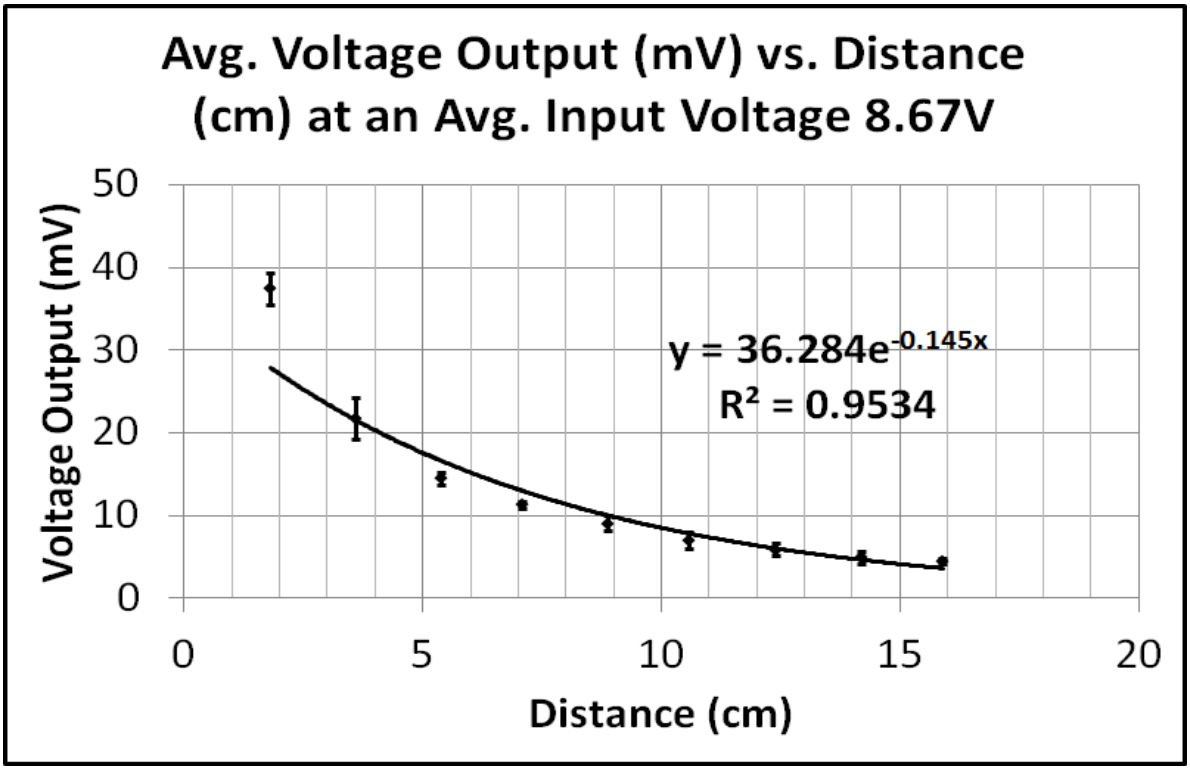

Figure 2: The graph demonstrates the relationship between the distance (cm) separating the coils and the voltage output (mV) at an average input voltage of 8.67V

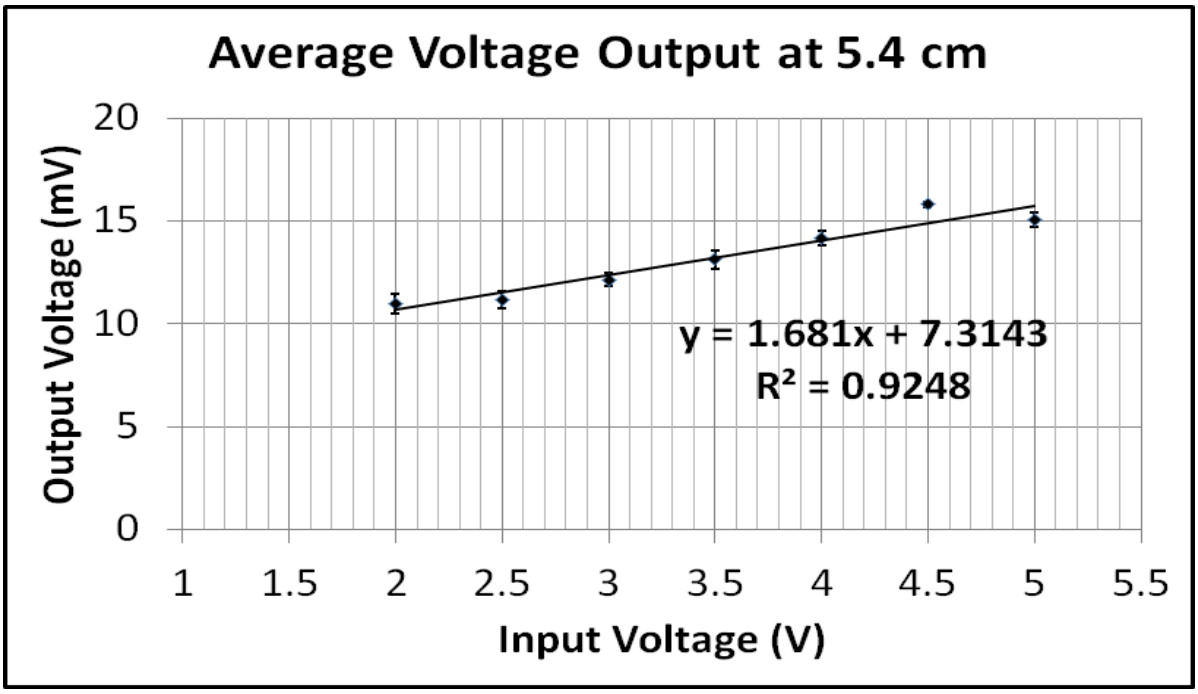

Figure 3: The graph to the side shows the change in the voltage output (mV) based on the voltage input (V) at a distance of 5.4 cm between the coils.

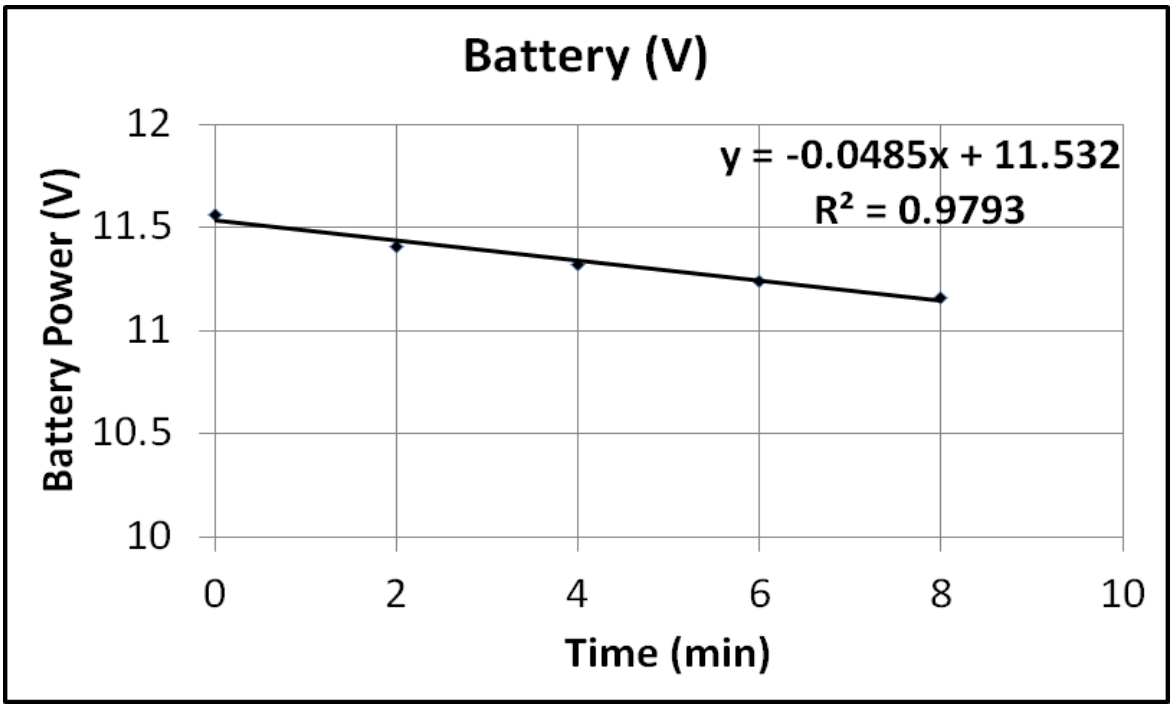

Figure 4: This graph shows the voltage decay of the battery (V) over 2 minute intervals.

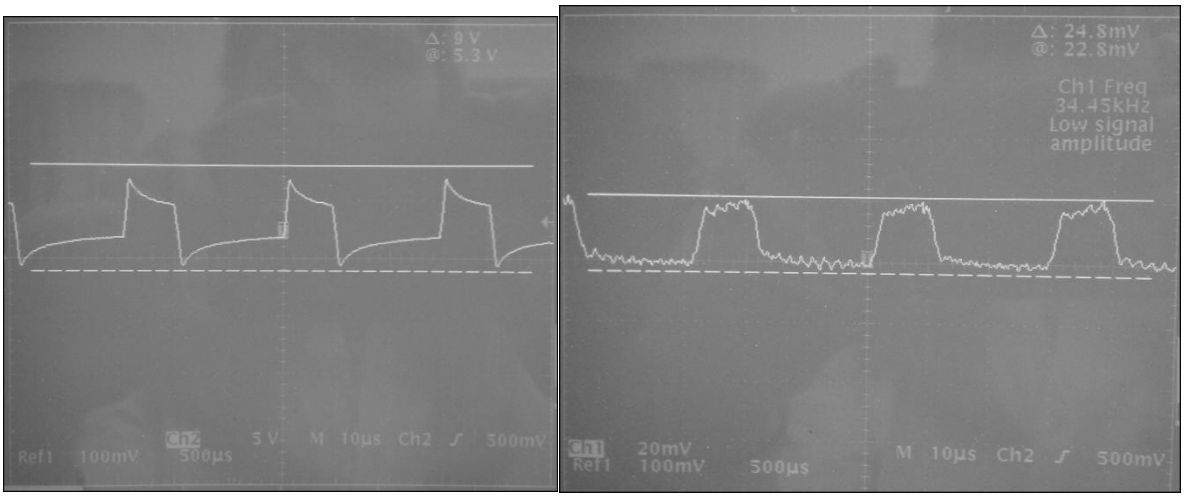

(5a) (5b)

Figure 5: The figure above displays the complete circuit schematic of both coils, emitter (a) and receiver (b) the EMI meter.

Conclusion

The experiments performed on the EMI sensor and robot itself revealed that they were functional and autonomous respectively. The EMI sensor was developed and is still in the testing phase, not yet able to be set up, used, and regulated for field uses. Overall, the resulted product is not ready for practical uses; given that the goal was to create an easy method (specifically non-penetrating) of acquiring electrical conductivity within soil and our EMI sensor has not been fully developed. However, the prospect of a field autonomous robot succeeded to an extent. Limitations within the control system persist such as the ability to survey an agricultural field at equal intervals across the field using GPS in order to ensure consistency of the input EMI data throughout the whole of the field. The bot still needs to be thoroughly tested for field readiness such as the ability to maneuver in various types of terrain, the battery life efficiency, and weather durability. Possible developments for the future would include improvements of the limitations by developing a technique to program the robot to report to various pre-distributed points across the agricultural field using GPS coordinates to obtain data readings, the inclusion of a finished EMI sensor, the addition of a radio transmitter using the GPS to transmit the robot's location within the field for retrieval purposes and inclusion of one or more sensors such as soil moisture to aid in assessing the condition of the soil. All in all, a GPS could also be integrated into the system in order to provide coordinates for the data points and where they were collected. In this way, a map can be generated displaying the varying degrees of electrical conductivity which can reveal elements such as soil pH, ion content, and moisture.

Literature Cited

Breen, A. (1964). Principles in designing instruments for electromagnetic ore prospecting. *Geoexploration*, *2*(3), 159–168. Retrieved from http://ac.els-cdn.com/0016714264900079/1-s2.0-0016714264900079-main.pdf?_tid=2e18f504-4d3d-11e3-8b83 00000aacb35f&acdnat=1384441271_f9cb4ddc32600e34da2e4393d8d3371d

Pentjuss, A. (2011). Improving precision agriculture methods with multiagent systems in latvian agricultural field. *Engineering For Rural Development*, 109-114. Retrieved from http://tf.llu.lv/conference/proceedings2011/Papers/020_Pentjuss.pdf

Zanwar, S. R. (2012). Agricultural robot for cultivation process. *Excel Journal of Engineering Technology and Management Science, 1*(1), 1-6. Retrieved from http://excelpublication.com/issue/Vol-/Agricultural_Robot_For_Cultivation_Process pdf

The Effect of River Proximity on the Microbial Phyllosphere of the Sycamore Tree, *Platanus occidentalis*

Cooper Thome
Central Magnet High School, Murfreesboro

Abstract

This study was conducted to determine whether proximity to rivers had any effect on the number of microbes contained within the phyllosphere of Sycamore (*Platanus occidentalis)*. The hypothesis was that the number of colonies on leaves of trees closest to the river would be elevated due to increased moisture. Sycamore leaf samples were taken from ten trees in four different locations; two were alongside rivers. Leaves were pressed onto Tryptic Soy and MacConkey agar plates, incubated for 48hr, and colonies counted. Data collected was conflicting and showed no statistically significant relationship between colonization of bacteria and proximity to rivers. These inconclusive findings suggest the need for further study including more samples and controls for other factors such as leaf age and leaf location on the tree.

Introduction

The most immense habitat of the world is camouflaged to the human eye in the form of leaves of plants–the phyllosphere. The term "phyllosphere" is used in reference to the above-ground portions of plant surfaces that act as a habitat for various microorganisms. It is estimated that this living areal habitat's surface area covers about 6.4×10^8 km^2, which is 125% of the earth's entire surface**.** The phyllosphere is an extremely harsh area for life subject to great changes in temperature, random bouts of rainfall, and long exposure to damaging sunlight. Despite these intense conditions, microorganisms such as fungi, yeast, and bacteria flourish on plant leaves. The majority of these microorganisms, bacteria, are typically measured to have around 10^6 or 10^7 cells/cm^2 in the phyllosphere (Leveau, 2009; Lindow, 2003).This huge number of bacteria per cm^2, multiplied by the amount of surface on which they are able to live, results in massive numbers of diverse microbes inhabiting the phyllosphere.

Variance in microbial populations is thought to be caused by many factors. Geographical distance is a noteworthy factor that has been considered in the study of microbial population variance. Studies concerning the effect of distance between host plants on the microbial habitats have brought up varying results. One study conducted in 2010, while focused mostly on the diversity of bacterial communities, did also include data comparing the difference of bacterial populations one of the *Pinus ponderosa* tree from different locations (Redford, 2010). Samples

were taken at four sites, two being in Colorado, USA, about 100 km apart, one being in California, USA, about 2000 km from the Colorado sites, and the last being in Canberra, Australia, about 14,000 km away from the Colorado sites (Redford, 2010). This species maintains comparable characteristics in most areas where it grows (Redford, 2010). The results introduced the notion that host species variation had a larger effect on the diversity of the phyllosphere (Redford, 2010).

Contrary to this finding, a more recent study in 2011 showed that, among three different species of *Tamarix* trees, the variance in the bacteria on the tree's leaves had a direct relationship to distance between samples (Finkel, 2011). For example, two sets of samples taken roughly 100 km apart showed very little similarities in the percentages of different bacterial inhabitants (Finkel, 2011). A similar experiment was conducted a year later, yet with attempts to limit change in environment while still using increased geographical distances (Finkel, 2012). The study suggested that distance and environmental factors both affect the variable phyllospheres of *Tamarix* trees for certain bacteria, yet more information is needed to make a solid conclusion (Finkel, 2012). Two environmental factors, heat and drought, have, however, been found to increase species richness and diversity for epiphytic microbes, while lowering the richness of the microbes of the leaf as a whole (Hunter, 2010).

Other factors that have been speculated to cause change in the phyllosphere are much different than distance or environmental factors. The leaf morphology itself may play a role in microorganism colonization. Like all habitats, leaves seem to have a carrying capacity for microorganisms; it has been shown that characteristics such as a waxy surface may decrease this carrying capacity (Lindow, 2003). A rather recent study found that differences in size, shape, crenulations, and blistering of the plant could affect the flow of air, water, and soluble nutrients, thus affecting microbial colonization (Penuelas, 2012). Penuelas *et al.* went even further, to speculate that the very occurrence of veins, cell walls, and other microscopic features may determine the ability of bacteria to form and prosper on plant surfaces (Penuelas, 2012). Furthermore, characteristics such as wax coating or nutrient secretion are shown to greatly benefit the life of bacteria on plants (Penuelas, 2012).

The research on the bacteria specifically found within the phyllosphere has proven this habitat to be both scientifically and economically important due to the complex commensalistic relationships with both plant host and other bacterial inhabitants of the same leaf (Lindow,

2003). Some of these relationships involve gram- negative plant-pathogenic bacteria as well as human-pathogenic bacteria. Effective preventative methods have been found to reduce high plant-pathogenic bacteria infestations in the phyllosphere leading scientists to work on the same for human-pathogenic bacteria (Lindow, 2003). However, in order to accomplish this, further information on the bacteria found within the phyllosphere of particular species in certain environments is needed first.

The abundance and diversity of microbes within the phyllosphere of trees near rivers and, more specifically, of *Platanus occidentalis* has received little attention. By building an understanding of where different microbes are able to grow, ideas about the greater importance and interactions of microbes can begin to be studied. The purpose of my study was to determine whether proximity to rivers had any effect on the number of microbes contained in the phyllosphere of *Platanus occidentalis*. The hypothesis is the number of microbes will be greater in the phyllosphere of the sycamore tree near a river.

Methodology

Leaf samples of *Platanus occidentalis* were taken from ten different specimens in four different locations. Two sample sites were located along the West Fork Stones River, about 15.3 kilometers (9.5 miles) from each other. The two other sample sites were not along rivers, but were each located closest to a river sample site. This site distribution was used in order to control for distance between locations instead of the proximity to the water. However, controlling for size and age of the tree was not within the scope of this study.

Four leaves were collected from each tree. The samples were taken 8 to 15 feet up, depending on the size of the specimen. With use of a branch pruner, the samples were removed using gloved hands and were placed into sterile autoclaved bags to control for contamination. The leaves made no contact with any other surface. The leaves and bags were labeled and placed in a cooler for the remaining collection time to prevent drying out and to suppress further bacterial growth. The leaves and sample sites were all given different codes for identification. After the collection on the same day, the samples were pressed onto growth medium. Two samples from each tree were pressed onto Tryptic Soy Agar (TSA) plates and the remaining two were pressed onto MacConkey Agar plates (Figure 1). In order to conserve plates, one plate was used for both the top and bottom of each singular leaf by dividing the plate down the middle via marks on the outside of the plate. The leaves were cut in half on the mid rib. The same cut half

was used for the top and bottom on either side of the same plate (Figure 2). To prevent contamination of other leaf samples, the scissors used to cut the leaves were disinfected by being submerged in isopropyl alcohol, exposed to flame by Bunsen burner, and left to cool. Alcohol sterilized gloves were worn for all leaf handling and were changed for each leaf. Pressing was done quickly and efficiently to reduce the time plates were exposed to the air. After pressing a leaf, the plate was sealed shut using parafilm, The plates were then placed in an incubator at 37°C for 48 hours. One unused plate of both types of media was also incubated as a control, to ascertain that the media was pure.

Figure 1. ***Pressing of a Platanus occidentalis leaf onto a MacConkey Plate*.** Leaves were cut in half using sterilized scissors. The top portion of the leaf was pressed onto one side of the agar plate while the bottom portion was pressed to the other. Alcohol sterilized gloves were worn for all leaf handling and were changed for each leaf. Pressing was done quickly and efficiently to reduce the time plates were exposed to the air. Once pressed, plates were sealed with parafilm and placed in the incubator at 37˚C for 48 hours.

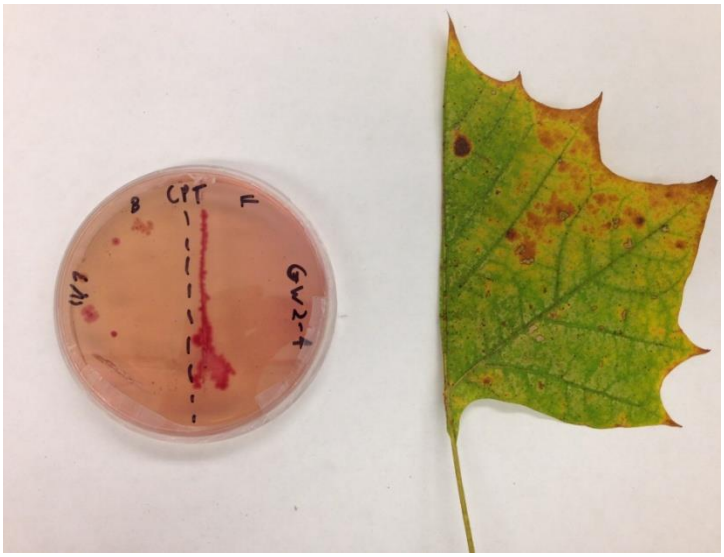

Figure 2. ***Cut leaf sample and corresponding MacConkey plate.*** All samples were cut down the midrib using sterilized scissors, top and bottom pressed onto the agar plate, and visually documented for use after plate 48 hour incubation.

After the 48 hours, the plates were removed from the incubator. The control TSA plate had one small colony, but the control MacConkey plate had none. Most of the TSA plates were overgrown with both bacteria and fungi and proved uncountable; the large growths removed any means of discerning individual colonies (Figure 3). However, all of the MacConkey plates showed discernible colonies and were then analyzed. Pictures were taken of all the plates and their respective leaves for documentation. The colonies on the left and right side of every MacConkey plate were tallied, representing the corresponding top and bottom portions of the leaf. A marker was used to show that a colony had already been counted in order to lessen mistakes. If a colony was touching another, neither was added to the total. The plate analysis took place on two days with the plates refrigerated in-between sessions to delay extra microbial growth.

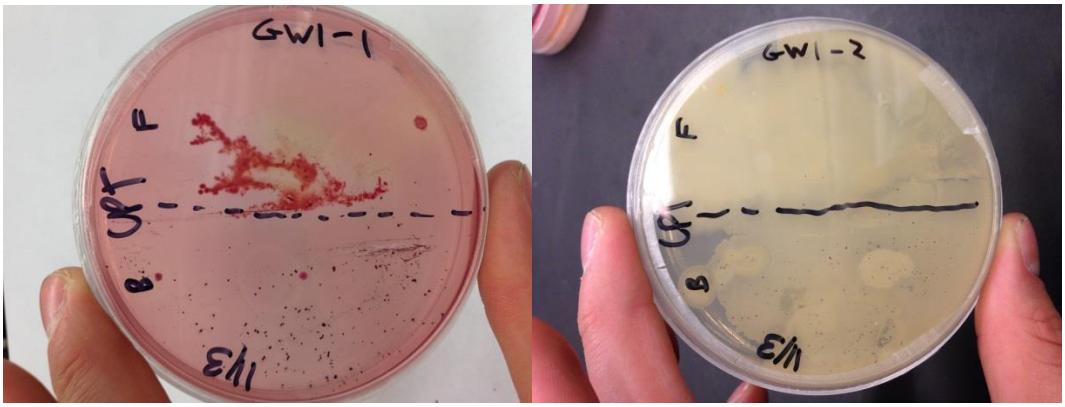

Figure 3. ***Countable MacConkey Plate (left) and overgrown TSA plate (right) from the same host tree.*** While the MacConkey plate exhibits some uncountable bacterial growth on the top portion here, it still contains discernable gram- negative colonies on the bottom that can be used for analysis, unlike the TSA plate. The TSA plate exhibits fungal overgrowth.

Results

All TSA plates were left out of the results, as not enough were countable and comparable. Only the MacConkey plates, and therefore gram-negative bacteria, were used for analysis. Eight out of the ten sampled trees showed a larger average number of microbial colonies on the bottom of the leaves, yet trees in Christiana showed the opposite for average number of microbial colonies on the bottom (see Figure 4). However, when analyzed statistically by use of a t-test, the data found no difference between colonization on the top or bottom of the leaves ($t=2.4$, $P=0.01$).

The leaves from the river sample site in Christiana had more individual bacterial colonies than the leaves of the corresponding non-river site. The other two site averages show this same trend. However, only one river tree from the Greenway river site sampling contained leaves with a higher number of bacterial colonies than the corresponding non-river trees. A one-way analysis of variance (ANOVA) statistical test was run determine if these differences in bacterial colony count at different locations were significant. While the colony counts in the data are not equal, the test found no significant difference in gram-negative bacterial counts based on river proximity ($F=0.62$, $P=0.44$).

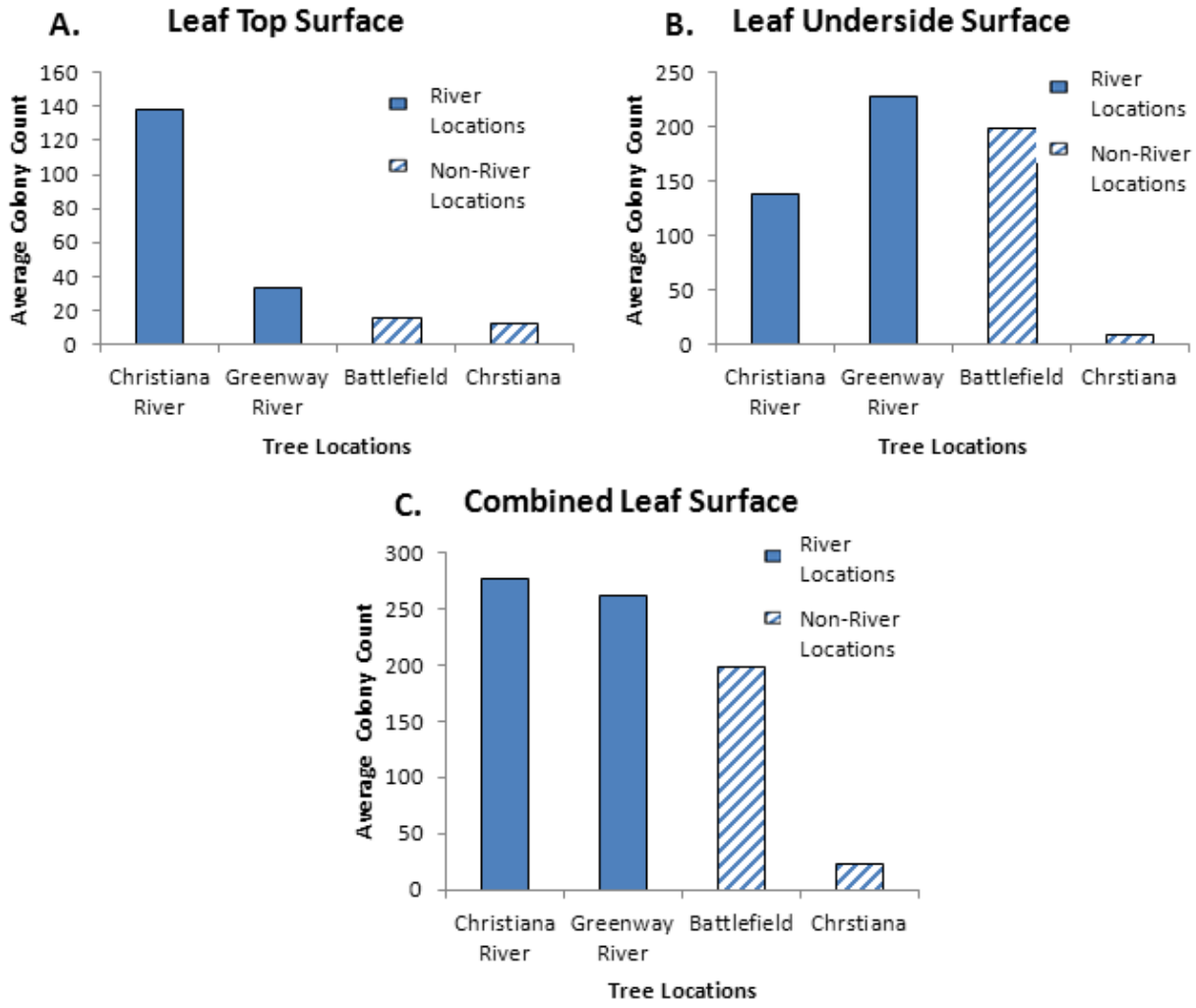

Figure 4. ***Average gram-negative bacterial colony counts based on leaf surface and river proximity*.** The two-three trees' colony counts from each site were averaged together to represent that specific location. While the colony counts in the data are not equal, one-way ANOVA testing found no significant difference in gram-negative bacterial counts based on river proximity (F=0.62, P=0.44).

Discussion

Statistical analysis did not support the hypothesis that the number of microbial colonies would be greater on trees closest to rivers. However, comparative studies show both possible explanations and ways to improve the study for future research. Controlling for age of the leaf, age of the tree, and size of both may be necessary. In this study, the trees collected at the

battlefield were older and taller than the other trees, and leaf age was not taken into account. According to Lindow, young leaves have a higher number of bacteria while older leaves have lower numbers (2003).

Research shows that season can also affect the amount of microbes found in the phyllosphere, specific to the plants growing season. The cooler, rainy months had larger resident microbes compared to the warmer, drier months (Lindow, 2003). Conflictingly, Hunter found that heat and drought increased species richness and diversity for epiphytic microbes. (2010). As the leaves in this study were collected in the late Fall, it seems they should have had more microbes with less species richness and diversity. However, there was difficulty in locating trees with collectable living leaves. Damaged leaves could change the leaf surface and morphology, which had been speculated to affect microbial colonization (Lindow, 2003; Penuelas, 2012).

Proximity to roads that receive a large amount of traffic may also have an effect on the microbial population on leaves. There were an interestingly lower number of bacteria on trees close to roads in this study which prompts the questioning of this possibility. There has been no past finding to suggest that this relationship exists. Further research is needed in this area with a larger sample size to make a solid conclusion.

For future studies, a larger sample size is advised to ensure validity of statistics as well as controlling for the variables previously discussed. While the data in the experiment showed no significant difference of colonization of microbes from trees alongside rivers and trees far from rivers, further research into this relationship is recommended with a larger sample size to ensure validity of statistics as well as adding controls for the variables previously discussed. With these improvements, information about the gram-negative microbial populations within the phyllosphere of this species and others could lead to research on preventative methods for the colonization of both plant-pathogenic and human-pathogenic bacterial species.

Literature Cited

Finkel O, Burch A, Elad T, Huse S, Lindow S, Post A, Belkin S. Distance-Decay relationships partially determine diversity patterns of phyllosphere bacteria on *tamrix* trees across the Sonoran Desert. Appl Environ Microbiol. 2012. [cited 2 Oct 2013]; 78(17): 6187-6193.

Finkel O, Burch A, Lindow S, Post A, Belkin S. Geographical location determines the population structure in phyllosphere microbial communities of a salt-excreting desert tree. Appl Environ Microbiol. 2011. 77(21): 7647-7655.

Hunter P, Hand P, Pink D, Whipps J, Bending G. Both leaf properties and microbe-microbe interactions influence within-species variation in bacterial population diversity and structure in the lettuce (*Lactuca* species) phyllosphere. Appl Environ Microbiol. 2010. 76(24): 8117-8125.

Leveau J. Life on leaves; the surface of plant leaves—the phyllosphere—is home to many microbes. A 'community proteogenomics' approach offers a fresh look at what it takes to survive and thrive in this unique habitat [Internet]. Davis (CA): University of California, Davis; 2009. Available from: http://ic.galegroup.com/ic/scic/AcademicJournalsDetails Page/AcademicJournalsDetailsWindow?failOverType=&query=&prodId=SCIC&windo wstate=normal&contentModules=&mode=view&displayGroupName=Journals&limiter= &currPage=&disableHighlighting=false&displayGroups=&sortBy=&source=&search_w ithin_results=&action=e&catId=&activityType=&scanId=&documentId=GALE%7CA21 0224918&

Lindow S, Brandi, M. Microbiology of the phyllosphere. Appl Environ Microbiol [Internet]. 2003. 69(4): 1875-1883. Available from: http://aem.asm.org/content /69/4/1875.full

Lindow S, Leveau J. Phyllosphere microbiology. Curr Opin in Biotech. 2002. 13:238-243.

Penuelas J, Rico L, Ogaya R, Jump A, Terradas J. Summer season and long-term drought increase the richness of bacteria and fungi in the foliar phyllosphere of *Quercus ilex* in a mixed Mediterranean forest. Plant Bio. 2012. 14:565-575.

Redford A, Bowers R, Knight R, Linhart Y, Fierer N. The ecology of the phyllosphere: geographic and phylogenetic variability in the distribution of bacteriaon tree leaves. Environ Microbiol. 2010. 12(11): 2885-2893.

Measuring Wetland Health with Geochemical Data Loggers

Dheeraj Namburu, Arturas Malinauskas, Gray Tettleton, and Daniel Mehus
School for Science and Math at Vanderbilt University, Nashville

Abstract

Wetlands are an integral component of a variegated and biologically sound ecosystem. As urban development and sprawl occurs, some wetlands are destroyed and replaced with compensatory wetlands created to emulate the destroyed wetlands conditions in order to harbor similar organisms and maintain the biological integrity of the site and its surroundings. The purpose of this project was to monitor compensatory wetlands to determine their effectiveness. Oxidation Reduction Potential and Dissolved Oxygen are measures of wetland health; low DOs correlate to healthy wetlands and organisms taking oxygen. The wetland soils should accept electrons making them reduced, creating low ORPs. To monitor these data, microprocessor controlled self-contained units, with sustainable energy (solar panels) and data logging capabilities were created. An apparatus was designed, built and coded. Microcontrollers for the sensors were mounted on PVC in waterproof housing and sensor ends were submerged in the groundwater at test sites. Initial results showed shifts occurred with weather changes, and multiprobe data showed seasonal shifts correlating to previous studies in similar wetlands. Showing that a data logger can be created and deployed, future directions include perfecting the recording mechanism and allowing both sensors (DO and ORP) to be managed by one microcontroller; eventually it is hoped that more representative guidelines to protect future created wetlands will be established and similar systems will be used to monitor the trajectory of both created and established wetlands.

Introduction

Wetlands are an integral part of the ecosystem due to their ability to sequester carbon, filter out harmful pollution and excess nutrients, and harbor unique wildlife and microbial life. Increasing population and urbanization has required the destruction of many natural wetlands (Brown, 2001). This depletion of natural wetlands has begun to take its toll on ecosystems; attempts to recreate natural wetlands (otherwise known as mitigation wetlands, wetland mitigation banking is the practice of creating, restoring, enhancing, or preserving large off-site wetlands to compensate for authorized impacts to natural wetlands) are often ineffective in adequately replacing all previous functions of the original wetlands (Brown, 2001). Significant chemical indicators of a wetlands health are dissolved oxygen (DO) and oxidation reduction potential (ORP) (Hunt, 2004). With data collected from a chemical monitoring system, a better understanding of wetland ecology can be gained and can assist in creating more efficient

wetlands. This study is necessary due to a dearth of research studies that monitor geochemical wetland characteristics over extended time periods with short temporal resolutions. The objective of the research study was to create a robust long term monitoring system that would collect DO and ORP readings accurately over time. A long term monitoring system will need to be water resistant, structurally robust, and will need the ability to take measurements over long periods of time in adverse weather conditions in the field while being powered by a natural source of energy in order to conclusively determine the progress of a created wetland.

The sites that will host said monitoring systems will be Shelby Bottoms Greenway and Nature Park and Bells Bend Park. Bells Bend is a large municipal park on the floodplain of the Cumberland River that was researched and characterized by TDEC as a possible site for a mitigation wetland. The Shelby Bottoms wetland is a natural wetland that has been established for a long time. Measurements taken at this established wetland will be used to determine the baseline for the new constructed wetland at Bells Bend. Since both wetlands are on the Cumberland River Floodplain, using the established wetland at Shelby Bottoms provides a more accurate approach to determining the progress of the created wetland rather than using a general wetland assessment protocol because they share many properties such as geographical location and a main water source. Using this information, it was possible to determine the proper thresholds for DO and ORP and the unit of time with which the loggers will take measurement to choose a unit of time that will compromise between battery usage and fluctuation resolution.

Figure 1- The two sampling sites. The leftmost pentagon represents the Bell's Bend site, and the one towards the right represents the Shelby park site.

Figure 2-This image shows the monitoring site at Shelby Park, which is outlined in white. (Represented by the rightmost pentagon in figure 1.)

Figure 3- The site at Bell's Bend where initial research was performed. (Represented by the left pentagon in figure 1.)

A primary focus of the research was to improve the efficacy of various types of wetlands, such as restored and natural wetlands, and the functionality of wetlands themselves (Albuquerque, 2009, Brown, 2001, Reddy, 1997). The efficacy of wetlands has traditionally been observed through pollutant removal, resilience to invasive species, and rejuvenation rates of plant life (Reddy, 1997). Information collected in these studies included chemical properties and variables that affect wetlands such as vegetation types and quantity, nutrient levels such as

nitrates and phosphates, DO, ORP, electrical conductivity (EC), pH, and temperature (Hunt, 2004) (Reddy, 1997). Chemical properties that were observed frequently amongst the scientific papers gave this study direction and shed light on which properties were more significant and indicative of the health of wetlands (Hunt, 2004).

Design

A long-term monitoring system for measuring the progress of a mitigation wetland was designed to measure ORP, DO, temperature, and water level in a series of wells that would be dug at a site in the wetland. This apparatus would be 5 feet tall, but the lower 18 inches of the device would be below the surface in order to make contact with groundwater. It needed to house the circuitry in two separate areas, a higher location for the microcontroller and its power supply (solar panel), and a lower location for the DO and ORP stamps. The separation of components was done to make the device more secure from potential animal interference or flooding and allow the probes to be placed deeper into the groundwater. A liquid trap was included between the two circuit's locations to prevent liquids from getting into the sensitive wiring.

Construction

Figure 4- The final apparatus while deployed at a test site.

The final apparatus is shown above in figure 4. The apparatus's wiring was first planned out and figure 5 displays the wiring used between the microcontroller and the stamp to operate the sensor. Two of the microcontrollers were used in each device, one to operate the DO sensor and the other to operate the ORP sensor. It was coded to take a measurement every two hours and write it to the controller's EEPROM.

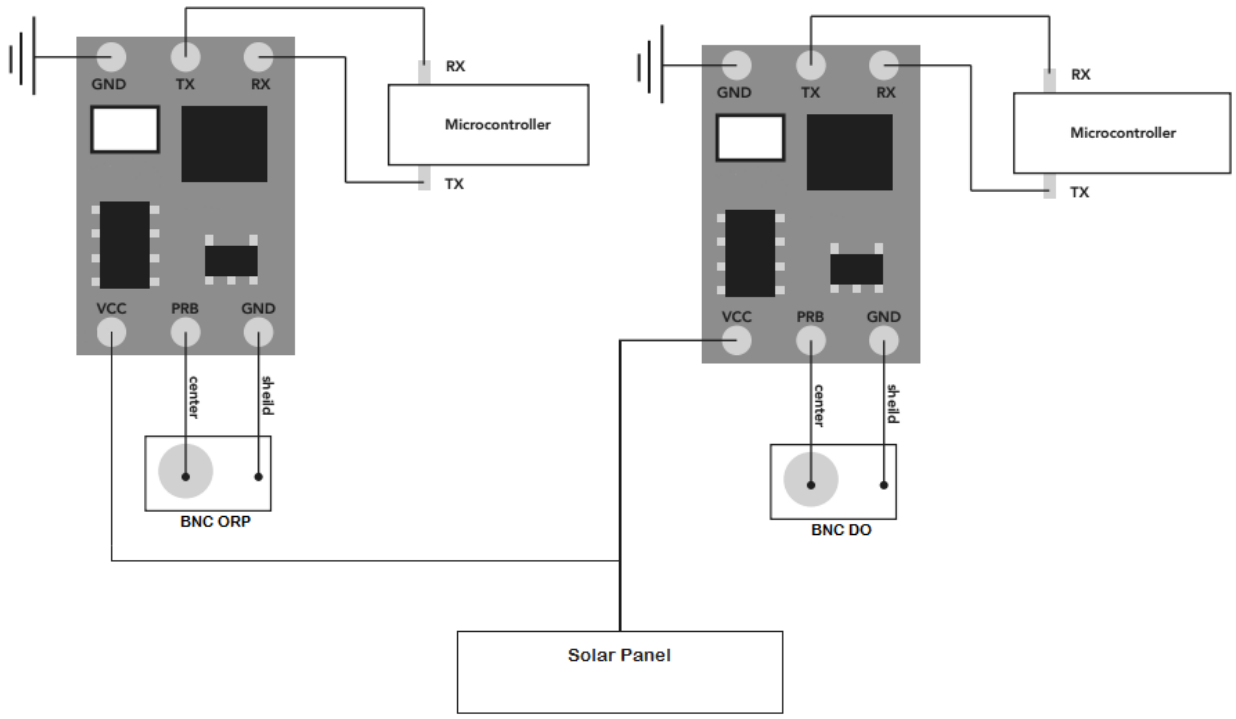

Figure 5- Basic wiring used to connect the sensor (BNC port) to the microcontroller. This was done twice, once for DO and once for ORP. Power went from the solar panel and was fed to both microcontrollers, in parallel.

Waterproof housings were used to house the circuits. A two inch diameter hole was drilled in the bottom of the larger, primary housing. A ring was cut out of Styrofoam and placed around the hole and a PVC joint to reseal the box. Hot glue was used to seal the outside and caulk was used to bind the joint to the box on the outside. A half inch hole was also drilled in the bottom of the larger junction box for the cable connecting the microcontrollers to the solar panel. This hole was sealed with a gasket that was attached to the cord. On top of the primary housing, the solar panel was put inside a transparent map case and attached to the housing. The cable from the primary housing connected the microcontroller to the solar panel. The secondary housing was not modified; a one to two inch connection pipe was used to accommodate the smaller outflow. The circuits were then placed inside the housing. The microcontroller was placed in the primary housing and the stamps for the sensors were put in the secondary housing. Kat5e cable was used to connect the stamps to the controller, and it was soldered at the connections. Appropriate lengths of PVC were cut for the main body, and the liquid trap. The main body is around 66 inches tall, (see figure 1 for the PVC assembly). To connect the PVC pipes, they were first cleaned with PVC cleaner. Immediately afterward, PVC cement was applied to the edge where

two pipes would connect, on both pipes and then glued together. The DO and ORP probe went from the secondary housing into the main PVC chamber where it reached groundwater. A water level sensor was put inside the chamber as well (it didn't need to be connected to the microcontroller; it had its own independent power supply and controller). This sensor took pressure readings that were corrected with a similar sensor attached to the outside of the monitoring system in order to determine water level depth.

Testing

Throughout the construction process, the code and electronics were tested to ensure proper functionality before field deployment. Breadboards were used initially to test the ability of the microcontroller to run off of solar power and produce accurate measurements of samples with known values of DO or ORP. Water was applied to areas that were supposed to be watertight to ensure there were no leaks. Finally, when the monitoring system was fully assembled, it was deployed in a wetland overnight, in the rain. A second system was also assembled and was to be deployed at Bell's Bend, but the lack of groundwater meant the system was not able to take measurements. The first system was able to take accurate readings throughout a test night and was powered by stored solar power. Additional data was taken throughout a few seasons in established wetlands with multi-probes to ensure our test results for the monitoring system were valid. It also was used to establish a baseline of an established wetland that could be used to identify the progress of a mitigation wetland.

Results

The purpose of this experiment was to create a long term wetland monitoring unit that can take readings for both ORP and DO. The technology being used is only just past the development phase, therefore, the results being presented are mainly to prove the functionality of the monitoring units and to establish a baseline for future research using these units. Figure 2 is a representation of the area in which all of the presented results were collected. Graphs 1 and 2 both display data gathered at the site pictured in figure 2. Graph 1 shows the dissolved Oxygen Readings gathered from the monitoring site over the course of three seasons, and Graph 2 shows the ORP readings from our multiprobe. Both of these were used because the monitoring units were expected to read both ORP and DO. The DO graph shows what would be expected, that the

DO level would decrease during the hotter drier weather of the summer. The ORP graph shows higher levels during the winter and spring and lower levels during the summer. As lower ORP is preferable to wetland plant life, it appears that the summer this year was best for plant growth while the spring and summer were not as much. Referring to Graph 3, displaying the data gathered during the overnight functionality test, The results vary from -20mV to -140 mV, which makes sense for the season in which they were gathered. At this point, the data logger would be about ready to proceed with useful, relevant research use.

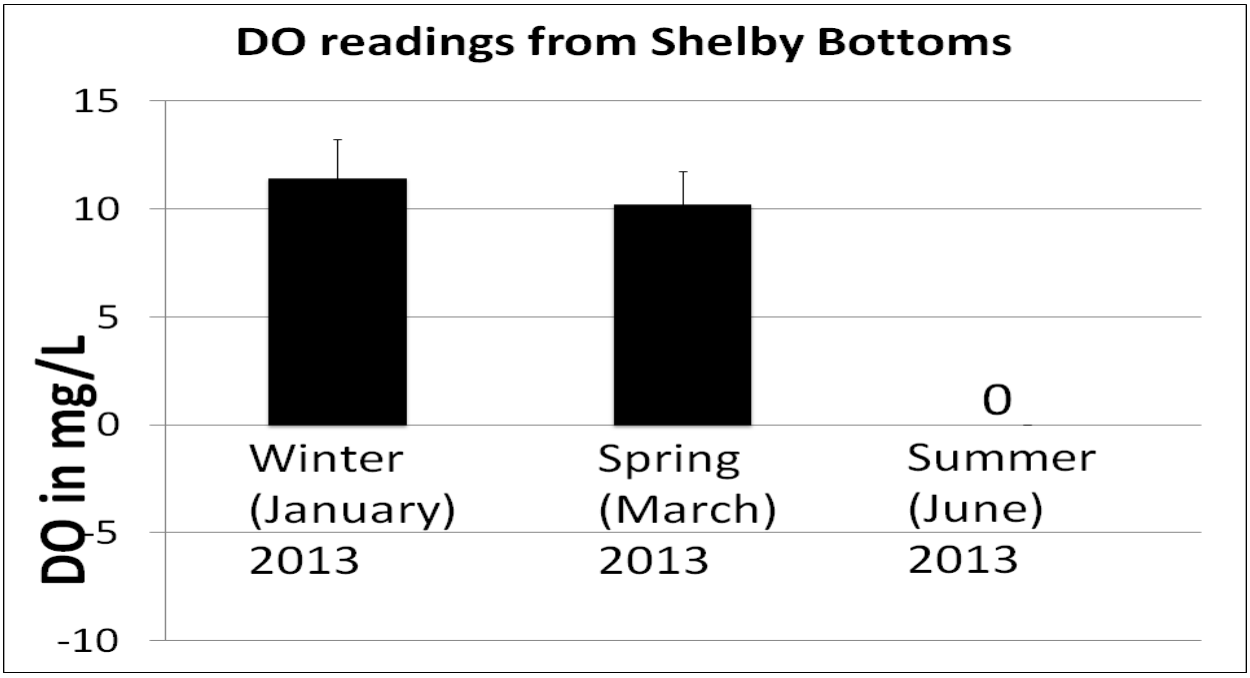

Graph 1- Dissolved oxygen readings received from the field site at Shelby Park over different seasons.

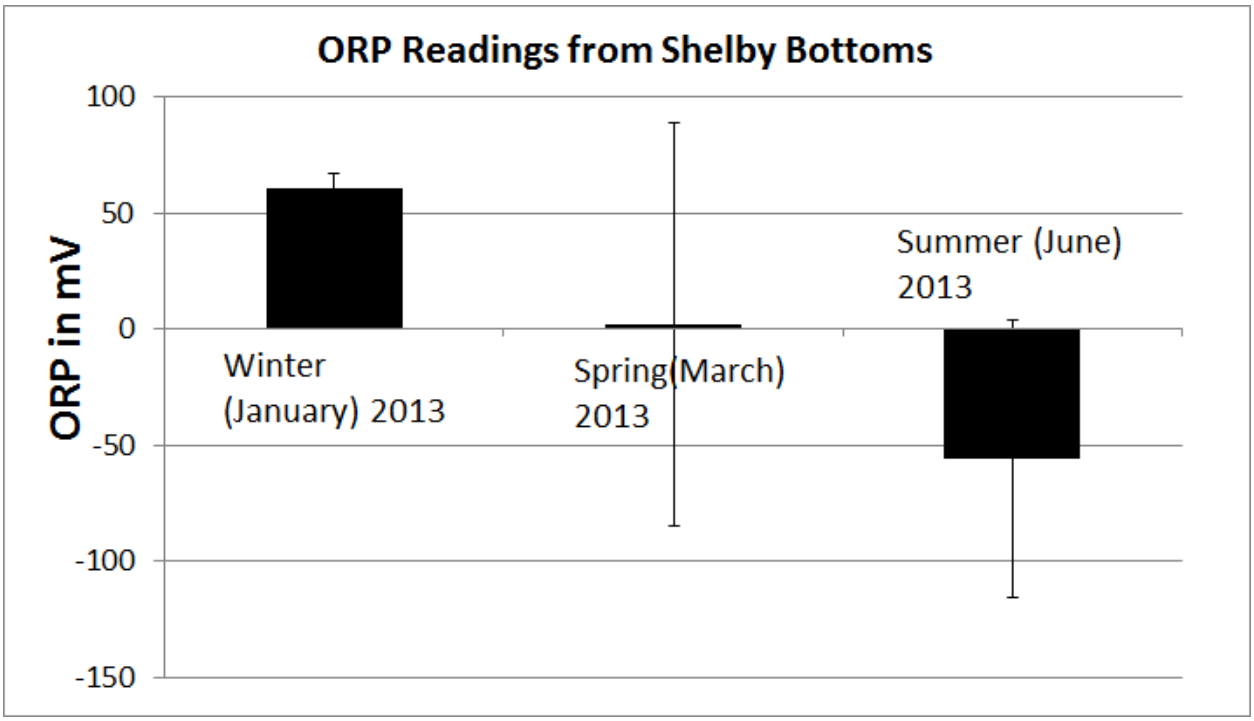

Graph 2- Oxidation Reduction Potential readings gathered at Shelby Park, also over the course of three seasons.

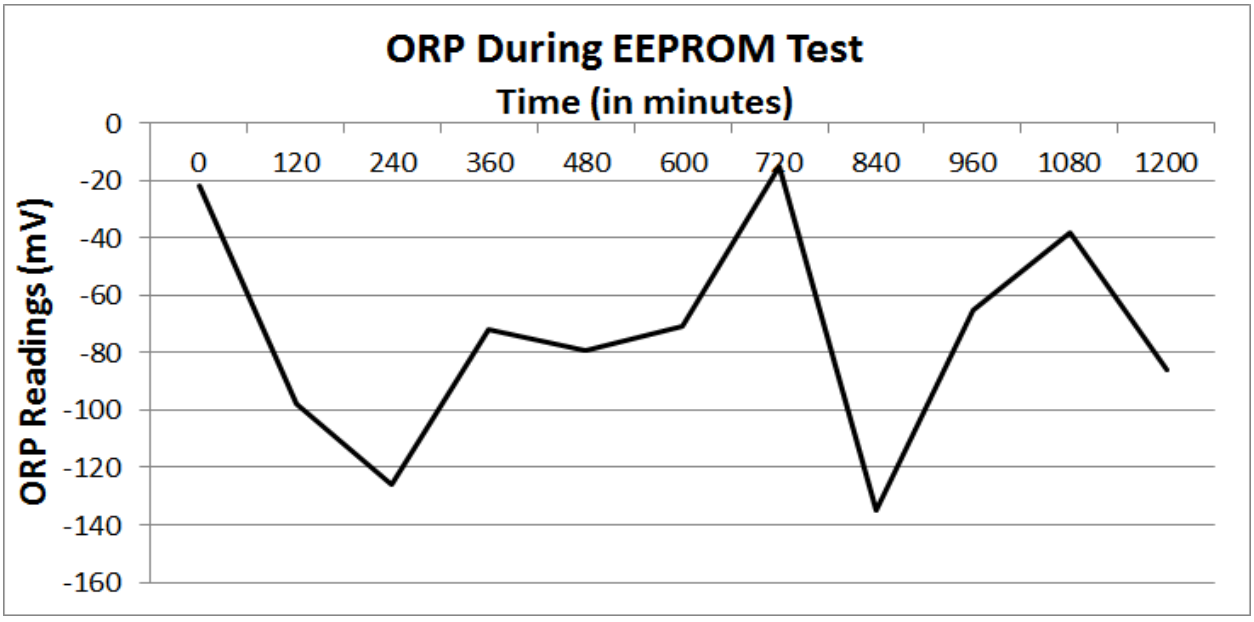

Graph 3- Temporal variability of ORP during an overnight 20-hour field deployment test at the Shelby Bottoms wetland.

Conclusion

Based on multiprobe data, ORP and DO readings increased during wetter months and

decreased in the dry summer. This was confirmed due to seasonal fluctuations found in several field visits. The monitoring system took measurements every hour, a temporal resolution suitable for wetland fluctuation data logging; we found large fluctuations when taking measurements every hour using the data monitoring systems. When field visits were conducted ORP and DO did not change significantly in smaller temporal units. Based on the multiprobe readings, DO probes were functional and gave correct readings, the ORP probes may need more fine-tuning and calibration. Our setup was waterproof and stayed powered on throughout the night without sunlight. The successful probe setup is a novel method that can be used to monitor and assess created wetlands in the future, and will allow for the further development of quantitative guidelines and assessment protocols rather than current qualitative measurements. This study's results also correlate with trends determined by a research study with similar wetlands (Hunter, 2004).

In the future we would like to optimize our code to utilize an ENV data logger stamp and make our setup run using only one microcontroller. Furthermore we would like to successfully deploy three functional units in a wetland and collect data once water levels have returned within twelve inches of the surface. Further investigation would include a comparison of a potential wetland's properties to an established one and revision of the weatherproofing of the data loggers. The use of different wires and mounting equipment will be needed to use our device for a long-term application and improve the durability of the devices.

Acknowledgements

We would like to thank the School for Science and Math for being our research facility. Furthermore we would like to thank the instructors at the School for Science and Math, particularly Dr. Chris Vanags and Dr. Mary Loveless for and assisting us through our various problems. We would like to thank the Tennessee Department of Transportation for their generous grant facilitated through Friends of Bells Bend for allowing us to conduct our research. We would also like to thank Atlas Scientific for providing technical support. We would further like to thank Randy Phillips of the Tennessee Department of Environmental Conservation for supporting our research and for helping us with field research.

Literature Cited

Albuquerque, a, Oliveira, J., Semitela, S., & Amaral, L. (2009). Influence of bed media characteristics on ammonia and nitrate removal in shallow horizontal subsurface flow constructed wetlands. Bioresource technology, 100(24), 6269–77. doi:10.1016/j.biortech.2009.07.016

Brown, S. C., & Veneman, P. L. M. (2001). Effectiveness of compensatory wetland mitigation in Massachusetts, USA. Wetlands, 21(4), 508–518. doi:10.1672/0277-5212(2001)021[0508:EOCWMI]2.0.CO;2

Hunt, P. G., Sadler, E. J., & Evans, D. E. (2004). Characterization of oxidation-reduction processes, *20*(2), 189–200.

Reddy, K., & D'Angelo, E. (1997). Biogeochemical indicators to evaluate pollutant removal efficiency in constructed wetlands. Water Science and Technology, 35(5), 1–10. http://www.sciencedirect.com/science/article/B6VBB-3T7J1NV-2/1/d661fd859ef02d960d6fc97c2acae812

Low Levels of Caffeine Protect the Brain Following Stroke

Faris Wasim
Montgomery Bell Academy, Nashville

ABSTRACT

Stroke is the fourth leading cause of permanent disability in industrialized nations.[1] There are many risk factors for Stroke, and treatment is available. However, the treatment has to be administered within 3 hours of stroke onset and it cannot repair damage caused to the blood vessels in the brain.[2, 3] The purpose of this study was to evaluate whether lower levels of caffeine can protect the brain in the event of stroke. This study showed that low levels of caffeine increase nitric oxide production leading to vasodilation of blood vessels in the brain. The vasodilation leads to increased locomotor behavior, reduced infarct volume and increased expression of Adenosine receptor type 2b, KDR and Flt1 receptor expression. These receptors are known to contribute to new blood vessel formation.

INTRODUCTION

Stroke is the leading cause of permanent disability in industrialized nations.[1] Stroke leads to an interrupts blood flow to the brain. The interrupted flow causes a lack of oxygen to the brain cells which causes damage and death of the brain cells. Loss of these cells in the brain may lead to impaired speech, memory and movement. There are many risk factors for stroke: being over 53 years old, a family history of stroke, high cholesterol, smoking, being overweight, and high blood pressure.[4] Eventhough treatment is available for stroke, it cannot repair damage caused to the blood vessels in the brain.

There are two main types of stroke: Ischemic[5] and hemorrhagic[6] stroke. Ischemic stroke is more common and occurs in more than 75% of the population.[1] This type of stroke occurs due to the fatty material build up in an artery in the brain. The buildup leads to a clogging of the artery and leads to restriction of blood flow to the brain. Ischemic stroke can also occur if a clot travels from a different part of the body and lodges in the brain thus preventing further blood flow to the brain cells. A hemorrhagic stroke is less common and occurs when a blood vessel in the brain ruptures and bleeds into the space between the brain and the skull. Once a stroke has occurred, the patient has to be rushed to the hospital for treatment. If the patient is treated within two hours of the onset of stroke, the damages can be reversed. However, patients do not usually arrive to the hospital within the three-hour window, leading to damage to the blood vessels of the brain.[1]

Since caffeine is a commonly consumed active ingredient worldwide, several studies have focused on the effect of caffeine on the brain and stroke.[7] A majority of the studies report that higher consumption of caffeine leads to detrimental effects in the brain.[7] In this study we hypothesized that lower levels of caffeine protect the brain in the event of stroke and that it can promote new blood vessel formation in the brain following stroke.

METHODS

Animals. A total of 21, nine week old, Sprague Dawley rats were used in this experiments. All protocols were approved and every effort was made to minimize pain and the numbers of animals used for this study. Animals were divided into three groups of 7 animals each: untouched controls, stroke alone and stroke+caffeine. All reagents were obtained from Fisher Scientific (Waltham, MA) unless otherwise noted.

Nitric Oxide production in Rat Brain Endothelial cells. Rat brain endothelial cells were commercially obtained (Cell Applications, Inc; San Diego, Ca) and grown per manufacturers protocol. Twenty thousand cells were seeded per well of a 96 well plate (BD biosceinces; San Jose, CA) and either left untreated, treated with increasing concentrations of caffeine (0.25mM, 0.5mM, 0.75mM and 1mM). L-Argnine was added to each well to provide the cofactor for nitric oxide production. 4-amino-5-methylamino-2',7'-diflurescein diacetate (DAF-FM), a fluorescent dye used to measure nitric oxide production was also added to each well at a concentration of 10uM. DAF-FM diacetate passively diffuses across cell membranes and becomes deactylated by nitric oxide to produce a fluorescent DAF-FM product. The fluorescent product can then be quantified on a plate reader. The cells were placed in a plate reader (Biotek; Winooski, VT) and the amount of Nitric Oxide produced measured in relative fluorescence units.

Caffeine Administration. Caffeine (0.25mM) was dissolved in water and administered IP once before stroke was induced in the animals.

Endothelin-1 (ET-1) model of stroke. Animals were acclimated to their environment and their behavior recorded in a Phenotyper cage. Animals were subjected to ET-1 induced stroke; seven animals received a stroke alone and seven animals received a low dose (0.25mM)

of caffeine prior to the stroke. Et-1 causes an ischemic stroke.[8] Briefly, rats underwent an intracranial placement of a guide cannula, followed by induction of Middle Cerebral Artery Occlusion (MCAO) using Endothelin-1 (ET-1) as previously described.[8] Briefly, rats were anesthetized with 5% Isoflurane and maintained under 2% Isoflurane in a stereotaxic frame (Stoelting Co, Wood Dale, IL) for the duration of both procedures. For the cannula, a midline incision was made to expose the skull, and a stainless steel guide cannula was implanted into the right hemisphere using the following stereotaxic coordinates [+1.6mm anterior, +5.2mm lateral, -4.5mm ventral relative to Bregma]. After three days of recovery, the rats underwent MCAO by infusing 3ul of 80umol (1ul/minute) ET-1. All animal surgeries were performed by a trained technician.

Automated Open Field Assessments. Locomotor activity was tracked via the center point, nose point, and tail base of the animal. Rats were video recorded in the Noldus Phenotyper cage (Noldus Information Technology; Leesburg, VA) for 2 hours pre-stroke and 24hrs post-stroke. The Phenotyper cage was divided into 'zones' using the Ethovision XT software. Separate zones were created for the water-spout area and feeder tray area, as well as the four walls of the cage for rearing frequency. Data was analyzed using EthoVision XT software, using the following parameters: distance moved (distance travelled (cm) by defined body point), nose at water spout frequency (number of times nose point enters defined 'water spout zone' during recording period), Nose at feeder tray frequency (number of times defined nose point enters defined 'feeder zone' during recording period), and rearing frequency (number of times defined body point enters defined 'wall zones' during recording period).

Infarct Size Quantification. To confirm presence of stroke, animals were sacrificed at 24 hours post stroke and tissue infarct was determined by staining 2 mm coronal sections with 3,5-triphenyltetrazolium chloride (TTC). Infarct size was quantified using Image J software as previously described.[8]

Gene Expression analysis. Following the behavior, animals were sacrificed and their brain removed, flash frozen in liquid nitrogen and stored at -80 degrees till ready for analysis. Brain samples were homogenized and mRNA extracted from each sample per manufacturers protocol (BioRad; Hercules, CA). DNASEI was used to remove any contaminating genomic

DNA from the samples. The harvested mRNA was then reverse transcribed into cDNA using iScript (BioRad; Hercules, CA). Gene specific primers were used to amplify genes for Adenosine receptor type 2b, KDR and Flt1.

Data Analysis. All statistical analysis was performed using the Students t-test or one-way ANOVA (GraphPad Software, Inc. La Jolla, CA, USA). A p value of less than 0.05 was considered to be significant and is indicated on subsequent graphs with an asterisk.

RESULTS

To determine whether lower concentrations of caffeine sustained high levels of nitric oxide production, a DAF-FM assay was conducted on rat brain endothelial cells in vitro. Figure 1 shows that nitric oxide production was highest at the lower concentrations of caffeine. Increasing concentrations of caffeine lead to decreasing concentrations of nitric oxide production.

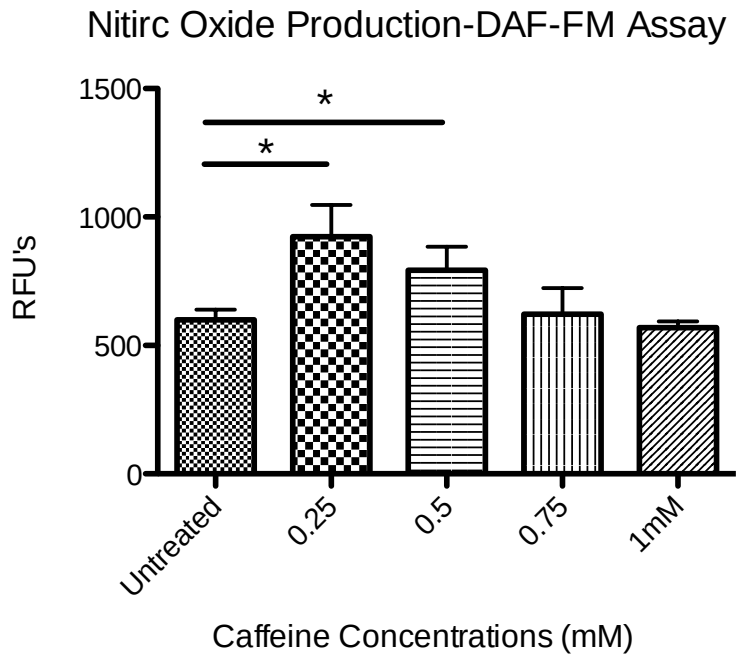

Figure 1. Nitric oxide Production by Rat Brain Endothelial Cells. Rat brain endothelial cells were treated with increasing concentrations of caffeine and the amount of nitric oxide generated was measured using DAF-FM. Nitric Oxide production was highest at the 0.25mM concentration of caffeine and lowest at 1mM of caffeine. *p<0.05

Figure 2 shows a representative track plot of an animal pre stroke (Figure 2A) and post stroke (Figure 2B) and post stroke+caffeine. The turquoise path delineates the nose, red

delineates the center of the animal and purple delineates the tail base of the animal. Visual inspection of the tracks created by the animals before and post stroke indicated that animals displayed a healthy exploratory behavior prior to the stroke in an open field, and post stroke, a substantial decrease can be seen in the exploratory activity post-stroke, with activity that once comprised the entirety of the Phenotyper cage becoming limited to circling in the top-right of the arena. Closer inspection of the track plots also indicates the frequency of the nose spout at the feeder and water tray pre-stroke. Post stroke, however, the representative animals' nose was not recorded in the feeder or the water zone. Figure 2C shows a represeantative plot from an animal which received stroke+caffeine and the plot indicates that the animal had more mobility than the stroke alone animal. The distance which the animals moved were quantified as an assessment of mobility (Figure 2D). When compared to pre-stroke values, there was a significant decrease in the distance moved, pre-stroke: 5094±7825 cm vs. post stroke: 1748±876 cm; stroke+caffeine showed a significantly higher distance moved: 2937±1044. Rearing frequency showed a significant decrease post stroke (pre stroke=225±36 and post stroke=116±65). While the stroke+caffeine group did not exhibit a significant difference compared to stroke alone, there was a trend towards an increase in rearing frequency (Figure 2E). The nose point of the animals was defined to track their eating and drinking habits throughout the duration of recording. There was a significant reduction in the frequency that the animals spent at both the water bottle (Figure 2F; pre stroke: 68±28 and post stroke: 15±15) and the feeder tray (Figure 2G; pre stroke: 42±16 and post stroke: 15±10). The stroke+ caffeine group was significantly higher in both the feeder tray (50±16) and water bottle groups (28±9).

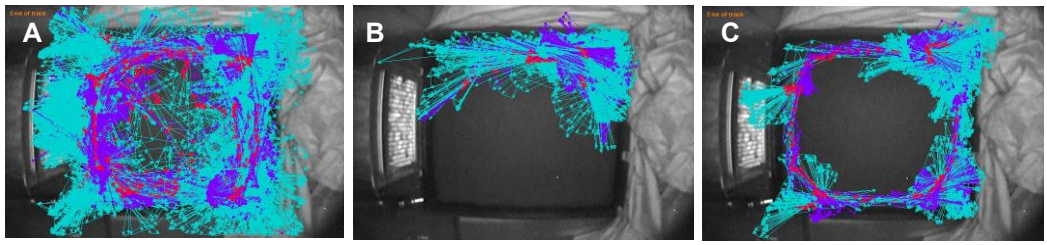

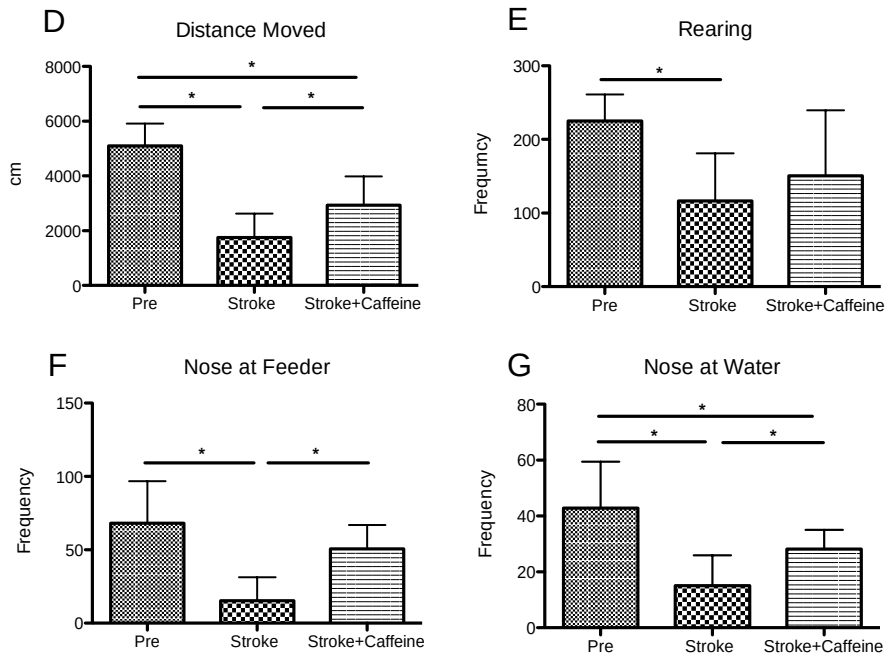

Figure 2. *Locomotor Behavior. Animals were placed in a Phenotyper cage pre –stroke and 24 hours post stroke to assess their behavior. The Phenotyper tracks the nose (turquoise), tail (purple) and center (red) of each animal. A. representative locomtor pre-stroke plot. B. Representative post stroke plot. C. Representative post stroke+caffeine plot. D. Total distance moved was significantly higher in the stroke+caffeine group compared to stroke alone. E. Rearing frequency was higher in the stroke+caffeine group (not statistically significant). F. Nose of the animals were detected more frequently at the feeder tray in the stroke+caffeine group. G. Nose of animals was detected more frequently at the water bottle in the stroke+ caffeine group. *P<0.05.*

It has already been widely reported that Stroke leads to a decreased blood flow to the brain.[8, 9] Since we have already shown that lower levels of caffeine lead to significantly higher levels of nitric oxide production (Figure 1), which in turn leads to vasodilation, we reasoned that the stroke+caffeine group would have higher blood flow to the brain. Figure 3 shows that the stroke+caffeine group did indeed have significantly higher blood flow to the brain compared to the stroke alone group (stroke alone=35±9, stroke+caffeine=156±52). The presence of white, non-stained (infracted) tissue in right cortex and striatum confirmed successful ET-1 induced ischemia in all of the animals in the stroke alone group. The stroke+caffeine group had significantly reduced infarct volumes (Figure 4) in the brain.

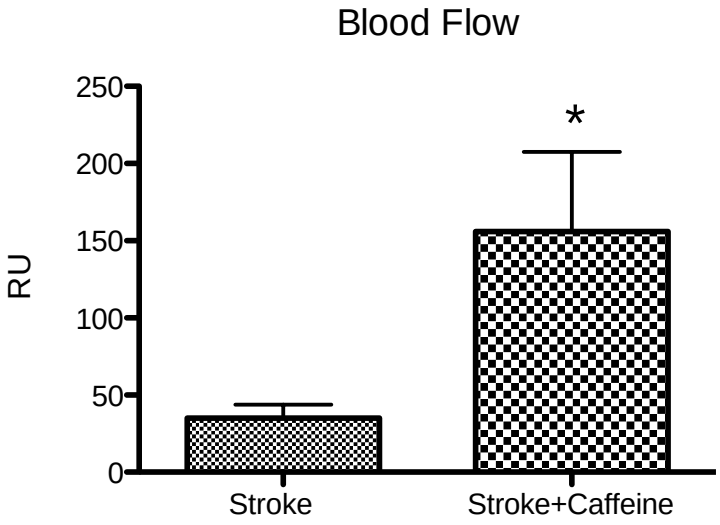

*Figure 3. Blood flow measurements. Blood flow was measured using a Doppler; blood flow was significantly higher in the stroke+caffeine group. *P<0.05*

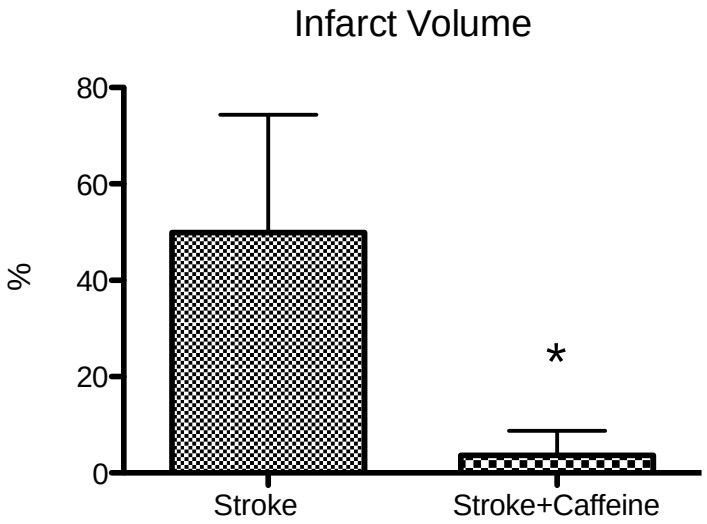

Figure 4. *Brain infarct volume following stroke. Infarct volume was significantly lower in the stroke+caffeine group indicating that caffeine was able to protect the brain during a stroke. *P<0.05*

Gene expression studies were done in an attempt to explain how the lower levels of caffeine were able to lead to a rescue of the brain following stroke. Levels of Adenosine receptor Type 2b (A2B), KDR and Flt1 were assessed. Figure 5 shows that all 3 receptors were significantly higher in the stroke+caffeine treated group.

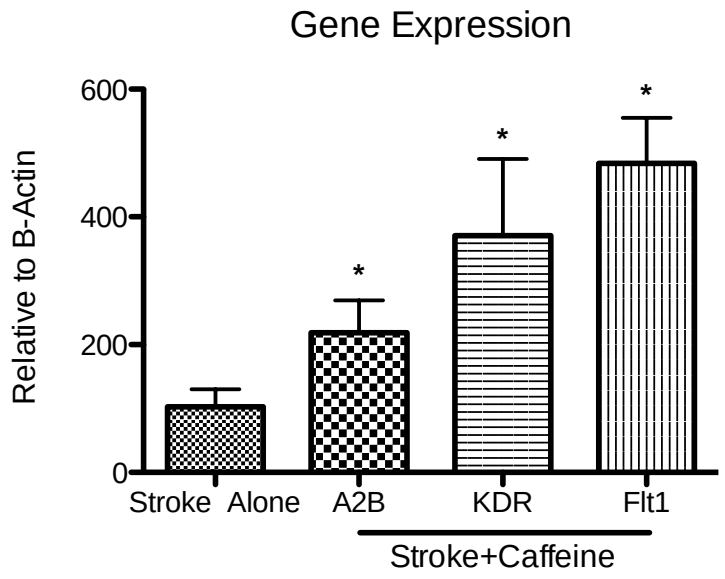

*Figure 5. Gene expression for A2B receptor, KDR and Flt1 was significantly higher in the stroke+caffeine group. *P<0.05*

DISCUSSION

This study supports the hypothesis that lower levels of caffeine protect the brain in the event of a stroke. The study showed that low levels of caffeine: increase nitric oxide production (Figure 1), increase locomotor behavior in animals (Figure 2), increase blood flow to the brain (Figure 3), reduce infarct volume to the brain (Figure 4) and increase expression of A2B, KDR and Flt1 receptors (Figure 5). Based on the in vitro data that showed that nitric oxide levels are increased with lower concentrations of caffeine, we infer that caffeine leads to vasodilation of the blood vessels in the brain. Vasodilation of blood vessels promotes blood flow to the brain[10] and prevents a severe stroke. This experiment was done invitro to avoid using large numbers of animals just to determine an effective concentration for the caffeine.

The locomotor behavior of the animals was assessed using an automated Phenotyper cage and the Ethovision XT software. This method provided detailed analysis of the motor behavior of the animal in the three groups and avoided subjective manual scores as used in other studies. The animals, understandably, moved less post stroke and this effect also showed a significant increase with the caffeine administration (Figure 2D). Rearing is a natural exploratory behavior for rodents, which also decreased post stroke. Even though we saw an increasing trend in rearing

behavior in the caffeine+stroke group, we did not see a significant increase in the rearing behavior post stroke, possibly due to a small 'n' in each group. The representative track plots clearly show that the animals' nose was detected at the feeder tray and the water bottle pre stroke and both of these frequencies decreased post stroke. Caffeine administration rescued this frequency towards the pre-stroke values. However, the mere presence of the animals' nose at the feeder tray or the water bottle does not indicate that the animals did actually eat or drink. One drawback of the software is that it only reports the presence of the nose at these points rather than an actual 'eating' or 'drinking' event.

Since the lower levels of caffeine do lead to increased nitric oxide production (Figure 1), it is reasonable to assume that the increased nitric oxide causes the vasodilation, hence the significantly higher blood flow to the brain in the stroke+caffeine group (Figure 3). If a vessel is already dilated in response to the caffeine, then the ET-1 probably cannot cause enough of a constriction of the brain blood vessels to cause a severe stroke, hence the reduced infarct volume (Figure 4).

While the gene expression studies implicate an upregulation of the A2b, KDR and Flt1 receptors, it remains to be seen whether this holds at the protein levels as well. Western blotting for the levels of these receptors and their downstream signaling molecules need to be evaluated to further confirm these results. Caffeine is structurally similar to Adenosine;[11] Adenosine binds to its receptor (A2B) and leads to new blood vessel formation.[12] In addition, activation of the A2B receptor also activates the KDR and Flt1 receptors, both of which are also responsible for augmenting new blood vessel growth.[13] An upregulation in the gene expression of all of these receptors indicates that low levels of caffeine may drive formation or repair of damaged blood vessels in the brain following stroke.

Further studies need to be conducted to confirm these preliminary data. Larger groups of animals need to be studied to get a better understanding of the true effects of lower concentrations of caffeine on the brain. It is entirely possible that even lower levels of caffeine exhibit significantly higher levels of protection for the brain. Additional experiments need to be conducted to ensure that the caffeine is indeed working through the Adenosine, KDR and Flt1 receptors. A nitric oxide inhibitor such as NG-Nitro-L-Arginine Methyl ester[14] needs to be administered prior to the caffeine to assess whether it abrogates the beneficial effects of low levels of caffeine. The caffeine in this study was also administered prior to a stroke, which

would benefit coffee drinkers, however, further studies should evaluate the effect of low levels of caffeine in non-coffee drinkers. In addition, the time course of caffeine administration should be increased to evaluate whether it can be administered 24 hours post stroke to achieve a similar benefit.

Literature Cited

1. Lloyd-Jones DM, Hong Y, Labarthe D, Mozaffarian D, Appel LJ, Van Horn L, Greenlund K, Daniels S, Nichol G, Tomaselli GF, Arnett DK, Fonarow GC, Ho PM, Lauer MS, Masoudi FA, Robertson RM, Roger V, Schwamm LH, Sorlie P, Yancy CW, Rosamond WD. Defining and setting national goals for cardiovascular health promotion and disease reduction: The american heart association's strategic impact goal through 2020 and beyond. *Circulation*. 2010;121:586-613

2. Tissue plasminogen activator for acute ischemic stroke. The national institute of neurological disorders and stroke rt-pa stroke study group. *The New England journal of medicine*. 1995;333:1581-1587

3. Chapman SN, Mehndiratta P, Johansen MC, McMurry TL, Johnston KC, Southerland AM. Current perspectives on the use of intravenous recombinant tissue plasminogen activator (tpa) for treatment of acute ischemic stroke. *Vascular health and risk management*. 2014;10:75-87

4. Machalinski B, Paczkowska E, Koziarska D, Ratajczak MZ. Mobilization of human hematopoietic stem/progenitor-enriched cd34+ cells into peripheral blood during stress related to ischemic stroke. *Folia histochemica et cytobiologica / Polish Academy of Sciences, Polish Histochemical and Cytochemical Society*. 2006;44:97-101

5. Neuhaus AA, Rabie T, Sutherland BA, Papadakis M, Hadley G, Cai R, Buchan AM. Importance of preclinical research in the development of neuroprotective strategies for ischemic stroke. *JAMA neurology*. 2014

6. Shovlin CL, Chamali B, Santhirapala V, Livesey JA, Angus G, Manning R, Laffan MA, Meek J, Tighe HC, Jackson JE. Ischaemic strokes in patients with pulmonary arteriovenous malformations and hereditary hemorrhagic telangiectasia: Associations with iron deficiency and platelets. *PloS one*. 2014;9:e88812

7. Lee SM, Choi NK, Lee BC, Cho KH, Yoon BW, Park BJ. Caffeine-containing medicines increase the risk of hemorrhagic stroke. *Stroke; a journal of cerebral circulation.* 2013;44:2139-2143

8. Regenhardt RW, Desland F, Mecca AP, Pioquinto DJ, Afzal A, Mocco J, Sumners C. Anti-inflammatory effects of angiotensin-(1-7) in ischemic stroke. *Neuropharmacology*. 2013;71:154-163

9. Min LJ, Mogi M, Tsukuda K, Jing F, Ohshima K, Nakaoka H, Kan-No H, Wang XL, Chisaka T, Bai HY, Iwanami J, Horiuchi M. Direct stimulation of angiotensin ii type 2 receptor initiated after stroke ameliorates ischemic brain damage. *American journal of hypertension*. 2014

10. Paulson OB, Strandgaard S, Edvinsson L. Cerebral autoregulation. *Cerebrovascular and brain metabolism reviews*. 1990;2:161-192

11. Ribeiro JA, Sebastiao AM. Caffeine and adenosine. *Journal of Alzheimer's disease : JAD*. 2010;20 Suppl 1:S3-15

12. Feoktistov I, Goldstein AE, Ryzhov S, Zeng D, Belardinelli L, Voyno-Yasenetskaya T, Biaggioni I. Differential expression of adenosine receptors in human endothelial cells: Role of a2b receptors in angiogenic factor regulation. *Circulation research*. 2002;90:531-538

13. Takagi H, King GL, Ferrara N, Aiello LP. Hypoxia regulates vascular endothelial growth factor receptor kdr/flk gene expression through adenosine a2 receptors in retinal capillary endothelial cells. *Investigative ophthalmology & visual science*. 1996;37:1311-1321

14. Losonczy G, Mucha I, Muller V, Kriston T, Ungvari Z, Tornoci L, Rosivall L, Venuto R. The vasoconstrictor effects of l-name, a nitric oxide synthase inhibitor, in pregnant rabbits. *British journal of pharmacology*. 1996;118:1012-1018

Microorganism Presence in the Decomposition of Flesh

Emily McRen

Pope John Paul 11 High School, Hendersonville

Abstract

The environment of decomposition often determines how fast flesh decomposes and the presence of microorganisms in decomposition. In this experiment, since pork most closely resembles human flesh, 5-pound cuts of ham were composted in varying levels of aeration and moisture in order to determine how the decomposition rate was affected. The hams in the warmer, moister environments were hypothesized to decompose much faster. Temperature was measured during data collection to indicate the levels of decomposition that could not be directly observed. After six weeks, the hams were uncovered and samples were taken in order to culture the microorganisms found during the process of decomposition. Both the qualitative level of decomposition and the cultures of bacteria and fungi further illustrated the role of environment in determining aerobic versus anaerobic decomposition in flesh. The results of this experiment did not necessarily confirm that warmer, moister environments were ideal for fastest decomposition. However, the results conclusively indicated that rather than temperature and moisture in the compost, oxygen levels were most indicative of decomposition speed, and that aerobic decomposition works more quickly than anaerobic decomposition

Introduction

In the forensic field, decomposition is defined as "physical disintegration, finishing when all organic material is converted into inorganic compounds" (Mann 1990). The study of decomposition potentially elucidates why certain variables change both the rate and illustration of decomposition in the human body (T. Saul, personal communication, October 22, 2012). Such variables can create ideal environments for bacteria, which play a crucial role in facilitating the aforementioned conversion of organic material into inorganic compounds (Mann 1990).

As noted in a tropical Pacific study on human decomposition, high temperatures, high humidity, and high rainfall "improved the conditions for bacterial growth and hastened the putrefaction of the tissues" (Spennemann & Franke, 1995). Of all meats, pork most closely resembles human flesh; therefore, in this experiment, five bone-in picnic hams were decomposed under a variety of conditions that would test the effects of higher temperature and greater moisture levels on bacterial growth in carrion. Insect activity may have also affected the samples, but for this experiment the focus will be on bacterial growth and activity within the hams.

During data collection, the hams were placed in wire cages in order to keep mammals from damaging the samples or interfering with decomposition (Schoenly 2006). Five hams decomposed on bare soil under varying conditions: (1) completely exposed to all elements, (2) buried in soil with aeration, (3) buried in soil with aeration and covered with a tarp, (4) buried in soil without aeration, and (5) buried in soil without aeration and covered with a tarp (M. Farone, personal communication, July 22, 2013). Using this method of "composting" the hams, a difference in temperature was achieved without the need for different locations. Keeping two of the samples aerated and leaving two undisturbed allowed a look into aerobic and anaerobic decomposition and also had an influence on the temperature of the specimens. Aerobic compost, theoretically, would decompose at a higher rate because the microorganisms that break down the meat have increased access to oxygen. Anaerobic decomposition does not require oxygen; however, while some anaerobic decomposers thrive without oxygen, anaerobic decomposition in organic matter progresses more slowly than aerobic decomposition (Kristensen et al. 1995). If the specimens of meat were placed in varying aerobic and levels of moistness, then the hams in warmer, moister environments will decompose most quickly, when anaerobic conditions generate and insulate more heat than aerobic conditions. The insulation of heat and moisture would encourage ideal conditions for bacteria to develop, and therefore facilitate the decomposition of organic matter into inorganic compounds. After several weeks, samples from each ham would be taken and cultured to determine the presence and level of microorganisms in each sample.

Materials and Methods

This experiment required five bone-in hams in a Boston butt cut, two raised 6'x18"x10" garden beds, two wood/chicken wire mats, compost-additive-free soil filler, and two 2'x2' squares of construction-grade non-insulating tarp, and six bungee cords. Additional materials included disposable gloves, a baking scale, an extendable internal meat thermometer, sterile q-tips, sandwich bags, plates poured with nutrient agar, a permanent marker, and a refrigerator.

Five bone-in Boston butts were used to emulate the decomposition of human flesh and were subject to different environmental factors to test the role of microorganisms in decomposition. The hams were placed in two raised garden beds, and wood/chicken wire mats were constructed over the beds, similar to a cage, to protect the samples from outside interference in decomposition. The wire mats were made by measuring wood to fit the perimeter

of each bed, securing one length of wood to the side of the bed, and stapling the chicken wire to the wood. The beds were filled with an expanse of bare soil and topsoil, without any added composting factors, and labeled numerically 1-5.

The weight and temperature were recorded for each ham using a baking scale (accurate to a fraction of an ounce) and an extendable internal meat thermometer. The samples were then placed in the beds with respect to their variable environment. Sample 1 was placed on top of the soil, 2-5 in the soil; 4 and 5 were also covered with a construction-grade non-insulating tarp. The beds were then shut and kept closed by three hooked bungee cords per bed. Two days later, the temperature was taken for all of the samples, and the weight was recorded for 1, 2, and 4. Due to the nature of the anaerobic samples, weight was not able to be measured in 3 and 5. Temperature was successfully measured with the extendable internal meat thermometer, which was able to determine the internal temperature of the samples without necessitating that the anaerobic compost piles be disturbed. Temperature was measured again in week 4 and week 6 day 4 (final day) of the experiment.

After the data collection period was over, each sample was swabbed two separate times with sterile swabs. The two swabs were used to inoculate two nutrient agar plates per variable ham, and the eight plates were labeled according to their number. The hams were disposed of using sealed plastic bags and thrown away. The soil was taken out of the beds, and the beds were recycled for their intended use. The samples were left in room temperature to grow for four days. After the fourth day, the plates were refrigerated to stop growth and then analyzed.

Data and Analysis

Each sample was numbered in order to indicate its tested variable, and will be referred to by number. Chart 1 provides the system by which they were numbered.

Chart 1

Sample	Condition
1	control exposed to all elements
2	aerobic exposed to moisture
3	anaerobic exposed to moisture
4	aerobic protected from moisture (covered)
5	anaerobic protected from moisture (covered)

During intervals in the experiment, both the weights and temperatures of the samples were taken. Because the anaerobic samples could not be exposed to oxygen, the method of measuring weight (including complete removal from soil and return to freshly turned soil) could not be used on samples Three and Five. Though weight was not included in the final data collection, the initial weight measurement was necessary to make sure that the size of the samples was as close as possible.

Figure 1

Sample temp. (^{0}F)	Week 1 Day 1 9/29/13 (initial)	Week 1 Day 3 10/1/13	Week 4 Day 1 10/20/13	Week 6 Day 4 11/14 /13 (final)
outside temp	62	78	61	36
1	62	88	--	--
2	62	79	65	41
3	62	79	80	61
4	62	88	65	45
5	62	87	65	52

Temperature could be successfully collected from all samples, shown in Figure 1. The outside temperature was recorded for each temperature sample as a relative temperature comparison. Initially, all of the samples had an identical temperature to their environment. Throughout its decomposition, Sample 1 maintained a higher temperature than most of the other samples due to the heat of insect activity. In later temperature recordings, 1 was no longer present due to high levels of insect activity, which hastened decomposition and finished off the sample within a week.

Temperature was taken two days later in order to determine their adjusted temperatures. The adjusted temperatures of samples 2-5 indicated their variable conditions: 2 and 3 were aerated and therefore maintained a similar temperature to outside. Samples 4 and 5 were protected from moisture using a construction-grade non-insulating tarp; however, the tarp may have afforded some insulation for the samples, and they measured higher in temperature by roughly 10 degrees Fahrenheit. The second temperature recording was done in the middle of the data collection period; samples 2, 4, and 5 had a similar temperature as outside, but 3 had a high temperature difference of about 15 degrees Fahrenheit. Because 3 was anaerobic and could not be disturbed, there was no way to account for the temperature variation. In the final temperature reading at the end of the data collection period, samples 2 and 4 were closest to outside

temperature, and sample 3 measured another notable temperature difference of about 20 degrees Fahrenheit.

Insect activity also played a role in decomposition, especially during some temperature readings. During the aeration of 2 and 4, blowfly maggot presence was noted on 2 but not 4, possibly due to the tarp covering 4 and the extra protection from insects it received. As it was the end of the data collection period, sample 3 (which had a notably higher temperature) was able to be disturbed, and blowfly maggot presence was confirmed on the sample. None of the other samples had insect activity at that point in the experiment. The singular insect activity in 3, therefore, would account for its temperature difference.

In terms of qualitative observations, samples 2 and 4 were closest to outside temperature, and when uncovered were noted to be mostly decomposed: both had nearly indiscernible visible differences between the soil except for distinctly hardened portions. The crumbly portions qualitatively indicated rapid decomposition in an oxygenated environment, identified through adipocere formation (the formation of soap from fat under high pH conditions) bound with sodium (Vass 2001). Sample 3, when uncovered, had a whitish discoloration and was greatly reduced in size, and Blow fly maggot presence was noted again. Sample 5 was the least decomposed of all samples, being undisturbed and covered with tarp for the full six weeks. Sample 5 still had its original shape, distinct discoloration, and a paste-like texture, which indicates a potassium bond within adipocere that may contribute to slower decay rates (Vass 2001).

After six weeks, the data collection period was finished and samples of each ham were taken to determine the presence and level of microorganisms in the meat during the decomposition process. For the four variable hams, each ham was swabbed twice separately in order to inoculate two plates. Because the data collection period was finished, two samples were taken from all variable hams (including anaerobic) in order to observe thoroughly the presence of microorganisms in the samples. The control ham (1), due to its exposure to all elements, was completely decomposed within the first week. Its presence in the experiment illustrated the varying decomposition rate of exposed ham versus composted ham (rather than the presence of microorganisms in exposed versus composted ham), therefore, no microorganism sample was taken. Chart 2 describes the presence and level of microorganisms on each plate.

Bacteria colonies on each plate were counted by dividing the plate into four quadrants,

and counting the least populated region. This method resulted in a relatively accurate count of the bacterial colonies, as shown in Plates 2.1 and 2.2 (two separate plates cultures based on separate samples from 2), in which the colony numbers were very close at 239 and 231 respectively. In samples from 3 and 4, the lawn of bacterial made individual colonies impossible to count, and were therefore labeled “Too numerous to count” (TNTC). Plate 5.1 yielded countable bacterial colonies, but 5.2 yielded a lawn.

Plate Number	Number of Colonies
2.1	239
2.2	231
3.1	too numerous to count (TNTC)
3.2	TNTC
4.1	TNTC
4.2	TNTC
5.1	329
5.2	TNTC

Chart 2

Figures 2a-5b indicate the appearance of the cultured plates. Plates from Samples 2, 4, and 5 indicated presence of both bacteria and fungi: the plate from Sample 3 was the only plate without fungi.

Figure 2a and Figure 2b

r 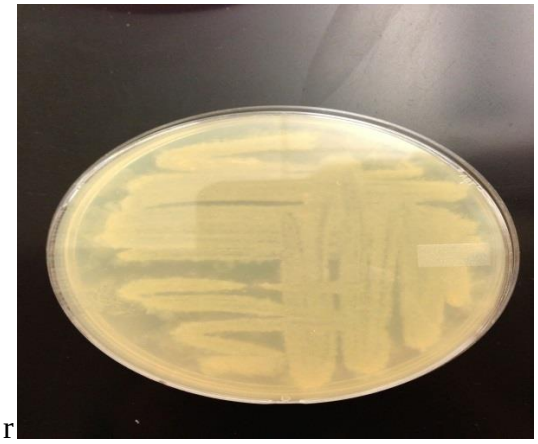 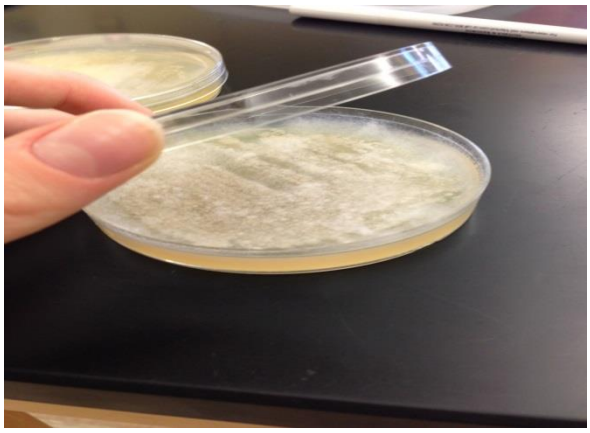

Figure 3a and Figure 3b

 

Figure 4a and Figure 4

Figure 5a and Figure 5b

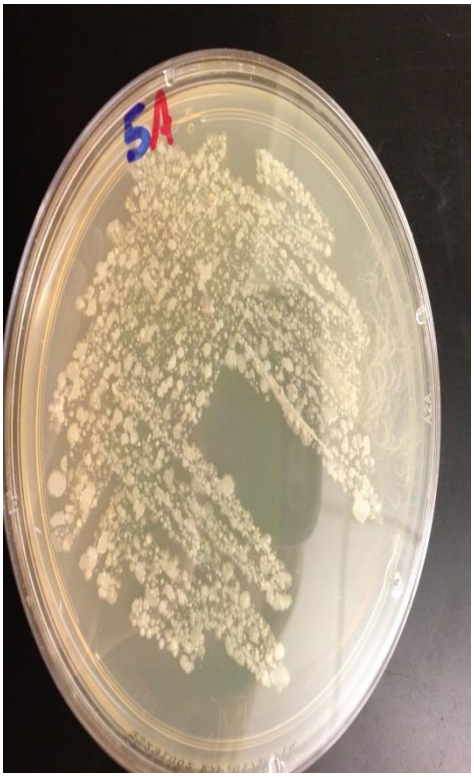

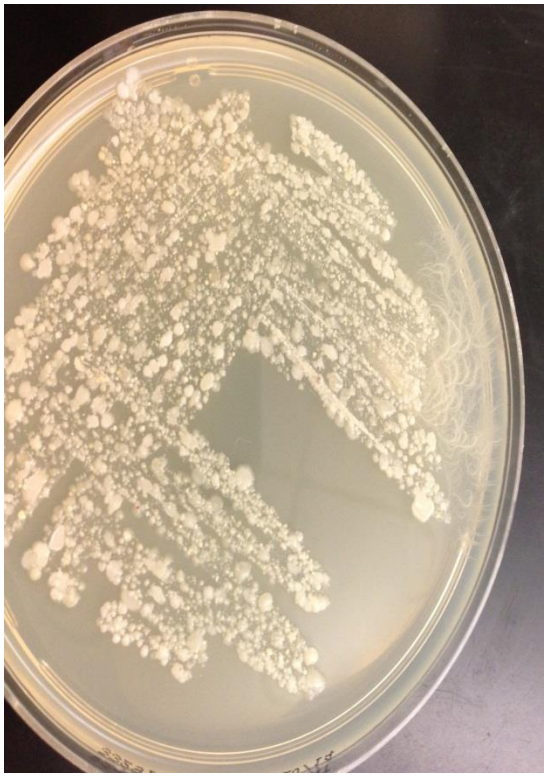

Conclusion

Over the course of six weeks, five hams were decomposed in varying environments in order to observe the role of environmental factors and microorganism activity in the rate of decomposition. After the data collecting period was completed, samples from each ham were taken and cultured, revealing that both bacteria and fungi were active on the decomposing meat and were varied according to the conditions in which the hams were decomposed. Initially, the specimens of meat placed in warmer, moister environments were predicted to decompose most quickly, and the specimens in colder, dryer conditions to decompose less quickly (Spennemann & Franke 1995).

Through the data collection period, however, the design of the experiment proved to have a different effect on the environments than the effect originally intended. The control ham, which was used to compare the decomposition rates of a completely exposed ham versus the composted hams, was quickly eaten away through a high level of insect activity. Therefore, the control was gone within a week, whereas the variable specimens lasted the six weeks of data collection. The materials used presented another unforeseen effect on the variable hams: the construction-grade non-insulating tarp afforded 4 and 5 more insulation than the uncovered specimens. Originally, the tarp was intended to protect samples 4 and 5 from any exposure to moisture (M. Farone, personal communication, July 22, 2013).

The cultured plates of 2 and 4 revealed active bacterial and fungal growth. The plates of 3 and 5 had bacterial growth, and one plate of 5 had some fungal growth; yet, the cultures were filled to a much lesser degree than those of 2 and 4.

Thus, the cultures of the microorganisms present on the samples reflected the level of decomposition for each ham. The specimen 2, exposed to moisture and aerated, decomposed the most quickly, followed by 4, the covered (and unintentionally insulated) and aerated sample. The remaining samples, 3 (uncovered, unaerated) and 5 (covered, unaerated) decomposed the third and least quickly, respectively.

The fastest decomposition was originally hypothesized to be with the more moist and heated samples, based on experiments with organic matter that indicate the movement of water increases the rate of decomposition, and the fact that warm, moist environments encourage the presence of microorganisms (Foote & Reynolds 1997, Spennemann & Franke 1995). In actuality, both aerated samples decomposed most quickly. Because of this, the results of this

experiment contribute to the assertion that aerobic decomposition progresses more quickly than anaerobic decomposition (Kristensen et al. 1995). In terms of microorganism presence, varied populations of both bacteria and fungi were found throughout the samples, with no clear correlation between a particular environmental variable and microorganism presence. Therefore, no conclusive statement can be drawn from the samples taken from the hams except that microorganisms played a role in the decomposition of each sample.

Such study of the factors that influence the rate of decomposition, like environmental factors and microorganism activity, can aid in forensic investigation. The understanding of key influences on decomposition, notably concerning oxygen-rich, moist environments, can be crucial when identifying a body or determining the time of death. Because the decomposition of pork most closely resembles that of human flesh, experiments investigating the role of such factors, especially when taken from the classroom - or rather, the backyard - and applied to daily life, can provide an accurate model for forensic investigation.

Literature Cited

Farone, M. (2013, July 22). Studying microorganisms in decomposition [E-mail to the author].

Foote, A. L., & Reynolds, K. A. (1997). Decomposition of saltmeadow cordgrass (Spartina patens) in Louisiana coastal marshes. *Estuaries*, *20*(3), 579-588.

Kristensen, E., Ahmed, S. I., & Devol, A. H. (1995). Aerobic and anaerobic decomposition of organic matter in marine sediment: Which is fastest? *Limnology and Oceanography*, *40*(8), 1430-1437.

Mann, R. W., M.A., Bass, W. M., Ph.D, & Meadows, L., B.A. (1990). Time since death and decomposition of the human body: variables and objectives in the case and experimental field studies. Journal of Forensic Sciences, 35(1), 103-111.

Saul, T. (2012, October 22). High school project [E-mail].

Schoenly, K. G., Haskell, N. H., Bieme-Ndi, C., Larsen, K., & Lee, Y. (2006). Recreating Death's Acre in the school yard: using pig carcasses as model corpses, to teach concepts of forensic entomology & ecological succession. The American Biology Teacher, 68(7), 402-410.

Spennemann, D. H. R., & Franke, B. (1995). Decomposition of human bodies and the interpretation of burials in the tropical Pacific. *Archaeology in Oceania*, *30*(2),

66-73.

Vass, A. A. (2001, November 1). *Beyond the grave - understanding human decomposition*. Retrieved July, 2013, from http://www.academia.dk/BiologiskAntropologi/Tafonomi/PDF/ArpadVass_2001.pdf

Acknowledgements

I am very thankful for the assistance of Jennifer Dye, who gave direction to my data collection, and provided feedback on the structure of my paper. I also thank Adam McRen for assistance in constructing the materials for this experiment and project disposal. Finally, I thank Dr. Mary Farone for providing invaluable advice on the structure and execution of this experiment.

Abstracts of Papers

Presented at the Annual Meeting
Belmont University
Nashville, Tennessee
Friday, April 25, 2014

Testing the Bayesian Model of Hypothesis Evaluation

Vijaya Dasari
White Station High School, Memphis

Abstract

Bayesian updating is a mathematical theory that describes how individuals update and revise beliefs based on new observations. The aim of this experiment was to 1) determine how well the Bayesian model explains subjects' hypothesis evaluation and 2) identify instances, if any, where subjects deviate from ideal Bayesian behavior. To this end, we used a modified version of the Wisconsin Card Sorting Test in which subjects guessed which stimuli, attribute, or rule, was relevant in a given trial and were given feedback on their guess. Additionally, we used probabilistic feedback to 1)dissociate the receipt of negative feedback and a rule change and 2) simulate the real-world uncertainty of evidence. We found that the Bayesian model accurately describes high-performing subjects' belief updating behavior. We can now use this model in future studies to pinpoint the areas that support hypothesis evaluation and make improvements in delusional patients who do not ideally evaluate their hypotheses.

Characterizing Unknown Microbial Species and Analyzing Microbial Stability in Cave Water Environments

Alex Jolly, Catherine English, Jacob Hill and Yae Eun yang
School for Science and Math at Vanderbilt, Nashville

Abstract

Assessment of microbial life is crucial for environmental analysis. Diversity of microbial cave life was studied within Mammoth Cave by analyzing various carbon preferences. Water samples were collected from stagnant and flowing water sources in Mammoth Cave in summer 2012/2013 and February 2013 and drip-water in Brush Hill Cave in summer 2013. These were analyzed using BioLog Eco plates. The hypotheses formulated stated that preferred carbon sources would change over time and location within the cave, but by no greater than 70% in

flowing water and 30% in stagnant. It was also hypothesized that there would be no change in the five most and least utilized carbon sources. Results demonstrated that the hypotheses were disproven: only 54.84% of carbon sources remained inside the 70% threshold for flowing water in Mammoth and 6.45% Brush Hill Cave, and 16.31% were within the 30% threshold in Mammoth and 38.71% in Brush Hill Cave; the hypothesis that the most/least utilized sources would remain unchanged was also incorrect. These results reveal that the cave water environments within these caves are not stable, which could negatively affect the overall health of their ecosystem, demonstrating that these changes are important to monitoring cave environments over time.

Evaluation of Primers for Microbial Source Tracking of Deer and Bovine in Middle Tennessee

Forrest Richardson
Hillsboro High School, Nashville

Abstract

PCR primer sets were tested for effectiveness in library independent microbial source tracking in middle Tennessee. Fecal samples were collected from middle Tennessee bovine and deer. Effectiveness of chosen DNA primer sets was tested using the bovine primer set to amplify its target sequence from DNA isolated from their respective fecal sources. Then, to evaluate host-specificity between primer sets, the bovine primer set was applied to DNA from deer feces and the deer primer set was applied to DNA from bovine feces in PCR. The DNA primer set for bovine targets the nifH gene sequence of Methanobrevibacter ruminatium. (1) The DNA primer set for deer targets a DNA sequence specific to Enterococcus mundtii. (2) Gel electrophoresis was used to display the results of PCR. The results showed the primers to be ineffective for source tracking, failing to amplify their target sequences of DNA from DNA isolated from bovine and deer fecal samples. Also, according to PCR and gel electrophoresis, the primers intended for bovine fecal source tracking target a sequence of DNA not specific to bacteria found in bovine feces. The primers intended for bovine fecal source tracking amplified their target sequence from DNA sample isolated from the deer fecal sample.

Voltage Measured Relative to Angle of Solar Panel

Sam Smith, Kyra Wilson, Christian Taylor
St. Andrew's-Sewanee School, Sewanee

Abstract

The world's population is growing. With more people on earth, our energy resources are stressed and people are in dire need of increasing the energy we produce in a stable and environmentally sustainable way. One of these new technologies is solar power. Although it is still in its infancy, solar panels are inefficient and are producing little electricity compared to its labor and resources used to make. Once the valuable resources are used to manufacture a solar panel, the most efficient form of collecting light is required to make this investment worthwhile for mankind. This paper explores how the relationship between the angle of a solar panel and the effects on the amount of sunlight collected throughout the course of a day. After data collection was finished a negative trend was found when comparing the average voltage collected throughout the day, and a negative trend when comparing peak voltages. The findings of this article result in a better understanding of solar technology and efficiency.

A Comparison of Water Parameters, Vegetation, and Macro-invertebrates of a Stream Before, after, and as it Passes Through Waterville Golf Course

Heidi Barringer
Cleveland High School, Cleveland

Abstract

This paper discusses the comparison of physical water parameters of a stream as it passes through Waterville Golf Course. The goal was to determine if the stream below the golf course is more degraded than the stream before it reaches the golf course. The data show that each site is about the same, concerning water quality. Each site has relatively healthy ranges of pH and temperature. However, the dissolved oxygen at each site was lower than the accepted value of 5.0mg/L at the beginning of the study. The dissolved oxygen levels eventually rose by the last two visits to the study sites. They also all had the presence of macro-invertebrates. However, the vegetation surrounding the stream is lacking and should be increased. A solution to the lack of vegetation is for less golf course construction around streams.

Biomass to Biofuels: An Economical Study

Rachel Baker
Camden Central High School, Camden

Abstract

This research and experiment will help determine if switch grass is a viable source for ethanol production that and its possible affect on the price of human or domestic animal feed. Information will be calculated from an experiment where ethanol levels from switch grass and corn fermentation will be recorded on a spreadsheet data base. This recorded information will show which biomass has the most ethanol energy potential to ferment into useable ethanol biofuel. Corn and switch grass will be studied to see which biomass has the most potential to create an efficient ethanol product. Ethanol levels will be taken from each sample using Vernier ethanol sensor and LabQuest. This data will be correlated into a spreadsheet data base.

This information will show the conclusion of which biomass crop is usable to produce a working ethanol biofuel. Further scientific investigation will be done to state whether or not the discovered biomass is a viable choice in large scale ethanol biofuel production, and on an economical sustainability stand point. Multiple factors must be considered to decide if the biomass would be best suited to be a long term economically efficient biofuel source.

Determination of Protein Molecular Weight

Aubrey Baxter and Carleigh Wilson
Northwest High School, Clarksville

Abstract

Proteins are essential to the way the human body works. In this project, the molecular weight of proteins was found. Making the gel and inserting the protein samples into the gel helped determine the weight. Measuring the distance from the wells in the gel to where the protein landed resulted in the findings of their weight. The discovery of the weight from the proteins in the gel showed that lighter proteins travel farther.

Anthropogenic Effects on the Water Quality of the Stones River in Murfreesboro, Tennessee

Morgan Bowling and Rachel Nichols
Siegel High School, Murfreesboro

Abstract

It is a grim fact that water running through urban areas comes into contact with a myriad of pollutants, especially when a landfill is near the flow. The study of the chemical quality of the Stones River is imperative because of its prominence as a drinking water and recreational resource in the community. With use of Vernier probes, water samples from two sites of the Stones River were tested for the presence of such pollutants. The first site was the Walter Hill Dam, which lies in close proximity to a landfill. The second site was downhill from the Murfreesboro Bark Park, a location where dogs can run and play, however, they often leave behind excrement. Dissolved oxygen, conductivity, temperature, and pH were tested to evaluate possible influences of the anthropogenic activities near these areas. Data from each site was compared using a two-sample student t-test. Additionally, the levels of dissolved oxygen in the water samples were determined to be higher than the EPA minimum. From the data, it was decided that some of the readings might have been affected by faulty probes, such as pH readings providing uncharacteristically acidic values for the Stone River.

Redox Reactions of Iron in the Body

Chardia Csizmadia and Abigail Schilling
Northwest High School, Clarksville

Abstract

Iron is essential to the human body. It makes up parts of blood and protein. Oxidation-reducingreactions are usually how iron is introduced to the body. In this situation iron II and iron III arebeing used. Redox reactions are any chemical reactions in which the oxidation number, in this case, of an ion changes by gaining or losing an ẽ. First, iron II ammonium sulfate solution or iron III chloride solution is dropped, by Beral-type pipet, into a well of a 24-well microplate. Next, a chemical solution is added to oxidize it. After, other chemical solutions will be added to the iron II and iron III solutions and is used to see if the oxidation-reduction reaction is evident or not. This is demonstrated in several different wells of the 24-well microplate.

Macroinvertebrates as Indicators of Anthropogenic Effects on Water Quality

Caroline Dodd, Julia Sculley and Christina Webb
Siegel High School, Murfreesboro

Abstract

Macroinvertebrate communities are a great way to indicate whether a river is healthy or not. Macroinvertebrates can be impacted by chemical, physical, and biological conditions of a stream such as, an abundance of nitrogen and phosphorus from runoff or changes in dissolved oxygen. Sample sites were chosen to evaluate the impact of human activity on water quality. There the macroinvertebrates were kicked into a net then sorted through and preserved in 95% ethanol. After, the macroinvertebrates were taken back to the lab and analyzed. The macroinvertebrates were identified by using a dissecting scope and field index key of the macroinvertebrate organisms. The macroinvertebrates were then sorted into three categories of rare, common, and dominant based on the number found. From here, the macroinvertebrates were placed into another group of sensitive, somewhat sensitive, and tolerant species.

The Influence of Hue, Lightness, and Saturation on Ants' Foraging Behavior

Susanna Edwards
Pope John Paul II High School, Hendersonville

Abstract

Appearance, the most immediate aspect of food, influences humans' choice of meal as well as animals', but what factors of appearance influence that choice the most? In an attempt to narrow down the most influential factors of appearance, this experiment tested ants for their selectivity of all three dimensions of color- hue, lightness, and saturation- while foraging. In trials for each dimension, an ant was placed in a small enclosure and allowed to choose between two sides that differed primarily in hue, lightness, or saturation of color and both contained reserves of sugar water. Because the ants selected most for hue and least for lightness when their ultimate choice of food was compared, it was concluded that the ants selected for hue and saturation about equally, but consistently selected for lightness the least.

The Process of Eutrophication and the Effects of Nuisance Algal Growth and Nutrient Enrichment

Anna Ferenchuk
Cleveland High School, Cleveland

Abstract

Eutrophication is a process of nutrient enrichment and algal growth. This study consisted of data collected at two streams to compare the indicators and observe the process of eutrophication. The data found showed that algae did affect dissolved oxygen concentrations. However, turbidity and pH were not affected, especially the latter. The streams were classified as mesotrophic and hosted the algae chlorophyta until the end of its growing season. Nuisance algal growth and low dissolved oxygen concentrations in a body of water are indicators of increased rate at which eutrophication occurs.